

Dissertation

submitted to the
Combined Faculties for the Natural Sciences and for Mathematics
of the Ruperto-Carola University of Heidelberg, Germany
for the degree of
Doctor of Natural Sciences

Presented by:

Maria Polychronidou

M.Sc. in Biochemistry

born in Holargos/Attica, Greece

Oral examination:

**Molecular analysis of the effect of the farnesylated nuclear membrane
proteins Kugelkern and Lamin Dm0 on nuclear architecture**

Referees: Prof. Dr. Herbert Steinbeisser
Prof. Dr. Jörg Großhans

Part of this work has been published in:

Polychronidou M., Hellwig A. and Grosshans J.: **“The Farnesylated Nuclear Proteins Kugelkern and Lamin Dm0 Affect Nuclear Morphology by Directly Interacting with the Nuclear Membrane”**

Mol Biol Cell. 2010 Aug 4. [Epub ahead of print]

Contents

Contents	4
Acknowledgements	7
Summary	8
Zusammenfassung	9
Abbreviations	11
1. Introduction	13
1.1 Nuclear shape.....	13
1.2 The nuclear membrane and the nuclear lamina.....	13
1.3 Lamins and lamin associated proteins.....	14
1.4 Laminopathies and the Hutchinson-Gilford progeria syndrome (HGPS).....	17
1.5 Kugelkern: a farnesylated INM protein that regulates nuclear shape in the <i>Drosophila</i> embryo.....	18
1.6 The C-terminal part of lamins and nuclear shape.....	21
1.7 Mechanisms of membrane deformation.....	21
1.8 The nuclear periphery and regulation of gene expression.....	22
1.9 Aim of the study.....	24
2. Materials and Methods	25
2.1 Materials.....	25
2.1.1 Chemicals.....	25
2.1.2 Radioactive substances.....	25
2.1.3 Enzymes.....	25
2.1.4 Antibiotics.....	25
2.1.5 Kits.....	25
2.1.6 Lipids.....	26
2.1.7 Bacterial strains.....	26
2.1.8 Yeast strains.....	26
2.1.9 Cell lines.....	26
2.1.10 Fly stocks.....	26
2.1.11 Primary antibodies.....	27
2.1.12 Secondary antibodies.....	28
2.1.13 Other reagents used in immunostainings.....	28
2.1.14 Buffers.....	28
2.1.15 Media used for bacterial cultures.....	29
2.1.16 Media and other reagents used for yeast cultures.....	29
2.1.17 Media and other reagents used for cell culture.....	30
2.1.18 Fly food.....	30
2.1.19 Apple juice agar plates for collection of <i>Drosophila</i> embryos.....	30
2.1.20 Chromatography.....	31
2.1.21 Other materials.....	31

2.1.22 Equipment.....	31
2.1.23 Software.....	32
2.1.24 Oligos used in the study.....	32
2.1.25 Constructs used in the study.....	35
2.2 Methods.....	37
2.2.1 Molecular cloning.....	37
2.2.2 Protein expression and purification.....	37
2.2.3 Total RNA isolation and cDNA synthesis by RT-PCR.....	38
2.2.4 PCR.....	38
2.2.5 mRNA injections.....	39
2.2.6 Immunostaining of <i>Drosophila</i> embryos.....	39
2.2.7 Mammalian cell culture.....	39
2.2.8 Generating the GFP-Kuk HeLa s/a cell line.....	40
2.2.9 <i>Drosophila</i> cell culture.....	40
2.2.10 dsRNA synthesis and RNAi treatment of <i>Drosophila</i> cells.....	41
2.2.11 Immunostaining of <i>Drosophila</i> cells.....	42
2.2.12 FTI treatment of cultured cells.....	42
2.2.13 Western Blotting.....	42
2.2.14 Collection of embryos with different number of maternally and zygotically provided copies of <i>kuk</i>	42
2.2.15 Liposome assays.....	42
2.2.16 Yeast transformation.....	43
2.2.17 Inducible protein expression in yeast.....	43
2.2.18 Fractionation of nuclei.....	44
2.2.19 IgG pull down of ZZ-Kuk.....	44
2.2.20 Silver staining of SDS-gels.....	44
2.2.21 GFP-pull down using GBP-beads in NIH-3T3 cell lysates.....	44
2.2.22 Filter assay for testing the activity of recombinant farnesyltransferase.....	45
2.2.23 Imaging.....	45
2.2.24 Electron microscopy.....	45
2.2.25 DamID.....	45
3. Results.....	47
3.1 The farnesylated proteins Kuk and lamin Dm0 affect nuclear morphology by directly interacting with the nuclear membrane.....	47
3.1.1 The extra nuclear membrane structures formed upon Kuk overexpression show an asymmetric composition.....	47
3.1.2 The nuclear membrane blebs formed upon Kuk overexpression are highly dynamic.....	49
3.1.3 Kuk and lamin Dm0 constructs used in the study.....	49
3.1.4 Expression of Kuk and lamin Dm0 constructs in mouse fibroblasts.....	53
3.1.5 Structure-function analysis of Kuk in the cellularizing <i>Drosophila</i> embryo.....	56
3.1.6 Maternally provided <i>kuk</i> is required for nuclear elongation during cellularization.....	59

3.1.7 Inhibition of farnesylation affects the localization of ectopically expressed and endogenous Kuk.....	62
3.1.8 Kuk and lamin Dm0 localize at the INM independently of a group of selected INM proteins.....	64
3.1.9 Kuk and LaminDm0 Δ N affect nuclear morphology even in the absence of a classical nuclear lamina.....	66
3.1.10 Farnesylation is not an absolute requirement for the binding of Kuk and lamin Dm0 constructs to protein free liposomes.....	67
3.1.11 Farnesylated Kuk and lamin Dm0 constructs deform protein free liposomes.....	71
3.2 Interplay between Kuk and chromatin.....	75
3.2.1 The GFP-Kuk HeLa s/a stable cell line: a system for studying ageing related cellular phenotypes.....	75
3.2.1.1 Characterization of the GFP-Kuk HeLa s/a cell line.....	75
3.2.1.2 Analysis of ageing related cellular phenotypes in the induced GFP-Kuk HeLa s/a cell line.....	76
3.2.1.3 The FTI ABT-100 reverses the ageing related cellular phenotypes observed in the induced GFP-Kuk HeLa s/a cell line.....	80
3.2.2 Identification of Kuk interacting partners.....	82
3.2.2.1 IgG pull down of ZZ-Kuk followed by mass spectrometry.....	82
3.2.2.2 Candidate approach for identifying Kuk interacting proteins.....	86
3.2.3 Analyzing the interplay of Kuk and chromatin by DamID.....	89
3.2.3.1 Identification of Kuk interacting genomic regions.....	89
3.2.3.2 Kuk overexpression increases chromatin accessibility in <i>Drosophila</i> Kc167 cells.....	91
3.2.4 Identification of a group of selected nuclear proteins that affect the localization of the X-chromosome in <i>Drosophila</i> S2 cells.....	93
4. Discussion.....	97
4.1 The nuclear membrane proteins Kugelkern and lamin Dm0 affect nuclear shape by directly interacting with the nuclear membrane via their farnesylated C-terminal part.....	97
4.2 Identification of potential Kuk interacting partners.....	100
4.3 The GFP-Kuk HeLa s/a cell line: a quantitative assay for studying ageing related cellular phenotypes.....	102
4.4 Analyzing the interplay of NM alterations and chromatin by DamID.....	103
4.5 Involvement of NM components in positioning of the X chromosome in male <i>Drosophila</i> cells.....	105
5. References.....	108
6. Appendix.....	117

Acknowledgements

First of all, I would like to thank my supervisor Prof. Dr. Jörg Großhans for offering me the opportunity to carry out my PhD work in his group and for always being available for answering questions, solving problems and discussing about my research.

I would also like to thank my first advisor Prof. Dr. Herbert Steinbeisser for offering me support throughout my PhD and for his helpful suggestions that contributed to the improvement of this work.

I would like to express my gratitude to Prof. Dr. Maarten Fornerod for offering me the opportunity to learn the DamID technique in his lab, for his help throughout the conduction of the DamID experiments, for the stimulating discussions and for his precious help with microarray data analysis.

I thank all present and past members of the Großhans lab, especially Dr. Fani Papagiannouli, Dr. Paweł Gawliński, Hung-Wei Sung and Felice Frey not only for helping me with the experimental part of my work but also for helpful discussions and for making my time in the lab enjoyable. I would also like to thank Andrea Hellwig, not only for performing the EM analysis, but also for her useful suggestions and for her help with technical problems.

A big thank you to the supervisor of my Diploma thesis Dr. Constantinos E. Vorgias, because all I learned in his lab, on so many different levels, and his valuable advice has been really beneficial throughout the conduction of my graduate studies.

Last but not least, I want to thank my parents for their endless support and for always being there for me.

A special thank you to Dr. Christian Wenzl, for helping me with experimental procedures, for providing constructive criticism on my work and most importantly for always standing by me where it matters the most, in life outside the lab.

Summary

Nuclear shape changes are observed during a variety of developmental processes, organismal ageing and pathological conditions among which the progeria syndrome HGPS. The mechanisms underlying nuclear shape changes in the above mentioned situations have mostly remained unclear. In order to address the molecular mechanism behind nuclear shape changes, it was analyzed in this work how the farnesylated nuclear envelope proteins Kugelkern, a *Drosophila* protein structurally and functionally related to lamins, and lamin Dm0 affect the structure of the nuclear membrane. It was found by expressing Kugelkern and a truncated lamin Dm0 variant in yeast, that the two proteins affect nuclear shape without requiring filament formation or the presence of a classical nuclear lamina. It could also be shown by RNAi experiments in *Drosophila* cultured cells that Kugelkern and lamin Dm0 do not depend on a group of selected inner nuclear membrane proteins for their localization to the nuclear envelope. Furthermore, farnesylated Kugelkern and lamin Dm0 recombinant protein constructs were found to induce changes in the morphology of protein free liposomes. Based on these findings it is proposed in this work that farnesylated proteins of the nuclear membrane induce nuclear shape changes by being asymmetrically inserted into the phospholipid bilayer via their farnesylated C-terminal part.

Aged cells, cells from progeria patients and cells overexpressing the farnesylated nuclear membrane protein Kugelkern or permanently farnesylated lamin variants, share a number of common cellular phenotypes among which abnormal nuclear shape and loss of heterochromatin. To elucidate the relation of altered levels of farnesylated nuclear membrane proteins with modified chromatin structure, a series of assays using Kugelkern were performed. By using the DamID technique in *Drosophila* cultured cells, it was found that Kugelkern overexpression results in increased accessibility of a number of genomic loci. In addition, by performing a screen in which a number of nuclear proteins were depleted by RNAi in *Drosophila* cells, it was found that a few genes among which *kugelkern* are required for peripheral localization and condensed morphology of the X chromosome in male cells. These results indicate that modification of the levels of nuclear membrane components can affect chromatin structure. Using a Kugelkern pull down assay followed by mass spectrometry a number of potential Kugelkern-interacting partners were identified, among which transcriptional regulators and proteins related to chromatin organization. These candidates may provide insight into the role of Kugelkern in modifying chromatin structure.

Zusammenfassung

Veränderungen in der Form des Zellkerns lassen sich in einer Reihe entwicklungsbiologischer Prozesse, während der natürlichen Alterung sowie bei einigen Erbkrankheiten, zu denen beispielsweise das Progeriesyndrom HGPS zählt, beobachten. Um einen Einblick in die größtenteils unbekanntem molekularen Mechanismen zu erlangen, die den genannten Änderungen der Kernmorphologie zugrunde liegen, wurde in der vorliegenden Arbeit untersucht, wie das farnesylierte Kernmembranprotein Kugelkern, ein *Drosophila* Protein mit funktioneller und struktureller Verwandtschaft zu Laminen, und Lamin Dm0 selbst die Struktur der Kernmembran beeinflussen. Durch Expression von Kugelkern und einer verkürzten Lamin Dm0-Variante in Hefezellen konnte gezeigt werden, daß beide Proteine die Kernmorphologie unabhängig von Filamentbildung oder dem Vorhandensein einer klassischen Kernlamina beeinflussen können. Zudem ließen sich Änderungen in der Morphologie von proteinfreien Liposomen durch den Einsatz von rekombinant hergestellten farnesylierten Kugelkern und Lamin Dm0 Proteinen induzieren. Darüber hinaus wurde durch den Einsatz von RNAi in *Drosophila* Kulturzellen gezeigt, daß die Kernmembranlokalisierung von Kugelkern und Lamin Dm0 nicht von einer Reihe bekannter Komponenten der inneren Zellkernmembran abhängt. Basierend auf diesen Ergebnissen wird in dieser Arbeit ein Modell vorgeschlagen, nachdem farnesylierte Kernmembranproteine die Form des Zellkerns durch die asymmetrische Insertion in die Phospholipid-Doppelschicht mittels ihrer farnesylierten C-Termini beeinflussen.

Alte Zellen, Zellen von Progerie-Patienten und Zellen, die das farnesylierte Protein Kugelkern oder dauerhaft farnesylierte Laminvarianten überexprimieren, weisen auffallend ähnliche zelluläre Phänotypen wie beispielsweise abnormale Kernform und Verlust von Heterochromatin auf. Um die Verbindung zwischen veränderten Levels farnesylierter Kernmembranproteine und Modifikationen in der Heterochromatinstruktur zu ergründen, wurden mit Hilfe von Kugelkern eine Reihe von Experimenten durchgeführt. So konnte durch die Verwendung der DamID Technik in *Drosophila* Kulturzellen gezeigt werden, daß die Überexpression von Kugelkern zu einer erhöhten Zugänglichkeit in einer Reihe genomischer Loci führt. In einem RNAi-Screen in *Drosophila* Kulturzellen, bei dem eine Reihe von Kernmembranproteinen depletiert wurden, konnte gezeigt werden, daß einige der getesteten Gene einschließlich *kugelkern*, für die periphere Lokalisation und die kondensierte Morphologie des X-Chromosoms in männlichen Zellen benötigt werden. Die Ergebnisse dieser beiden Experimente zeigen, daß durch die Manipulation von Komponenten der Kernmembran die Chromatinstruktur der DNA im Zellkern beeinflusst werden kann. Schließlich führte die massenspektrometrische Auswertung von Kugelkern Bindungstests zur Identifizierung potentieller Kugelkern-Interaktionspartner, zu denen auch eine Reihe von Transkriptions-

regulatoren und Proteinen mit bekannter Funktion in der Chromatinorganisation gehören. Eine weitergehende Analyse dieser Faktoren könnte ein besseres Verständnis für die Art und Weise wie Kugelkern die Chromatinstruktur modifiziert ermöglichen.

Abbreviations

aa	amino acid (s)
BAF	Barrier to Autointegration Factor
bp	base pairs
cDNA	complementary DNA
CMV	cytomegalovirus
d	day(s)
Dam	DNA adenine methyltransferase
DamID	DNA adenine methyltransferase identification
DAPI	4',6'-Diamidino-2-phenylindole
ddH ₂ O	double distilled water
dMAN1	<i>Drosophila</i> homolog or MAN1
DNA	deoxyribonucleic acid
dox	doxycycline
DTT	1,4-dithiothreitol
Δ	deletion
ΔC	C-terminal deletion
ΔN	N-terminal deletion
<i>E. coli</i>	<i>Escherichia coli</i>
EDTA	ethylenediaminetetraacetic acid
EGTA	ethyleneglycol-bis(β-aminoethyl)-N,N,N',N'-tetraacetic acid
EM	electron microscopy
ER	endoplasmic reticulum
FBS	fetal bovine serum
FCS	fetal calf serum
FL	full length
FPP	farnesyl pyrophosphate
FT	farnesyltransferase
FTI(s)	farnesyltransferase inhibitor(s)
g	gram (s)
GBP	GFP binding protein
GFP	green fluorescent protein
h	hour (s)
HEPES	N-(2-Hydroxyethyl)piperazine-N'(2-ethanesulfonic acid)
HGPS	Hutchinson-Gilford progeria syndrome
His	histidine
HP1	heterochromatin protein 1
Ig	immunoglobulin
INM	inner nuclear membrane
IPTG	isopropyl-β-D-thiogalactopyranoside
kb	kilobases
kDa	kilo Dalton
Kuk	kugelkern protein
<i>kuk</i>	kugelkern gene
l	liter (s)

La Δ 50	lamin A Δ 50 (progerin)
LB	Luria-Bertani medium
LBR	lamin B receptor
Leu	leucine
LEM	LAP2, emerin, MAN1
m	milli-
M	mol per liter
min	minute (s)
mRNA	messenger RNA
MSL	male specific lethal
MT(s)	microtubule(s)
MW	molecular weight
μ	micro-
n	nano-
NE	nuclear envelope
NLS	nuclear localization signal
NM	nuclear membrane
NPC	nuclear pore complex
Nup	nucleoporin
OD	optical density
ONM	outer nuclear membrane
p	pico- or plasmid (when in front of construct names)
PCR	polymerase chain reaction
PE	phosphatidylethanolamine
PI	phosphatidylinositol
PS	phosphatidylserine
RBBP4	retinoblastoma binding protein 4
RNA	ribonucleic acid
RNAi	RNA interference
rpm	revolutions per minute
RT	room temperature
s/a	silent but activatable
<i>S.cerevisiae</i>	<i>Saccharomyces cerevisiae</i>
SDS	sodiumdodecylsulphate
SDS-PAGE	SDS-polyacrylamide gel electrophoresis
TCL	total cell lysate
TNL	total nuclear lysate
Tris	tris(hydroxymethyl)aminomethane hydrochloride
UTR	untranslated region
v/v	volume per volume
w/v	weight per volume
WB	western blotting
wt	wild type
$^{\circ}$ C	degrees Celsius

1. Introduction

1.1 Nuclear shape

In all organisms the genetic material is found packaged and compacted, since the length of a linear DNA molecule would by far exceed the dimensions of the cellular compartment in which it has to be confined (Lewin, 2004). In prokaryotes, the supercoiled genetic material is found in the nucleoid, which is not separated by a membrane from the cytoplasm (Thanbichler *et al.*, 2005). On the other hand, in eukaryotic cells the main genetic material is housed in a membrane-enclosed organelle, the nucleus, which is the main site of DNA replication and RNA synthesis and processing (Alberts, 2002). Compartmentalizing the genetic material in the nucleus, offers to the eukaryotic cells multiple levels of regulation of gene expression i.e. by a complex and tight regulation of transcription or by selective export of mRNAs for translation in the cytoplasm.

Even though the nucleus of most cells has a round and smooth shape, nuclear shape and size changes are frequently observed during a variety of physiological processes such as cell cycle and differentiation, as well as in various pathologies. A prominent example of developmental nuclear morphology changes are the nuclei of neutrophil granulocytes (Olins and Olins, 2005). Granulocytes need to migrate through narrow tissue openings in order to reach sites of inflammation. During cell differentiation, the granulocyte nucleus adopts a lobulated shape, in order to facilitate cell function (Hoffmann *et al.*, 2007). Developmental nuclear shape changes are also observed during the early development of the *Drosophila* embryo (discussed in 1.5). Among the pathologies where nuclear shape changes are observed are cancer (Zink *et al.*, 2004) and diseases where nuclear membrane (NM) or nuclear lamina proteins are mutated (Capell and Collins, 2006).

The molecular mechanism that defines nuclear shape in the above mentioned situations remains unclear (Webster *et al.*, 2009). Nevertheless, an active role in determining nuclear shape is undoubtedly played by the NM, as indicated by the abnormal nuclear shapes observed in diseases caused by mutations in NM proteins (Chi *et al.*, 2009).

1.2 The nuclear membrane and the nuclear lamina

The NM (or nuclear envelope, NE) functions as a barrier isolating the genetic material from the cytoplasm and regulates the import or export of materials, from or to the cytoplasm. It is composed of two lipid membranes; the outer and inner NM (ONM and INM respectively). The ONM is continuous with the endoplasmic reticulum (ER) while the INM faces the interior of the nucleus and is characterized by the presence of a number of integral membrane proteins. The

ONM and INM are fused at the sites of the nuclear pore complexes (NPCs). In metazoans, a meshwork of proteins called the nuclear lamina is also found at the NM. The lamina underlies the INM to which it attaches via INM proteins and it also interacts with parts of the chromatin, either directly or via chromatin binding proteins. The lamina provides mechanical stability to the nucleus and anchors the nucleus to the cytoskeleton. When selected lamina components are affected, the mechanical properties of the nucleus such as elasticity or stiffness are impaired (Lammerding *et al.*, 2004; Lammerding *et al.*, 2005; Lammerding *et al.*, 2006; Rowat *et al.*, 2006) and the nucleus-cytoskeleton connection is destroyed (Ji *et al.*, 2007). Apart from regulating nuclear mechanics, the lamina participates in a variety of non structural processes among which NPC positioning, docking chromatin to the nuclear periphery, apoptosis, DNA replication and transcription, disassembly and reassembly of the NM during mitosis, signal transduction, cell differentiation and cell cycle regulation (Mattout-Drubezki and Gruenbaum, 2003). The multiple cellular functions of the nuclear lamina are highlighted by the wide variety of diseases that arise from mutations in NE and lamina proteins (Broers *et al.*, 2004; Cohen *et al.*, 2008; Chi *et al.*, 2009).

1.3 Lamins and lamin associated proteins

The nuclear lamina is composed of lamins and lamin related proteins. Lamins are nuclear specific Type V intermediate filaments, divided in A- and B-type depending on their posttranslational modifications and their expression pattern (Hutchison *et al.*, 1994). A-Type lamins are developmentally regulated and expressed in a cell-type and tissue-specific manner while B-Type lamins are uniformly expressed in all nucleated cells. A- and B-type lamins were thought to behave differently during mitosis, with the A-type dissociating from the NM and the B-type lamins remaining associated with NM vesicles. This idea has been revised since increasing evidence indicates that both types are solubilized at the onset of mitosis (Beaudouin *et al.*, 2002).

In vertebrates, there are three lamin genes, *LMNA*, *LMNB1* and *LMNB2* that encode lamins A, C, AΔ10 and C2, B1 and B2-B3 respectively. In *Drosophila* there are two lamin genes coding for lamin Dm0 and lamin C and in *C.elegans* only one (Goldman *et al.*, 2002). In *S.cerevisiae* there are no lamins and typical lamin associated proteins (Erber *et al.*, 1998). It is unknown whether a structural or functional equivalent to the nuclear lamina is found in yeast (Hattier *et al.*, 2007). The absence of lamins from yeast and the higher number of lamins and inner nuclear membrane (INM) proteins in vertebrates indicate an increase in complexity of the nuclear lamina during evolution. It has been suggested that the emergence of lamina proteins in animal cells is related to the transition from a closed to an open mitosis (Cohen *et al.*, 2001).

Lamins show a common polypeptide structure, consisting of a short N-terminal head domain followed by an α -helical rod domain and a globular C-terminal tail domain. The C-terminal tail domain contains the nuclear localization signal (NLS), the immunoglobulin fold and a CaaX motif. The CaaX motif (where 'C' is a Cysteine, 'a' is an aliphatic amino acid and 'X' is any amino acid), gets farnesylated, thus rendering the protein lipophilic and promoting its association with the NM (Kitten and Nigg, 1991; Krohne, 1998). In A-type lamins the modified CaaX motif is cleaved during the maturation of the polypeptide, while B-type lamins remain permanently farnesylated (Meshorer and Gruenbaum, 2008). Lamin C does not contain a CaaX motif and it is not farnesylated.

The α -helical rod domain of lamins is composed of four coiled coil segments 1A, 1B, 2A and 2B interconnected by linkers L1, L12 and L2 (Herrmann *et al.*, 2009). The rod domain participates in the formation of intermediate filaments (IF). Formation of head-to-tail coiled coil dimers initiates the assembly of the IF (Stuurman *et al.*, 1998). On a first level, lamins form homodimers and they can subsequently form linear multimers. A-type and B-type homodimers may be combined in order to associate in mixed polymers, a process that is thought to be important for the final assembly of the lamina network (Kapinos *et al.*, 2009).

Lamins interact with a wide variety of proteins. These interactions, which can either be direct or take place via other proteins, are thought to mediate the connection of lamins to the NM, to the cytoskeleton and to chromatin, depending on the properties of the binding partner (Foisner, 2001; Zastrow *et al.*, 2004). The current knowledge about selected binding partners of lamins is summarized in Table 1. In particular, lamins bind to partners related to the maintenance of nuclear structure, among which MAN1, lamina associated polypeptide 1 (LAP1), LAP2, lamin B receptor (LBR), SUN proteins and emerin and the *Drosophila* INM proteins otefin and YA. In addition to the NM related proteins, lamins interact with cytoskeletal proteins such as nesprins and actin, via which they participate in the maintenance of nuclear strength and nuclear positioning. Apart from interacting with structural proteins, lamins bind to chromatin associated partners, such as heterochromatin protein 1 (HP1), the NM-chromatin adaptor protein barrier to autointegration factor (BAF), histones, retinoblastoma protein (pRb), Rb binding protein 4 (RBBP4), RBBP7, the transcription factor c-Fos and the sterol response element binding protein (SREBP). Lamins A and C can also bind to DNA (Stierle *et al.*, 2003) either directly or via the formation of complexes with DNA-binding proteins (reviewed in Mattout-Drubezki and Gruenbaum, 2003).

Table 1: Summary of the current knowledge concerning the most prominent interacting partners of lamins. The interacting partners are divided in three categories: NM related, cytoskeleton related and chromatin related. The third column of the table describes the type of interaction, which can be either direct or mediated by other proteins.

	Partner	Lamin Type	Type of interaction	References
NM	Emerin	Lamin A/C	Direct	(Lee <i>et al.</i> , 2001), (Sakaki <i>et al.</i> , 2001), (Capanni <i>et al.</i> , 2009)
	LAP1	Lamin A/C and B	Direct	(Foisner and Gerace, 1993)
	LAP2 isoforms	Lamin B		(Gant <i>et al.</i> , 1999), (Yang <i>et al.</i> , 1997)
	LAP2 α	Lamin A/C	Direct	(Dechat <i>et al.</i> , 2000)
	LBR	Lamin B	Direct	(Ye and Worman, 1994)
	MAN1	Lamin A and Lamin B1	Direct	(Lin <i>et al.</i> , 2000), (Mansharamani and Wilson, 2005)
	Otefin	Lamin Dm0	Direct	(Goldberg <i>et al.</i> , 1998)
	YA	Lamin Dm0	Direct	(Goldberg <i>et al.</i> , 1998)
	SUN-proteins	Lamin A/C	Direct	(Haque <i>et al.</i> , 2006)
Cytoskeletal	Nesprins or SYNE proteins	Lamin A/C	Direct & via Emerin and SUN-1	(Mislow <i>et al.</i> , 2002)
	Actin	Lamin A	Direct & via nesprins	(Sasseville and Langelier, 1998), (Houben <i>et al.</i> , 2007)
Chromatin related	BAF	Lamin A/C and B	Direct & via LEM proteins	(Holaska <i>et al.</i> , 2003), (Shumaker <i>et al.</i> , 2001), (Bengtsson and Wilson, 2006), (Capanni <i>et al.</i> , 2010)
	c-FOS	Lamin A/C	unknown	(Ivorra <i>et al.</i> , 2006)
	Histones	Lamins A/ C and B	Direct	(Taniura <i>et al.</i> , 1995)
	HP1	Lamin B	Direct & via LBR	(Ye <i>et al.</i> , 1997)
	pRb	Lamin A/C	via LAP2 α	(Ozaki <i>et al.</i> , 1994), (Markiewicz <i>et al.</i> , 2002)
	RBBP4	Lamin A	Direct	(Pegoraro <i>et al.</i> , 2009)
	RBBP7	Lamin A	Direct	(Pegoraro <i>et al.</i> , 2009)
	SREBP	Lamin A	Direct	(Lloyd <i>et al.</i> , 2002)
	DNA	Lamin A/ C	Direct & indirect via other proteins	(Stierle <i>et al.</i> , 2003), (Mattout-Drubezki and Gruenbaum, 2003)

1.4 Laminopathies and the Hutchinson-Gilford progeria syndrome (HGPS)

Mutations resulting in defective NE proteins i.e. emerin, LBR and lamin A are associated to many human diseases (Chi *et al.*, 2009). A large number of NE related diseases arise from mutations spanning the entire *LMNA* gene and are collectively called laminopathies (Capell and Collins, 2006). Laminopathies include neuromuscular disorders, i.e. Emery-Dreifuss muscular dystrophy (EDMD) and dilated cardiomyopathy (DCM), partial lipodystrophies and progeria syndromes i.e. Werner syndrome and HGPS.

HGPS is one of the more severe laminopathies and its striking phenotype has received increasing attention. Patients of this very rare disease (incidence 1 in 4-8 million births) are born healthy. At an average age of 12 months they start exhibiting characteristics of accelerated ageing and eventually die at a mean age of 13 years due to severe atherosclerosis leading to heart attacks (DeBusk, 1972). The phenotype of HGPS includes failure to thrive, loss of subcutaneous fat, skeletal abnormalities including osteoporosis, hair loss, sclerodermatous changes of the skin, small and beaked nose and wrinkled skin. HGPS children show no neurodegeneration and their mental and emotional development is corresponding to their age, even though they look much older.

Despite the fact that HGPS was first described by Hutchinson and subsequently by Gilford more than one hundred years ago (Hutchinson, 1886; Gilford, 1904), the mutation causing the syndrome was only recently identified. In most cases, a point mutation in exon 11 of *LMNA* activates a cryptic splice site, which leads to the formation of the permanently farnesylated lamin A variant La Δ 50 or progerin (De Sandre-Giovannoli *et al.*, 2003; Eriksson *et al.*, 2003). During normal lamin A processing, the prelamin A polypeptide is farnesylated in its CaaX motif by farnesyltransferase (FT), and after cleavage of the aaX motif by the ZMPSTE24 protease, the free farnesylcysteine is carboxyl-methylated and the last 15 aa are cleaved by ZMPSTE24 giving rise to mature lamin A (Young *et al.*, 2006). La Δ 50 lacks the second endoproteolytic ZMPSTE24 cleavage site and therefore cannot be processed to form mature lamin A.

The permanently farnesylated La Δ 50, due to its irreversible attachment to the NM induces a variety of nuclear defects. One of the most prominent consequences of La Δ 50 accumulation is the large and abnormally shaped nuclei of the patient's fibroblasts (Goldman *et al.*, 2004). In addition, heterochromatin markers such as HP1 and tri-methylated histone 3 lysine 9 (tri-me-H3K9) are found to be reduced and there is increased DNA damage (Scaffidi and Misteli, 2006). The formation of mixed polymers of La Δ 50, lamin A and lamin B is thought to impair lamin A and lamin B polymerization and function (Delbarre *et al.*, 2006).

The phenotypic similarities of La Δ 50 expressing cells and *Zmpste24* deficient cells (Moulson *et al.*, 2005; Navarro *et al.*, 2005), led to the idea that the permanently farnesylated state of La Δ 50 was responsible for the HGPS cellular phenotype. Indeed, it was shown that *Zmpste24*^{-/-}*Lmna*^{+/-} mice, in which the prelamin A synthesis is reduced to half the normal amount, are protected from abnormalities related to the *Zmpste24* deficiency (Fong *et al.*, 2004). Farnesylation was also shown to be required for the activity of La Δ 50 on nuclear shape, by the use of farnesyltransferase inhibitors (FTIs), which prevent and even reverse the nuclear shape defects (Toth *et al.*, 2005; Yang *et al.*, 2005).

Interestingly, cellular phenotypes similar to the ones observed in HGPS have been described as a result of physiological aging in *C.elegans*, humans and *Drosophila* (Haithcock *et al.*, 2005; Scaffidi and Misteli, 2006; Brandt *et al.*, 2008). This indicates that changes in nuclear architecture are not an exclusive characteristic of laminopathies but are also related to normal cell physiology.

1.5 Kugelkern: a farnesylated INM protein that regulates nuclear shape in the *Drosophila* embryo

During the early stages of embryonic development in *Drosophila* (shown in Figure 1A and reviewed in Mazumdar and Mazumdar, 2002), after fertilization and fusion of the parental nuclei, the nucleus of the zygote undergoes a series of mitotic divisions that are not followed by cytokinesis. This results in the formation of a syncytium, where the nuclei are located in the interior. With the onset of the ninth division, most of the nuclei migrate to the periphery and the syncytial blastoderm is formed. After the thirteenth division, membrane starts to invaginate from the surface to enclose the nuclei and with this process, called cellularization, the syncytial blastoderm gives rise to the cellular blastoderm. During cellularization, the shape of the cortical nuclei changes from spherical to ellipsoidal, together with a 2,5-fold increase in length (Figure 1B). This elongated nuclear shape is maintained until gastrulation. In addition to the increase in length, the nuclei show apical ruffling of the NM. At the same time as nuclear elongation, start of zygotic transcription and formation of pericentromeric chromatin are observed. The mechanism that lies beneath this change in nuclear morphology remains unknown. The microtubules (MTs) surrounding the nucleus (Figure 1B), seem to be required for maintenance of the elongated nuclear shape, since MT destruction by the use of MT depolymerizing drugs results in the loss of nuclear elongation (Brandt *et al.*, 2006; Pilot *et al.*, 2006).

A screen for genes affecting various aspects of cellularization, led to the identification of *kugelkern* (*kuk*), a gene that is required for nuclear elongation in the early fly embryo. In the *kuk*

mutant embryo the nuclei remain round and smooth by the end of cellularization and formation of the apically located chromocenter is impaired (Brandt *et al.*, 2006). Despite the defects observed during cellularization, *kuk* mutant embryos develop normally and the flies are viable and fertile, without any apparent defects.

How Kuk regulates nuclear morphology during cellularization remains unknown. One possible explanation might be that Kuk induces NM growth, required for the expansion of the NM when the nucleus elongates and ruffles apically. Another possibility is that Kuk serves as a link between NM and MTs or other cytoskeletal elements and in this way stabilizes the elongated nuclear shape. This could be achieved by Kuk interaction with “linkers of the nucleoskeleton to the cytoskeleton” (LINC) complexes i.e. with SUN proteins, INM proteins known to serve as linkers of NM and cytoskeleton (Razafsky and Hodzic, 2009).

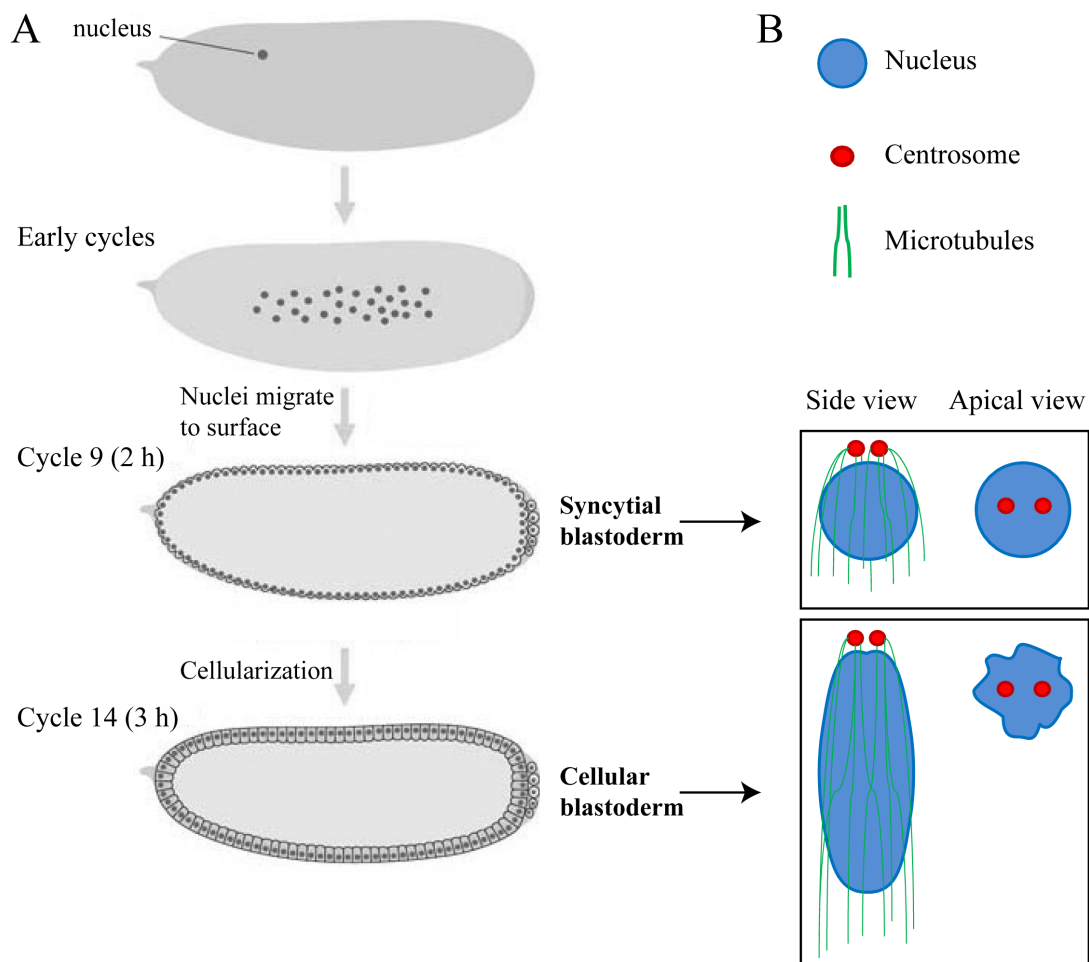


Figure 1: Nuclear morphology in the early *Drosophila* embryo.

A. Scheme of the early *Drosophila* embryo development (adapted from Morgan, 2007). In the preblastoderm (cycles 1-9) the nuclear divisions take place in the interior of the embryo and in cycle 8-9 most of the nuclei migrate towards the periphery and form the syncytial blastoderm. In cycle 14, during cellularization, the nuclei are enclosed in membrane and give rise to the cellular blastoderm. B. Scheme of nuclear shape in syncytial blastoderm stage and in late cellularization stage. Side and apical view of the nuclei (blue) is shown. The microtubules (green), arising from the pair of centrosomes (red) located apically to the nucleus, elongate towards the interior of the embryo.

Kuk was found to be an INM protein, consisting of 570 aa and containing a putative coiled coil motif in its N-terminus (aa 137-185), a NLS (aa 440-447) and a CaaX motif in the C-terminus (Brandt *et al.*, 2006). The structure of the Kuk polypeptide is shown in Figure 2. No apparent homologues of Kuk in higher organisms could be identified by BLAST analysis. Kuk is conserved within arthropods and the highest percentage of aa identity between different *Drosophila* (*D. melanogaster* and *D. grimshawi*) and mosquito species (*A. gambiae* and *A. aegypti*) was found in the aa sequences 353-404 and 453-473 (alignment shown in Figure 8). According to *in silico* analysis, the two sequences do not seem to contain any known functional motifs. Even though the predicted MW of Kuk is 60 kDa, the protein runs at approximately 120 kDa on SDS-PAGE. So far there is no evidence for Kuk dimer formation, which could explain its abnormal electrophoretic behavior.

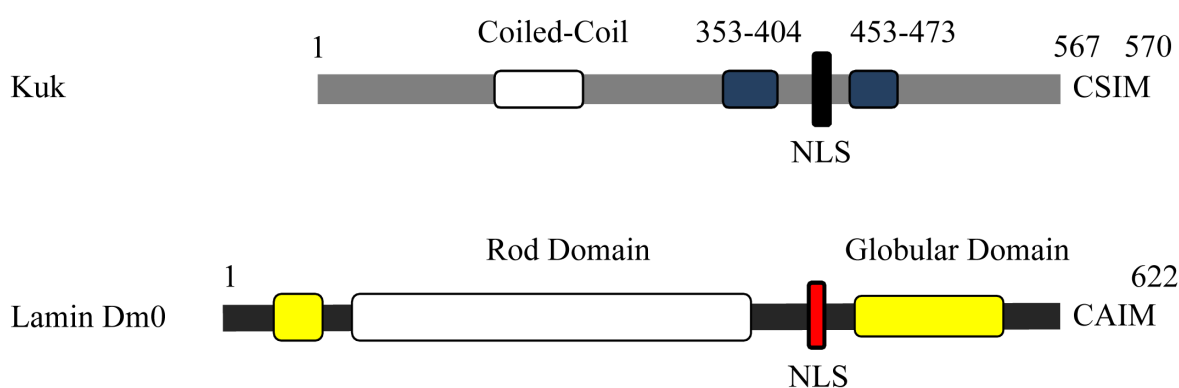


Figure 2: Schematic representation of Kuk and lamin Dm0 protein structures.

The putative coiled coil motif of Kuk (aa 137-185) is shown in white. The two highly conserved aa sequences 353-404 and 453-473 are shown in blue and the NLS in black. In the lamin Dm0 polypeptide scheme the NLS is shown in red, the rod domain in white and the N-terminal head domain and the C-terminal globular domain in yellow.

The polypeptide structure of Kuk is similar to the one of lamins (comparison of Kuk to lamin Dm0 is shown in Figure 2). Apart from lamins, Kuk is so far the only known farnesylated nuclear protein. The coiled coil motif of Kuk is much shorter compared to the rod domain of lamins and so far there is no evidence that Kuk could form filaments. Interestingly, apart from the structural similarities, Kuk also shares functional similarities with lamins, since overexpression of Kuk or farnesylated lamin variants results in comparable nuclear phenotypes (Brandt *et al.*, 2006; Brandt *et al.*, 2008). In particular, overexpression of Kuk results in the formation of abnormally shaped nuclei, with similar defects as in the case of La Δ 50 overexpression i.e. heterochromatin reduction, NPC clustering and DNA damage. Strikingly, tissue specific Kuk overexpression in the adult fly induces life span shortening and ageing related phenotypes (Brandt *et al.*, 2008).

1.6 The C-terminal part of lamins and nuclear shape

Increased Kuk or LaΔ50 levels lead to the formation of abnormally shaped nuclei and induce NM infoldings. These effects of farnesylated nuclear proteins on the NM seem to be primarily due to their association with the NM via the lipophilic CaaX motif. B-type lamins containing a CaaX motif were shown to induce NM growth in cultured cells and zebrafish embryos, while *Drosophila* lamin C that does not contain a CaaX motif and non farnesylatable lamin B mutants containing a SaaX motif are not able to change nuclear shape (Prüfert *et al.*, 2004). The use of short GFP-tagged truncated lamin variants containing only the C-terminal part of lamins in the same study, led to the formation of lobulated, abnormal nuclei, thus showing that the N-terminal part of lamins is not required for their activity at the NM. Similar results were obtained by increased synthesis of lamin B1 and B2 in *Xenopus* oocytes and by expressing a chimeric GFP-NLS-CaaX construct in HeLa cells (Ralle *et al.*, 2004). According to the above mentioned studies, the CaaX motif of farnesylated lamins and potentially of Kugelkern seems to be sufficient for inducing NM growth, since even the chimeric construct GFP-NLS-CaaX, where the rod domain of lamin is completely absent shows activity on the NM. In contrast to the filament forming N-terminal part of lamin that has been extensively studied (Wiesel *et al.*, 2008; Ben-Harush *et al.*, 2009; Kapinos *et al.*, 2009) the analysis of the C-terminal part has been rather limited even though it has a clear activity on nuclear shape and it is associated with human diseases such as HGPS.

1.7 Mechanisms of membrane deformation

Curvature and dynamics of membrane shapes are frequently observed in all cells and are important for many cellular functions such as endo- and exocytosis or membrane trafficking. Membranes primarily consist of two components; lipids arranged in a phospholipid bilayer and membrane proteins. Changes in membrane structure can generally be achieved by two mechanisms which involve both membrane components, reviewed in Kozlov, 2010 and depicted in Figure 3. The first mechanism involves asymmetric composition of one of the two layers of the membrane bilayer. The asymmetry can be either due to the enrichment of one of the two monolayers in lipids of different shapes or simply by insertion of more lipid molecules in one monolayer (Figure 3, A). The contribution of proteins to the asymmetry is believed to be more significant than the one of the lipids and is achieved through their asymmetric insertion in only one side of the double layer (Figure 3, B). Proteins containing amphipathic α -helices or hydrophobic domains have been described to induce membrane curvature using this mechanism (Campelo *et al.*, 2008). According to the second mechanism, membrane bending is induced by contraction of boundaries between domains of different lipid phases. Lipid bilayers contain

patches of different phase states, i.e. ordered or disordered regions. The boundaries between patches of different phase state are areas of higher energy, which gives rise to line tension and results in constriction and bulging of the patch (Figure 3, C). In this model, protein molecules can act as scaffolds and stabilize membrane curvature i.e. by impressing their curved shapes on the bilayer (Figure 3, D). The two mechanisms do not exclude one another. As reported by Yu *et al.*, 2010, a synthetic mechanism of membrane bending in which both boundary contraction and asymmetric protein insertion are involved, is also possible.

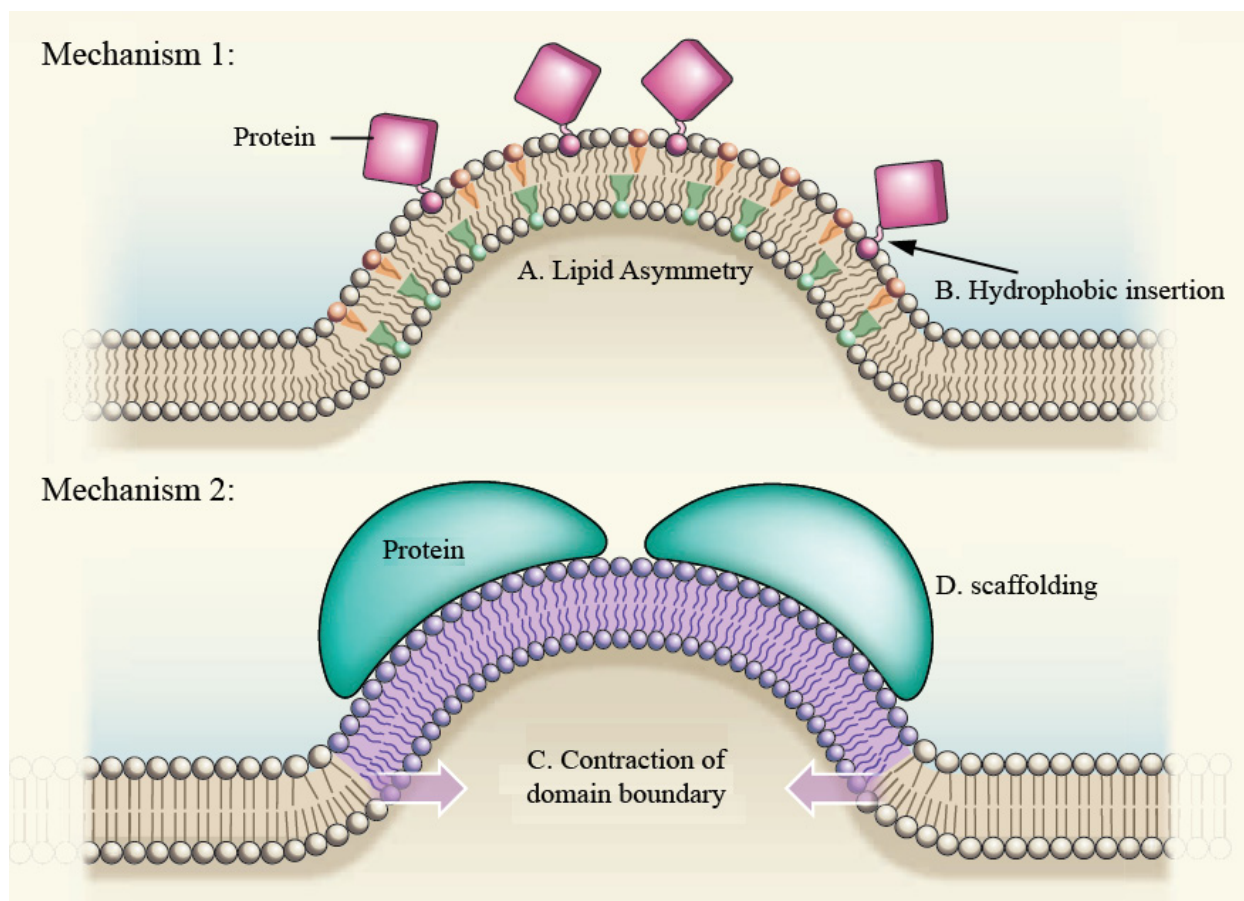


Figure 3: The two suggested mechanisms of membrane bending (adapted from Kozlov *et al.*, 2010). Mechanism 1 involves lipid asymmetry (A). The asymmetry may be enhanced by hydrophobic protein insertion (B). Mechanism 2 involves boundary contraction (C) which in some cases is stabilized by proteins (D).

1.8 The nuclear periphery and regulation of gene expression

Spatial arrangement of chromatin in the nucleus affects regulation of gene expression. Interaction of genes with the nuclear periphery has been associated with both transcriptional repression via interaction with components of the nuclear lamina and activation through interaction with the nuclear pores (reviewed in Akhtar and Gasser, 2007). Nuclear envelope proteins have been shown to transcriptionally regulate genes at the nuclear periphery by various mechanisms such as direct binding to transcription factors, recruitment of chromatin modifiers,

regulating the availability of signaling pathway components or modulating transcriptional complexes (reviewed in Shaklai *et al.*, 2007; Andres and Gonzalez, 2009).

Genomic elements that associate with the nuclear lamina have already been identified by characterizing lamin Dm0 interacting genomic regions in *Drosophila* cultured cells (Pickersgill *et al.*, 2006). In this study it was found that lamin Dm0 associates with mostly silenced, late replicating loci, lacking active histone marks. This comes in agreement with results from human cells, where lamin B1 and emerin were shown to associate with relatively inactive genomic regions (Guelen *et al.*, 2008). The idea that the nuclear periphery is mostly associated with inactive chromatin and is in general a non permissive environment for transcription is supported by experiments in which defined genomic loci were tethered to the INM in yeast or mammalian cells (Andrulis *et al.*, 1998; Reddy *et al.*, 2008; Finlan *et al.*, 2008; Kumaran and Spector, 2008). These studies showed that perinuclear tethering significantly reduces gene expression. The repression is reversible, since repositioning of the genomic locus away from the periphery results in increased expression of the previously silenced gene (Finlan *et al.*, 2008). Possible mechanisms of gene silencing at the nuclear periphery (discussed in Ruault *et al.*, 2008) include local accumulation of specific heterochromatin related factors (such as HP1), transcriptional repressors and histone modifying enzymes.

The pronounced loss of general heterochromatin markers in La Δ 50 overexpressing, Kuk overexpressing or aged cells (Scaffidi and Misteli, 2006; Brandt *et al.*, 2008; Pegoraro *et al.*, 2009) indicates that NM related defects have a global impact on chromatin structure. Modification of the NM properties due to the expression of increased amounts of farnesylated NM proteins seems to significantly disrupt heterochromatin structure, which may subsequently lead to altered gene expression. The mechanism linking the altered NM structure to the observed heterochromatin defects has not been analyzed yet.

1.9 Aim of the study

The nuclei of cells from patients with progeria syndromes, of aged cells or of cells overexpressing a farnesylated NM protein, share a number of similar phenotypes, summarized in Figure 4. The mechanism underlying the emergence of these phenotypes remains unknown. Given the similarity of HGPS and ageing with the situation of the overexpression of a farnesylated NM, the latter was here chosen for performing a series of different experiments, in order to analyze two phenotypes; abnormal nuclear shape and heterochromatin defects. In particular, the mechanisms by which farnesylated NM proteins induce nuclear shape changes and the interplay of Kugelkern and chromatin were investigated in this work.

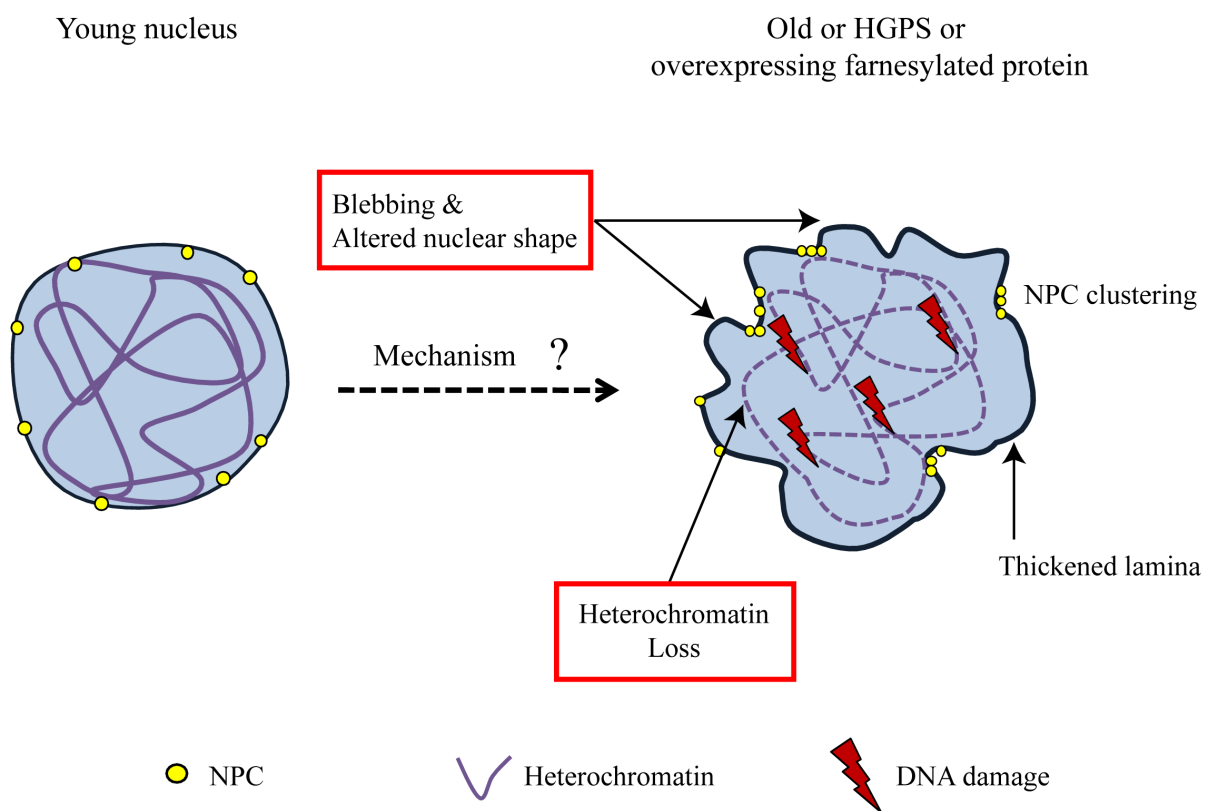


Figure 4: Schematic representation of the phenotype of a young nucleus compared to an old or HGPS or overexpressing farnesylated NM protein, nucleus. The nuclear periphery is indicated by dark blue color, the NPC in yellow, heterochromatin in purple and DNA damage in red.

2. Materials and Methods

2.1 Materials

2.1.1 Chemicals

All standard chemicals were purchased from Sigma-Aldrich (St. Louis, USA), AppliChem GmbH (Darmstadt), Invitrogen (Carlsbad, USA), Merck (Darmstadt), Gibco BRL (Eggenstein) or Roth (Karlsruhe) unless otherwise mentioned. The farnesyltransferase inhibitor (FTI) ABT-100 was provided by Abbott Laboratories.

2.1.2 Radioactive Substances

Farnesyl Pyrophosphate Triammonium Salt, [1-3H(N)]- (PerkinElmer)

2.1.3 Enzymes

All restriction enzymes were obtained from Fermentas (St. Leon-Rot) and New England Biolabs (Ipswich, USA) and used according to the manufacturer's instructions. In addition, the following enzymes were used.

- Shrimp Alkaline Phosphatase (Fermentas)
- Taq Polymerase (expressed and purified in the lab)
- Pfu DNA-Polymerase (expressed and purified in the lab)
- T4 DNA Ligase (Fermentas)
- T7 RNA polymerase (expressed and purified in the lab)
- Transcriptor Reverse Transcriptase (Roche)
- Advantage cDNA PCR mix (Clontech)

2.1.4 Antibiotics

- Ampicillin: stock (1000x) 100 mg/ml, used in a final concentration of 100 µg/ml
- Chloramphenicol: stock (1000x) 34 mg/ml, used in a final concentration of 34 µg/ml
- Kanamycin: stock (1000x) 50 mg/ml, used in a final concentration of 50 µg/ml

2.1.5 Kits

All kits were used according to the manufacturer's instructions.

- ECL plus Western Blotting Detection System (GE Healthcare/Amersham)
- Plasmid Midi Kit Nucleobond AX (Macherey-Nagel, Düren)

- mMESSAGE mMACHINE high yield capped RNA transcription kit (Applied Biosystems)
- PCR purification kit (QIAGEN)
- Gel extraction kit (QIAGEN)
- DNeasy Tissue kit (QIAGEN)
- Effectene transfection reagent (QIAGEN)

2.1.6 Lipids

- Brain extract from bovine brain, Folch fraction 1 (Sigma-Aldrich)
- Rhodamine-PE (Avanti Polar Lipids)

2.1.7 Bacterial strains

E. coli **DH5- α** F⁻, ϕ 80dlacZ Δ M15, Δ (lacZYA-argF)U169, *deoR*, *recA1*, *endA1*, *hsdR17*(rK⁻, mK⁺), *phoA*, *supE44*, λ^- , *thi-1*, *gyrA96*, *relA1*

E. coli **MC1061** F⁻, Δ (ara-leu)7697 [araD139]_{B/r} Δ (codB-lacI)3 galK16 galE15 λ^- e14⁻ mcrA0 relA1 rpsL150(strR) spoT1 mcrB1 hsdR2(r⁻m⁺)

E. coli **Rosetta(DE3)pLysS** F⁻, *ompT* hsdS_B(R_B⁻ m_B⁻) gal dcm λ (DE3 [lacI lacUV5-T7 gene 1 ind1 sam7 nin5]) pLysSRARE (Cam^R)

2.1.8 Yeast strains

AK725: MATa ura3-52 leu2 Δ 1 his3 Δ 200 trp1 Δ 63 NUP133-mCherry-KanMX6

NUP133 was tagged endogenously using standard PCR-based methods (Janke *et al.*, 2004) in the S288c background. Tagging was confirmed by colony PCR and microscopy. The strain was a gift from A. Khmelinskii and E. Schiebel.

2.1.9 Cell lines

- HeLa s/a (provided by D. Görlich)
- GFP HeLa s/a (provided by D. Görlich)
- GFP-Kuk HeLa s/a (this work, described in 2.2.8)
- Kc167 (Drosophila Genomics Research Centre)
- NIH-3T3 (provided by R. Grosse)
- S2 DRSC (Drosophila Genomics Research Centre)

2.1.10 Fly stocks

All fly stocks used in this study are part of the Großhans lab stock collection.

- *4xkuk*: w ; P[1]{*kuk*⁺, w⁺} ; TM3, *Sb Ser* / TM6B, *Tb Hu*

- *6xkuk*: w , P[1]{*kuk+*, w+} ; P[2]{*kuk+*, w+} *th st cu sr e ca* / TM3, *Sb Ser*
- *kukΔ15*: w ; *dur+*{w+} , *kuk15 e ca* / *dur+*{w+}, Df(3R)EX6176{w+} *e ca*
- wt: ore^R
- DF(3R): w; Df(3R)Exel6176, p{w[+mC]=XP-U}Exel6176 / TM3, *Sb*, *hb-lacZ*{ry+}
- *zz-kuk* ; *kukΔ15*: w; HS-H10-ZZ-*tev-kuk*{w+} ; *dur+*{w+} , *kuk15 e ca* / *dur+*{w+}, Df(3R)EX6176{w+} *e ca*

2.1.11 Primary Antibodies

All primary antibodies were used in the appropriate dilution in 0,5% BSA in PBS-T.

- mAb414 (Sigma-Aldrich)
- guinea-pig- α -BAF (provided by G. Krohne)
- rabbit- α -BAF (provided by P. A. Fisher)
- rabbit- α -dNC2b (provided by J. T. Kadonaga)
- mouse- α - β -Gal (Boehringer)
- rabbit- α -GFP (Torrey-Pines Biolabs)
- mouse- α -HA (Babco)
- mouse- α -HP1 (*Drosophila* HP1) (Developmental Studies Hybridoma Bank)
- mouse- α -HP1 (mouse HP1) (Chemicon)
- mouse- α -Hsp47 (Mabtec)
- rabbit- α -Kuk (Brandt *et al.*, 2006)
- rat- α -MSL3 (provided by A. Akhtar)
- mouse- α -Myc (clone 9E10, Santa Cruz Biotechnology)
- goat- α -Lamin A/C (Santa Cruz Biotechnology)
- mouse- α -Lamin C (Developmental Studies Hybridoma Bank)
- mouse- α -Lamin Dm0 (provided by H. Saumweber)
- guinea-pig- α -LBR (provided by G. Krohne)
- guinea-pig- α -dMAN1 (provided by G. Krohne),
- rabbit- α -Nup50 (Brandt *et al.*, 2006)
- guinea-pig- α -Otefin (provided by G. Krohne)
- rabbit- α -p55 (provided by J. T. Kadonaga)
- mouse- α -p- γ -H2A.X (Chemicon)
- rabbit- α -RBBP4 (Abcam)
- guinea-pig- α -Slam (Brandt *et al.*, 2006)

- mouse- α -Tubulin clone B-512 (Sigma-Aldrich)
- mouse- α -Tubulin clone DM1A (Abcam)

2.1.12 Secondary Antibodies

Alexa-coupled goat- α -guinea-pig, goat- α -mouse, goat- α -rabbit, goat- α -rat, and donkey- α -goat (Invitrogen) were used for immunofluorescence in a 1:500 dilution.

Horseshoe peroxidase coupled goat- α -rabbit, goat- α -guinea-pig and goat- α -mouse secondary antibodies (Sigma-Aldrich) were used for immunoblotting in a 1:10.000 dilution.

2.1.13 Other reagents used in immunostainings

- DAPI (4',6'-Diamino-2-phenylindole): used for DNA staining, in a final concentration of 0,2 μ g/ml (Sigma-Aldrich)
- Alexa-coupled Phalloidin: used for actin staining, in a final concentration of 6 nM (Molecular Probes)
- Mounting medium: Aquapolymount (Polysciences, Eppelheim)

2.1.14 Buffers

- FT freezing buffer: 50 mM Tris [pH 7,5], 50 μ M ZnCl₂, 5 mM MgCl₂, 10 mM β -mercaptoethanol, 10% Glycerol.
- FT Reaction Buffer: 50 mM Tris [pH 7,5], 50 μ M ZnCl₂, 5 mM MgCl₂, 5 mM DTT, 5 mM NaF.
- Fixation Buffer for mammalian cells: 2% FA in PBS supplemented with 0,2% TX-100 and 0,5% NP-40.
- "His"-Lysis Buffer: 20 mM Na-phosphate [pH 8,0], 500 mM NaCl, 20 mM Imidazol.
- "His"-Elution Buffer: 20 mM Na-phosphate [pH 8,0], 500 mM NaCl, 500 mM Imidazol.
- HK-Buffer: 25 mM HEPES, 150 mM KCl, [pH 7,4].
- HK-Farnesylation Buffer: 25 mM HEPES [pH 7,4], 150 mM KCl, 1 mM MgCl₂, 20 μ M ZnCl₂, 5 mM DTT, 5 mM NaF.
- Ion exchange chromatography Buffer A: 20 mM Tris [pH 7,5], 10 mM NaCl.
- Ion exchange chromatography Buffer B: 20 mM Tris [pH 7,5], 1 M NaCl.
- IP buffer: 50 mM Hepes/NaOH [pH7,5], 150 mM NaCl, 1% TritonX-100, 10% glycerol, 1,5 mM MgCl₂, 1 mM EGTA, one tablet of protease inhibitor cocktail per 7 ml IP buffer.
- Lämmli SDS-PAGE sample buffer, 2x: 90 mM Tris-HCl [pH 6,8], 6% SDS, 0,6% bromophenol blue, 20% glycerol, 6% β -mercaptoethanol.

- Lithium acetate/ TE buffer: 1 volume 10x TE [pH 7,5], 1 volume 1 M lithium acetate, 8 volumes ddH₂O.
- Lithium acetate/ TE/ PEG buffer: 1 volume 10x TE [pH 7,5], 1 volume 1 M lithium acetate, 8 volumes PEG 4000 50% (w/v).
- Nuclear fractionation buffers:
Buffer A: 0,35 M sucrose, 15 mM Hepes/KOH [pH 7,5], 10 mM KCl, 5 mM MgCl₂, 0,5 mM EGTA, 1 mM DTT.
Buffer B: 0,8 M sucrose and all other components are the same as in Buffer A.
Buffer C: 15 mM Hepes/KOH [pH 7,5], 10 mM KCl, 3 mM MgCl₂, 1 mM DTT.
- PBS (Phosphate Buffered Saline) [pH 7,4]: 10 mM Na₂HPO₄, 2 mM KH₂PO₄, 137 mM NaCl, 2,7 mM KCl.
- PBS-T: PBS with 0,1% Tween-20 (for immunostainings) or 0,25% Tween-20 (for Western Blotting).
- Permeabilization buffer for mammalian cells: PBS supplemented with 0,5% TX-100 and 0,5% Saponin.
- Silver staining solutions:
Fixation buffer: 0,1% (v/v) acetic acid in 50% (v/v) EtOH.
Farmer Reducer solution: 250 ml ddH₂O with a spatula tip of kalium hexacyanoferrate III and a spatula tip sodium thiosulfate.
Silver solution: 0,1% (w/v) AgNO₃.
Equilibration solution: 2,5% (w/v) sodium carbonate.
Developing solution: 0,1% (v/v) FA (stock solution of FA, 37%), 2,5% sodium carbonate.
Stop solution: 5% (v/v) acetic acid.
- TE: 10 mM Tris/HCl [pH 8,0], 1 mM EDTA.

2.1.15 Media used for bacterial cultures

- LB: 1 l: 10 g Bactotryptone (Becton, Dickinson), 5 g Yeast extract (Becton, Dickinson), 10 g NaCl. 15 g Bactoagar (Becton, Dickinson) was added for making agar plates.
- SOB: 1 l: 20 g Bactotryptone, 5 g Yeast extract, 500 mg NaCl, 10 mM MgSO₄, 2,5 mM KCl.
- SOC: SOB supplemented with 20 mM glucose (from a 1 M stock solution).
- 2xYT: 1 l: 16 g Bacto Tryptone, 10 g Bacto Yeast Extract, 5 g NaCl.

2.1.16 Media and other reagents used for yeast cultures

- YPD: 1 l: 10 g Yeast extract (Becton, Dickinson), 20 g Peptone (Gibco), 20 g Bactoagar (Becton, Dickinson), 900 ml ddH₂O. Supplemented with 20 g glucose (in 100 ml ddH₂O

autoclaved separately). One tablet NaOH and 20 g Agar were added when YPD plates were prepared.

- SD: 1 l: 6,7 g Yeast nitrogen base without aminoacids, 0,6 g aa-mix without His, Trp, Leu, Ura. Supplemented with 20 g glucose or raffinose (in 100 ml ddH₂O autoclaved separately). One tablet of NaOH and 20 g Agar were added when SD plates were prepared.

- Amino acids/Uracil:

Uracil, 100x stock: 2,4 mg/ml. Used: 24 mg/l

Histidine, 100x stock: 2,4 mg/ml. Used: 24 mg/l

Leucine, 100x stock: 7,2 mg/ml. Used: 72 mg/l

Tryptophane, 100x stock: 5 mg/ml. Used: 50 mg/l

2.1.17 Media and other reagents used for cell culture

- BPYE Medium: 1 l: 2,5 g Bactopeptone, 1 g yeast-extract, 1 small bottle of M3 powder (Sigma-Aldrich), dissolved in 950 ml of water. The medium was filter sterilized using a 0,22 µm filter (Millipore) and stored at 4°C in the dark.

- Dulbecco's Modified Eagle Medium (DMEM) (Gibco Invitrogen)

- Leibovitz's L-15 medium (Gibco Invitrogen)

- Schneider's *Drosophila* medium (Gibco Invitrogen)

- Doxycycline (Sigma-Aldrich)

- Fetal Bovine Serum (FBS) (Gibco/Invitrogen)

- Fetal Calf Serum (FCS) (Gibco/Invitrogen)

- L-Glutamine 100x (Gibco/Invitrogen) : used at a final concentration of 2 mM

- Ganciclovir (Sigma-Aldrich): used in a final concentration of 10 µM

- Puromycin 10 mg/ml (Sigma-Aldrich): used in a final concentration of 5 µg/ml

2.1.18 Fly Food

20 l of water were cooked for 2 h with 160 g thread agar. After 2 h, 500 g fresh baker yeast, 200 g soja bean meal and 440 g molasses were added and cooked another 2 h. After 2 h cooking 1,6 kg malt extract, 1,6 kg corn meal and 125 ml of propionic acid were added, mixed and the food was filled in vials.

2.1.19 Apple juice agar plates for collection of *Drosophila* embryos

70 g of Agar was dissolved in 3 l of hot water. In parallel, 100 g of sucrose was dissolved in 1 l of apple juice. The two solutions were mixed and poured in Petri dishes.

2.1.20 Chromatography

- HisTrap HP affinity columns (Amersham)
- PD-10 Desalting columns (Amersham)
- Q-Sepharose (Amersham)

2.1.21 Other materials

- 1 kb DNA Ladder (New England Biolabs)
- 8-well chamber μ - slides (Ibidi)
- BSA/Albumin Fraktion V (Applichem)
- Complete Mini (EDTA free) Protease Inhibitor Cocktail (Roche)
- dNTPs 100mM stock (Invitrogen)
- IgG Sepharose Fast Flow (Amersham)
- Lab-TEK Chambered Coverglass (Nunc, Wiesbaden)
- PageRuler™ Unstained Protein Ladder (Fermentas)
- Polycarbonate membranes 0,1 μ m (Avanti Polar Lipids)
- Poly-L-lysine 10x concentrated (Sigma)
- Prestained Protein Molecular Weight Marker (Fermentas)
- Protran Nitrocellulose Membrane (Whatman/Schleicher & Schuell)
- Ribonucleoside Triphosphate set (Roche)
- RNase inhibitor (Roche)
- RotiSzint EcoPlus scintillation liquid (Roth)
- Salmon sperm DNA (Stratagene)
- TRizol Reagent (Invitrogen)
- VoltaLef Halocarbon Oil 10s (Lehmann & Voss & Co.)
- Whatman 3MM Chr Blotting Paper (Whatman, Springfield Mill, GB)

2.1.22 Equipment

- Agarose gel registrator: Raytest IDA (Image Documentation & Analysis)
- Fuji Medical X-Ray Film, 13x18 cm
- Gene Pulser™ Electroporator (BIO-RAD)
- Glass needle maker Narishige PN-30 (Japan)
- Image Screens BAS-MS 2040 (Fujifilm)
- Leica DMIRE 2 confocal microscope (Leica)
- Microfluidizer: EmulsiFlex-C5 (Avestin, Canada)
- Microinjector: FemtoJet (Eppendorf)

- Mini Extruder (Avanti Polar Lipids)
- Protein purifier Äkta prime, (Amersham Pharmacia Biotech)
- Rotavapor Rotary evaporator (Buchi)
- Thermocycler: PTC-200 Peltier Thermal Cycler (MJ Research)
- Trans-blot SD Semi-Dry Transfer Cell (BIO-RAD)
- Zeiss Axiovert 200 M PerkinElmer Ultra-View Spinning Disc confocal microscope (Carl Zeiss)
- Zeiss Axioplan 2 Fluorescence microscope (Carl Zeiss)

2.1.23 Software

- Adobe Photoshop CS3
- ImageJ 1.38x
- Leica Confocal Software 2.61
- PerkinElmer UltraView 2.0.0.009
- Lasergene 8.1.0
- Alignments of protein sequences were performed using the ClustaIW2 alignment program (<http://www.ebi.ac.uk/Tools/clustalw2/index.html>)
- The Protein Homology/AnalogY Recognition Engine (PHYRE) was used for identifying structured domains in the Kuk protein sequence (<http://www.sbg.bio.ic.ac.uk/~phyre/>)

2.1.24 Oligos used in the study

All oligos were synthesized by MWG Biotech AG (Ebersberg, Germany). Sequences recognized by restriction enzymes are shown in **bold letters**. Start (ATG) or Stop (TAA) codons are shown underlined. Insertions are shown in underlined italics.

Table 2: List of oligos used in the study.

Oligos used for clonings	
MP6f	cgggatcctccacgcgagccacgccat
MP6r	cgggaagctttacataatggcgactt
MP7f	cgggaattcctccacgcgagccacgccat
MP7r	cggctcgagttacataatggcgactt
MP15f	ggactagtatgagcaagggcgaggagctg
MP14r	ggctgcagttacataattgagcagatgg
MP17f	cgggaattctcgagcaaatcccgacgtgc
MP17r	cggctctagattacataatggcgactt
MP22f	cgccatggtgtcgcgccaagcgcgc

MP22r	gttcccgggttacataattgagcagatggatcg
MP23f	agaactagtatgagcaagggcgaggagctg
MP23r	gactcagttacataatggcgcacttctcg
MP41r	ggaggcctttacataattgagcagatg
MP42r	ggaggcctttacataattgaggagatg
MP44f	gcgctcagattctccaaggcaacaatcg
MP44r	gactcagttacataattgagcagatggatcg
MP45f	cgggaattcatgagcaagggcgaggag
MP45r	ggactcagttacataattgagcagatgg
MP46r	ggactcagttacataatggcgcacttc
MP47f	ggagatcttatgtaagcaaaatggc
MP49f	cgggatccgccgtggccaatctgg
MP49r	cggatatctcggtagtgggatac
MP50f	cgggatccgagaagtgcgcc
MP57f	cgggaattcatgagcaagggcgaggag
MP57r	cgtctagattactgtacagctcgtc
MP58f	cgggatccatgagcaagggcgaggag
MP58r	cgggaattcctgtacagctcgtcc
MP59f	cgggaattcatgctgggcacatcgag
MP59r	cgtctagaccatgactgtacattattcg
Oligos used for insertions or deletions of nucleotide sequences	
MP4f	gggatatctcgcgtctggagccgaacagt
MP4r	gggatatccaaattcaggctgaacaagtc
MP13f	ggcatatgtcattttcattctttggccgtg
MP12r	ggcatatgctgggcgaaagtgcgagccc
MP43f	ctgtttagaggtggaagctgatgtgcc
MP43r	ggcaacatcagcttccacctctacaacag
MP51f	<u>aagcgcaaacgcgcctg</u> accgggtcgacggatccgc
MP51r	cgggggcgaagaagttgtccatattggccacg
MP52f	gagcggataacaattataatagattcaattgtgagc
MP52r	<u>cacggcgcgtttgcctt</u> acctatggtagcggagctgc
MP53f	<u>aagcgcaaacgcgcctg</u> accgggtcgacggatccg
MP53r	<u>cacggcgcgtttgcctt</u> acctatggtagcggagctgcc
Oligos used for amplification of the cDNA arising from the two <i>kuk</i> transcripts	
MP11f	tccactagcgcgttggtta
MP11r	atccttattctcggcaccca
MP12f	gattacattccatactgaa
Oligos used for amplification of the cDNA arising from the <i>bottleneck</i> transcript	
MW-B1	gtaatacactcactatagggcgttcgtactcaacctcaac

MW-B2	gtaatacgactcactatagggcggcttgctggggcatcag		
dsRNA oligos containing the T7 promoter sequence at the 5'(shown in <i>italics</i>) (The oligos are shown in pairs, as used for the respective gene.)			
		Annotation ID	Gene
MP18f	<i>gtaatacgactcactatagggctgctgctcactacatcag</i>	CG5857	Ndc1
MP18r	<i>gtaatacgactcactatagggtagtatactatcttctc</i>	CG5857	Ndc1
MP19f	<i>gtaatacgactcactatagggatttctgctcagcctctg</i>	CG4236	Caf-1, p55
MP19r	<i>gtaatacgactcactataggggtggtccgtcctcagc</i>	CG4236	Caf-1, p55
MP20f	<i>gtaatacgactcactatagggatcgattcaagaaatcagc</i>	CG4453	Nup153
MP20r	<i>gtaatacgactcactatagggcgcgtgaaggaaatcaaa</i>	CG4453	Nup153
MP21f	<i>gtaatacgactcactataggggtgaagaaggcactcaaggc</i>	CG32067	Simjang, p66
MP21r	<i>gtaatacgactcactatagggggcatttgggtggtatcact</i>	CG32067	Simjang, p66
MP26f	<i>gtaatacgactcactatagggcgacggcgggtgtctt</i>	CG6743	Nup107
MP26r	<i>gtaatacgactcactatagggatgagcagtagtaggctattag</i>	CG6743	Nup107
MP27f	<i>gtaatacgactcactatagggctcccagcagctactcgt</i>	CG12399	Mad
MP27r	<i>gtaatacgactcactatagggcgatggtgctattctgttc</i>	CG12399	Mad
MP28f	<i>gtaatacgactcactatagggcttgcacaaactacagttac</i>	CG4257	STAT92E
MP28r	<i>gtaatacgactcactatagggcgactgtgggtgagttgtt</i>	CG4257	STAT92E
MP29f	<i>gtaatacgactcactatagggagagccaggcgaagag</i>	CG6476	Su(Var)3-9
MP29r	<i>gtaatacgactcactatagggcaacggcgcctagcac</i>	CG6476	Su(Var)3-9
MP30f	<i>gtaatacgactcactatagggtaatcgacatcaggaacag</i>	CG1594	Hopscotch
MP30r	<i>gtaatacgactcactataggggtgtggcctcggaggtg</i>	CG1594	Hopscotch
MP31f	<i>gtaatacgactcactatagggccaaagtttttcatcatctca</i>	CG12389	Fpps
MP31r	<i>gtaatacgactcactatagggagccaagtcaaaagcaag</i>	CG12389	fpps
MP32f	<i>gtaatacgactcactatagggatggtgagcaagggcgagga</i>	-	eGFP
MP32r	<i>gtaatacgactcactatagggatgccgttctctcgttctcgt</i>	-	eGFP
FP1	<i>gtaatacgactcactatagggcgagatgatgctaccgttgaga</i>	CG5145	Kuk
FP2	<i>gtaatacgactcactatagggcgaggtgcctatttctcagagg</i>	CG5145	Kuk
AB7	<i>gtaatacgactcactatagggcgaggatcgtttccatgact</i>	CG7380	BAF
AB8	<i>gtaatacgactcactatagggaaaggacgaggagctgttca</i>	CG7380	BAF
AB11	<i>gtaatacgactcactatagggctcttcttaatgctcggaggt</i>	CG8274	Mtor
AB12	<i>gtaatacgactcactatagggctctccttctcgcacaaaactt</i>	CG8274	Mtor
JL5	<i>gtaatacgactcactatagggctacgggtgaagaggatattgatga</i>	CG17952	LBR
JL25	<i>gtaatacgactcactatagggcaaatgacagaacgcagatagtg</i>	CG17952	LBR
JL8	<i>gtaatacgactcactatagggcaacgccagatatacgaaaa</i>	CG1664	Sbr
JL28	<i>gtaatacgactcactataggggtgttatccccaaatagagaa</i>	CG1664	Sbr
JL9	<i>gtaatacgactcactataggggaagaccagcagttgcatca</i>	CG9703	Axs
JL29	<i>gtaatacgactcactatagggcgatcgggtacacatacctg</i>	CG9703	Axs
JL17	<i>gtaatacgactcactataggggtggtcgtatgtgggaagt</i>	CG9424	Bocksbeutel
JL37	<i>gtaatacgactcactatagggccgactaaaggcacaatca</i>	CG9424	Bocksbeutel
JL21	<i>gtaatacgactcactatagggggctttatttgaacacggat</i>	CG5581	Otefin
JL41	<i>gtaatacgactcactataggggcagaagatcacatcaagt</i>	CG5581	Otefin
JL22	<i>gtaatacgactcactatagggctgtaaggctgttcaacaagg</i>	CG6944	Lamin Dm0

JL42	<i>gtaatacgactcactatagggacaaacgaacgaagattcagg</i>	CG6944	Lamin Dm0
JL46	<i>gtaatacgactcactataggggtgccttaagagttggtggg</i>	CG8409	HP1a,Su(var)2-5
JL64	<i>gtaatacgactcactataggggccctctggcaataatcaa</i>	CG8409	HP1a,Su(var)2-5
JL47	<i>gtaatacgactcactataggggctcaagtcgctgttctcc</i>	CG10119	Lamin C
JL65	<i>gtaatacgactcactataggggcacctcgcaaaaagaaaag</i>	CG10119	Lamin C
JL48	<i>gtaatacgactcactataggggttcttaattttgacaataatcac</i>	CG3167	D-MAN1
JL66	<i>gtaatacgactcactatagggatccagcgactattaagagaa</i>	CG3167	D-MAN1
JL60	<i>gtaatacgactcactataggggccattcgcttatgcagctgttca</i>	CG8593	Quemao
JL78	<i>gtaatacgactcactataggggtgcaattgagcgtgttctggtggg</i>	CG8593	Quemao

2.1.25 Constructs used in the study

Table 3: Constructs used in the study

Constructs designed and constructed in this study		
Construct	Oligos	Cloning Strategy & Construct information
pCS2-GFP	MP57f / MP57r	EcoRI / XbaI fragment in pCS2
pCS2-GFP-EcoRI	MP58f / MP58r	BamHI / EcoRI fragment in pCS2 (no stop codon, EcoRI site for making GFP-fusion constructs)
pCS2-GFP-BAF	MP 59f / MP59r	EcoRI / XbaI fragment in pCS2-GFP-EcoRI (the construct contains BAF 3'UTR)
pCS2-HA-Kuk-ΔHelix	MP44f / MP44r	PCR with MP44f / MP44r (template: pQE-H ₁₀ -zz-DN437Δhelix), XhoI fragment in pCS-HA-KukCDS (sequenced for orientation)
pCS2-HA-LaminDm0ΔN	MP7f / MP7r	EcoRI / XhoI fragment in pCS2-HA
pCS2-HA-LaminDm0	MP17f / MP17r	EcoRI / XbaI fragment in pCS2-HA
pMM6-GFP-Kuk	MP15f / MP14r	SpeI / PstI fragment in pMM6
pMM6-GFP- LaminDm0ΔN	MP23f / MP23r	SpeI / XhoI fragment in pMM6
pQE-H ₁₀ -GFP-LaminDm0ΔN	MP6f / MP6r	BamHI / HindIII fragment in pQE-H ₁₀ -GFP
pQE-H ₁₀ -ZZ-Kuk-ΔN437	MP22f / MP22r	NcoI / SmaI fragment in pQE-H ₁₀ -ZZ
pQE-H ₁₀ -ZZ-KukΔN437ΔHelix	MP43f / MP43r	Insertion of GAA (Glu) by PCR with MP43f / MP43r
pQE-H ₁₀ -GFP-C-term	MP49f / MP49r	BamHI / HindIII fragment in pQE-H ₁₀ -GFP
pQE-H ₁₀ -GFP-CaaX	MP50f / MP49r	BamHI / HindIII fragment in pQE-H ₁₀ -GFP
pQE-H ₁₀ -GFP-NLS-C-term	MP51f / MP51r MP52f / MP52r and MP52f / MP51r	PCR with MP51f / MP51r (template: pQE-H ₁₀ -GFP-C-term). PCR with MP52f / MP52r (template: pQE-H ₁₀ -GFP-C-term). The purified PCR products were mixed, the single stranded overhangs filled by a round of elongation and then PCR was performed with MP52f / MP51r. EcoRI / BamHI fragment cloned in pQE-H ₁₀ -GFP.
pQE-H ₁₀ -GFP-NLS-CaaX	MP52f / MP53r MP53f / MP51r and MP52f / MP51r	PCR with MP52f / MP53r (template: pQE-H ₁₀ -GFP-CaaX). PCR with MP53f / MP51r (template: pQE-H ₁₀ -GFP-CaaX). The purified PCR products were mixed, the single stranded overhangs filled by a round of elongation and then PCR was performed with MP52f / MP51r. EcoRI / BamHI fragment cloned in pQE-H ₁₀ -GFP.

pNDamMyc-Kuk	MP47f / MP41r	BglII / StuI fragment in pNDam
pNDamMyc-KukC567S	MP47f / MP42r	BglII / StuI fragment in pNDam
pCS2-GFP-Kuk-Δ353-404	-	pQE-H ₁₀ -GFP-Kuk cut with EcoRI / NheI and the 830bp fragment was cloned in pCS2-Δ353-404
pCS2-Kuk-Δ353-404	MP13f / MP12r	Deletion of sequence coding for aa 353-404 by PCR with MP13f / MP12r using pCS2-Kuk as a template. The primers insert a NdeI restriction site.
pCS2-Kuk-Δ453-473	MP4f / MP4r	Deletion of sequence coding for aa 453-473 by PCR with MP4f / MP4r using pCS2-Kuk as a template. The primers insert a EcoRV restriction site.
pCS2-GFP-NLS-C-term	MP45f / MP46r	PCR with MP45f/ MP46r (template pQE-H ₁₀ -GFP-NLS-C-term), EcoRI / XhoI fragment in pCS2
pCS2-GFP-NLS-CaaX	MP45f / MP46r	PCR with MP45f/ MP46r (template pQE-H ₁₀ -GFP-NLS-CaaX), EcoRI / XhoI fragment in pCS2

Plasmids constructed or provided by others	
pBI-F3	Provided by D. Görlich
pBI-F3-GFP-Kuk	Constructed by A. Frank
pCAGGS-Flpe-IRES-Puro	Provided by D. Görlich
pCS2-HA	Constructed by C. Wenzl
pCS2-HA-Kuk	Constructed by Y. Kussler-Schneider
pCS2-Kuk	Constructed by Y. Kussler-Schneider
pCS2-Kuk-C567S	Constructed by Y. Kussler-Schneider
pCS2-Kuk-ΔC328	Constructed by Y. Kussler-Schneider
pCS2-Kuk-cc+ΔN185	Constructed by J. Laumann
pCS2-Kuk-ΔN136	Constructed by Y. Kussler-Schneider
pCS2-Kuk-ΔN185	Constructed by J. Laumann
pCS2-Kuk-ΔN437	Constructed by Y. Kussler-Schneider
pLI-GCN4	Provided by B. Schwappach
pMPM-359 (His-FT subunit)	Provided by M. P. Mayer
pMPM-369 (GST-FT subunit)	Provided by M. P. Mayer
pNDamMyc	Provided by M. Fornerod
pNDamMyc-LaminDm0	Provided by M. Fornerod
pNDamMyc-LaminDm0ΔC	Provided by M. Fornerod
pQE80-H ₁₀ -ZZ	Provided by D. Görlich
pQE-H ₁₀ -ZZ-Kuk	Constructed by Y. Kussler-Schneider
pQE-H ₁₀ -ZZ-KukΔN185	Constructed by S. Lawo

2.2 Methods

2.2.1 Molecular cloning

All methods used for molecular cloning and recombinant DNA isolation were performed according to Sambrook and Russel, 2001.

2.2.2 Protein expression and purification

Expression of recombinant proteins in *E.coli* Rosetta(DE3)pLysS was induced with 0,1 mM IPTG for 4 h at 37°C (H₁₀-ZZ-Kuk and H₁₀-ZZ-KukΔN185, H₁₀-GFP-LaminDm0ΔN, H₁₀-GFP-NLS-C-termDm0 and H₁₀-GFP-NLS-CaaX), or 6 h at 18°C (H₁₀-zz-KukΔN437). Expression of FT was induced in MC1061 cells cotransformed with the plasmids pMPM359 and pMPM369 expressing the two subunits of the FT, by addition of L-Arabinose overnight at room temperature (RT). The cells were lysed in “His”-Lysis Buffer in the presence of Lysozyme (1 mg/ml), PMSF (1 mM) and DNase I by incubating on ice for 30 min, followed by passing 6 times through a microfluidizer. The lysate was cleared by centrifugation (two times, 20 min at 12.000 rpm). The proteins were purified by chromatography as described below, and stored at -80°C.

- H₁₀-ZZ-Kuk and H₁₀-ZZ-KukΔN185:

The proteins were purified from the cleared lysate by nickel chelate chromatography followed by ion-exchange chromatography. For storage, the buffer was changed to PBS using PD-10 desalting columns and 20% Glycerol was added prior to freezing.

- FT:

The protein was purified by nickel chelate chromatography. For storage the buffer was changed to FT freezing buffer.

- H₁₀-ZZ-KukΔN437, H₁₀-GFP-LaminDm0ΔN, H₁₀-GFP-NLS-C-term and H₁₀-GFP-NLS-CaaX:

The proteins were purified from the cleared lysate by nickel chelate chromatography. For storage, the buffer was changed to PBS using PD-10 desalting columns and 20% glycerol was added prior to freezing.

- Ras:

The purified protein was provided by M. P. Mayer.

- GFP:

The protein was purified by J. Paijo.

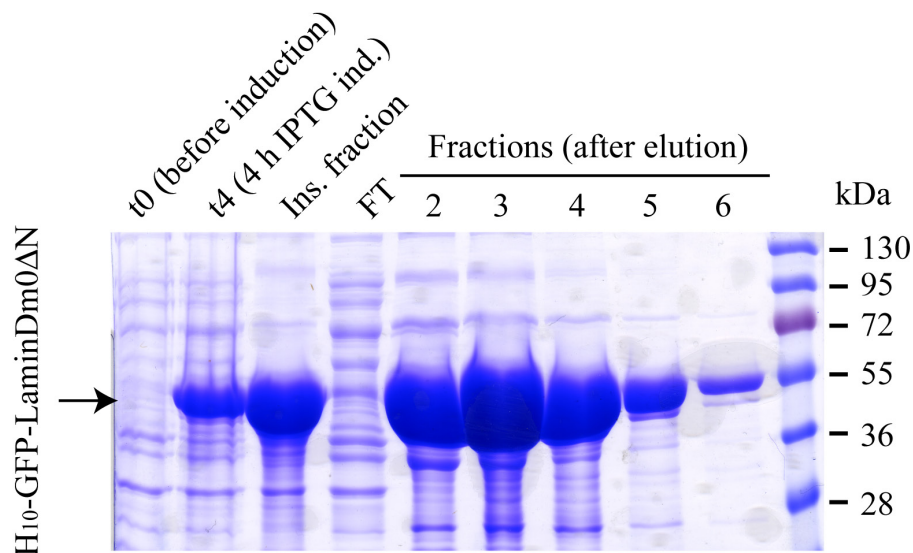


Figure 5: Purification of GFP-LaminDm0 Δ N shown as an example of protein purification. SDS-gel showing samples from the different steps of GFP-LaminDm0 Δ N purification. 4h after IPTG induction the band representing GFP-LaminDm0 Δ N is visible on the gel (second lane). A part of the protein remained in the insoluble fraction after clearing the lysate (third lane). Almost no protein is visible in the flow through (FT) sample (fourth lane), after binding to the His-Trap column. The protein was eluted from the column in five 1 ml fractions (fifth to ninth lane), which were pooled together and frozen after the buffer was exchanged to PBS.

2.2.3 Total RNA isolation and cDNA synthesis by RT-PCR

Total RNA was isolated from ten handpicked staged *Drosophila* embryos using 800 μ l TRIzol reagent and following the manufacturer's instructions. 20 μ g tRNA were added after homogenization in TRIzol. cDNA synthesis was performed using Transcriptor Reverse Transcriptase, Oligo-d(T) and 1 μ g of RNA as template in a final volume of 20 μ l. The cDNA was subsequently used as template for PCR.

2.2.4 PCR

PCR reactions were performed using Taq or Pfu DNA polymerase. For standard PCR reactions the following reagents were mixed: 50-200 ng DNA template, 0,4 μ M forward and reverse primers, 50 μ M dNTP (each), 10x PCR buffer (polymerase dependent), 1-2 units (per 50 μ l of reaction) Taq or Pfu polymerase. The reactions were performed under the following conditions:

Step 1 (initial denaturation): 95°C for 1 min

Step 2 (denaturation): 95°C for 30 sec

Step 3 (annealing): 50-60°C (depending on the annealing temperature of the respective oligos) for 1min

Step 4 (elongation): 72°C for 1min per kb to be amplified

Step 5: repetition of steps 2-4 for 30 times

Step 6 (final elongation): 72°C for 7 min

2.2.5 mRNA injections

Capped transcripts were synthesized using the SP6 mMACHINE high yield capped RNA transcription kit. Linearized plasmid (all constructs used were cloned in the pCS2 vector) was used as a template for the mRNA synthesis. 0-30 min old *kukΔ15* embryos were collected and dechorionated by treating with 50% bleach for 1 min. After washing with water, the embryos were aligned on a piece of apple juice agar, glued on a glass coverslip and dried for 9 min in a desiccating chamber. The embryos were covered by Halocarbon Oil 10s and injected with ~ 50-100 pl mRNA at their posterior part. After injection, they were incubated at 25°C for ~ 2,5 h, until developing to late cellularization stage. The embryos were removed from the coverslip by washing with heptane, fixed and immunostained. Injected embryos were not treated with methanol. The vitelline membrane was manually removed instead.

2.2.6 Immunostaining of *Drosophila* embryos

Embryos were dechorionated by incubating with 100% bleach until they detached from the apple juice agar plate and collected in a net which was subsequently placed in a glass vial containing 4 ml heptanes and 5 ml of 4% formaldehyde in PBS solution. The embryos were fixed for 30 min on a shaking platform. The fixation solution (lower aqueous phase) was then removed, 4 ml of methanol were added and the vial was vortexed until the embryos popped out of the vitelline membrane and fell on the bottom of the vial. The embryos were transferred in an eppendorf tube with a pasteur pipette and after washing two times with methanol and two times with PBS-T, they were blocked with 5% BSA in PBS-T for 45 min on a rotating wheel. They were then washed once with PBS-T and incubated for 2 h at RT or overnight at 4°C with the primary antibody solution. After incubation with the primary antibodies the embryos were washed 4x 15 min with PBS-T on a rotating wheel and incubated with the secondary antibodies for 2 h at RT. After washing 4x 15 min with PBS-T, DAPI (and Phalloidin, when required) staining was performed. The incubation times were 5 min for the DAPI staining and 20 min for the Phalloidin staining. Afterwards, the samples were briefly washed in PBS-T and mounted in Aquapoly mount on glass slides.

2.2.7 Mammalian cell culture

NIH-3T3 cells were maintained in DMEM supplemented with 10% FBS and 2mM L-Glutamine in a humidified incubator at 37 °C in the presence of 5% CO₂. HeLa cells were maintained under the same conditions, except that tetracycline-free FCS was used instead of FBS. For transient transfections, the cells were plated on glass coverslips at 50% confluency and transfected using Effectene according to the manufacturer's instructions. 24 h after transfection the cells were used

for immunostaining or western blotting. For immunostaining, the cells were fixed for 20 min, washed once with PBS, permeabilized for 10 min and washed once with PBS. After blocking for 30 min with 5% BSA in PBS-T, the coverslips were incubated o/n at 4 °C with the primary antibody solution. The next day the coverslips were washed twice in PBS and incubated for 2 h at RT with the secondary antibodies and DAPI. Finally the coverslips were washed twice in PBS and once in water and mounted on glass slides using Aquapolymount. For timelapse recordings, NIH-3T3 cells were transfected with pCS2-GFP-Kuk Δ 353-404 in 8-well chamber μ -slides. 24 h after transfection, prior to recording, the medium was changed to Leibovitz's L-15 medium supplemented with 10% FBS.

2.2.8 Generating the GFP-Kuk HeLa s/a cell line

Cells from the mother clone HeLa s/a (Weidenfeld *et al.*, 2009) were plated in a 6-well plate. The next day, when the cells were nearly confluent, they were transfected with 2 μ g of pCAGGS-Flpe-IRES-Puro and 2 μ g of targeting vector (pBI-F3-GFP-Kuk) using the Effectene transfection reagent. The molar ratio of plasmids was \sim 1:1. After o/n incubation the cells were transferred to a 10 cm dish and puromycin (5 μ g/ml) was added for the selection of cells transfected with the pCAGGS-Flpe plasmid. 36 h later the medium was changed and the cells were selected with Ganciclovir (10-50 μ M) for recombinants (loss of the HygTK-cassette). The medium was replaced by fresh selective medium every day for 1 week. After the 1 week long Ganciclovir selection, 10 clones were picked, amplified in selective medium and induced with Doxycycline (dox) at a concentration of 250 ng/ml in order to confirm GFP-Kuk expression. The protein expression was tested by western blotting and by immunofluorescence.

2.2.9 *Drosophila* cell culture

S2 *Drosophila* cells were maintained in Schneider's medium supplemented with 10% FBS, at 25°C. S2 cells were transfected using Effectene according to the manufacturer's instructions for suspension cells. 24 h after transfection the cells were seeded on poly-L-Lysine glass coverslips and immunostained. Kc167 *Drosophila* cells used for the DamID experiments were maintained in BPYE medium supplemented with 5% FCS, at 23,5°C. Kc167 cells used for DamID were transfected by electroporation. 20 μ g of the plasmid in the appropriate TE volume was placed in the electroporation cuvette and 800 μ l of cell suspension (\sim 6x10⁶ cells) were added. The cells were electroporated at 1000 μ F and 250V. 680 μ l of cells were added to a 10 cm dish (cells used for DamID) and 100 μ l of cells were added to one well of a 12 well plate (cells used for the immunofluorescence assay). When the cells were transferred from the cuvette to the dishes, it was

avoided to transfer the dead cells floating at the surface. 18 h after transfection, the cells used for the immunofluorescence assay were heat-shocked at 37°C for 2 h in order to induce expression of the Dam-fusion or Dam constructs. After heat-shock, the cells were incubated for 24 h at 23,5°C before being fixed and immunostained.

2.2.10 dsRNA synthesis and RNAi treatment of *Drosophila* cells

dsRNA was synthesized by *in vitro* transcription of a PCR generated template containing the T7 promoter sequence on both ends. The template was synthesized using the following reagents in 100 µl final volume: 1 µg fly genomic DNA (template), 0,4 µM forward and reverse primers, 50 µM dNTP (each), 10x PCR buffer for Taq polymerase (supplemented with MgCl₂), 4 units Taq polymerase. RNase free solutions and materials were used throughout the procedure. The reactions were performed under the following conditions:

Step 1: 95°C for 2 min

Step 2: 95°C for 30 sec

Step 3: 55°C for 1 min

Step 4: 72°C for 1 min 30 sec

Step 5: repetition of steps 2-4 for 6 times

Step 6: 95°C for 30 sec

Step 7: 55°C for 1 min

Step 8: 72°C for 40 sec

Step 9: repetition of steps 6-8 for 30 times

Step 10: 72°C for 7 min

The output of a 100 µl reaction was ~8 µg of PCR product. dsRNA synthesis was performed using the following reagents in 50 µl final volume (in DEPC treated sterile ddH₂O): 2 µg PCR product (template), CTP, ATP, GTP, UTP 7,5 µM each, 10x Transcription buffer for T7 polymerase (Roche), 2,5 units Pyrophosphatase, 4 units T7 RNA polymerase. The reactions were incubated at 37°C for 4 h, and the dsRNA was cleaned by Phenol/Chloroform extraction followed by EtOH precipitation. The output of a 50 µl reaction was ~250 µg of RNA.

RNAi treatment of cultured *Drosophila* cells was performed as previously described (Worby *et al.*, 2001). 5 d after RNAi treatment the cells were collected for immunostaining or western blotting.

2.2.11 Immunostaining of *Drosophila* cells

Drosophila (S2 or Kc167) cells were seeded on poly-L-lysine coated glass coverslips, left to settle for 15 min, washed once by briefly dipping the coverslip in PBS, fixed in 2% FA in PBS for 20 min, permeabilized in 0,5% NP-40 in PBS for 10 min, blocked in 5% BSA in PBS-T 0,1% and immunostained.

2.2.12 FTI treatment of cultured cells

NIH-3T3 cells were transiently transfected in medium supplemented with the FTI ABT-100 (Abbott laboratories) at a concentration of 6,25 µg/ml and were fixed and immunostained 24 h after transfection. HeLa s/a cells were incubated in dox containing medium supplemented with ABT-100 at a concentration of 6,25 µg/ml for the appropriate number of days depending on the experiment. S2 cells were incubated in medium supplemented with ABT-100 at a concentration of 6,25 µg/ml for 5 d.

2.2.13 Western Blotting

- Western Blotting (WB) using single embryos (WB shown in Figure 18): Single embryos of different genotypes at late cellularization stage were hand-picked, dechorionated in 100% bleach, transferred in an Eppendorf tube and lysed with a needle. 10 µl IP buffer and 10 µl 2x Lämmli buffer were added.
- WB using cultured cell lysates: Cells were harvested by pipetting (*Drosophila* cells) or scraped off (mammalian cells) and centrifuged at 2.000 rpm for 2 min. The medium was removed and 80 µl IP buffer was added to the cell pellet. The cells were lysed by pipetting and 20 µl 5x Lämmli buffer was added to the lysate. The equivalent of 10⁵ cells was loaded on an SDS-gel.

2.2.14 Collection of embryos with different number of maternally and zygotically provided copies of *kuk*

The crosses shown in Figure 17 were performed and staged 3-4 h old embryos were collected and immunostained. Embryos with one zygotically provided copy of *kuk* were distinguished by β-gal staining from the ones without any zygotically provided *kuk*. The nuclear morphology of the embryos of the different genotypes was analyzed by confocal microscopy.

2.2.15 Liposome assays

Liposomes were prepared from total bovine brain lipids (Folch fraction I, mainly consisting of Phosphatidylserine PS and Phosphatidylinositol PI) supplemented with 3% v/v Rhodamine-

Phosphatidylethanolamine (PE). 1 ml of lipid mixture (1 mg/ ml in chloroform) was dried under vacuum using a rotary evaporator and resuspended in 800 μ l HK Buffer supplemented with 10% sucrose. After homogenization by 10 freeze (by immersion in EtOH/ dry ice) -thaw (by immersion in a 37 °C waterbath) cycles, liposomes were prepared using a mini extruder and polycarbonate membranes (pore size, 100 nm). The lipid solution was subjected to 21 extrusions. The expected average size of the liposomes was 100 nm. For the liposome binding assay 30 μ l of liposomes were incubated with 400 μ l 4% BSA in HK Buffer for 30 min, spun at 15.000 g for 10 min (at RT) and protein, FT and farnesyl pyrophosphate (FPP) in 100 μ l HK-farnesylation buffer were added to the pellet. FPP was not added to the non farnesylated samples. After incubation for 3 h the samples were spun, the supernatant was collected and the pellet was washed twice with HK Buffer. Supernatant and pellet were used for SDS-PAGE. For analysis of liposome morphology, 10 μ l of liposomes were mixed with 2 μ g of protein, FT, FPP (FPP was only added to the farnesylated samples) and HK farnesylation buffer in a final volume of 20 μ l, incubated for 10 min and analyzed by fluorescence microscopy. The final protein concentrations in this mixture, referring to the situation where 1x protein amount was used are shown in Table 6. Liposomes were stored at 4 °C for not longer than 5 d and lipid stock solutions (in chloroform) were maintained at -20°C for maximum 5 months.

2.2.16 Yeast transformation

The AK725 yeast strain was grown in YPD medium at 30°C to an OD₆₀₀ of 0,5. 10 ml of culture were used per transformation aliquot. The cells were collected at 2000 rpm for 4 min, washed once with 1 ml sterile ddH₂O and once with 1 ml 100 mM Lithium Acetate/TE buffer and were finally resuspended in 50 μ l Lithium acetate/TE buffer. 50 μ g carrier salmon sperm DNA, 1 μ g of the appropriate pMM6 plasmid and 300 μ l Lithium acetate/TE/PEG buffer, were added to the cell suspension. The transformation mixture was incubated for 30 min at 30°C and subsequently heat shocked for 15 min at 42°C after addition of 35 μ l DMSO. After heat shock the cells were plated on SD glucose (-Leu) agar plates.

2.2.17 Inducible protein expression in yeast

AK725 cells transformed with pMM6-GFP-LaminDm0 Δ N or pMM6-GFP-Kuk were grown in synthetic dropout medium (-Leu) supplemented with 2% raffinose to mid-log phase and were induced by the addition of 2% galactose. 16 h later the cells were fixed in 4% FA, collected in 1,2 M sorbitol and mounted on poly-L-lysine coated slides.

2.2.18 Fractionation of nuclei

Apple juice agar plates with overnight (0-12 h old) *kuk* Δ 15 or *zz-Kuk* ; *kuk* Δ 15 embryos were heat shocked for 45 min at 37°C in order to induce *ZZ-Kuk* expression which is under the control of a heat shock promoter. The *kuk* Δ 15 embryos without the *zz-kuk* transgene were used as control. After the heat shock the embryos were incubated at 25°C for 30 min in order to recover from the heat shock. After recovery, the embryos were collected from the apple juice plate, dechorionated using 100% bleach and frozen in liquid nitrogen. For nuclear fractionation, 1 g of dechorionated *Drosophila* embryos were homogenized in 7 ml Buffer A and centrifuged at 4.000 rpm for 10 min. The supernatant (cytoplasmic fraction) was discarded and the pellet (nuclei) was gently resuspended in 7 ml Buffer A. The suspension was carefully placed on top of 14 ml Buffer B and centrifuged at 4.600 rpm for 10 min. The pellet (nuclei) was washed three times with Buffer C and used for IgG pull down of *ZZ-Kuk*.

2.2.19 IgG pull-down of *ZZ-Kuk*

Nuclei isolated as described in 2.2.19 were lysed by addition of 2 ml IP buffer and homogenizing in a Dounce homogenizer (not more than five strokes). The lysate was incubated for 15 min on a rotating wheel at 4°C and subsequently cleared by centrifugation at 15.000 rpm for 10 min. The cleared lysate was added to 15 μ l IgG beads, pre-equilibrated by washing three times with IP buffer. The mixture was incubated for 40 min on a rotating wheel at 4°C, centrifuged for 2 min at 2.000 rpm and the supernatant (unbound fraction) was collected. After washing two times with IP buffer, the proteins were eluted from the beads first with 2x 100 μ l 1M NaCl and then 2x 100 μ l 1,5 M MgCl₂. The eluates were TCA precipitated and resuspended in 30 μ l 2x Lämmli buffer. 50 μ l 2x Lämmli buffer was added to the beads and all samples were subjected to SDS-PAGE.

2.2.20 Silver staining of SDS-gels

The 5% to 17% gradient SDS gel was fixed for 30 min, washed twice with ddH₂O, incubated for 2,5 min in Farmer reducer solution, washed twice with ddH₂O and incubated for 30 min in silver solution. After washing 2x 30 sec with ddH₂O, the gel was equilibrated and developed until bands appeared. The developing was then stopped and the gel was stored in stop solution.

2.2.21 GFP pull down using GBP-beads in NIH-3T3 cell lysates

NIH-3T3 cells were cotransfected with pCS2-HA-Kuk and pCS2-GFP-BAF or pCS2-GFP (control plasmid) in 10 cm dishes and the cells were collected 24 h post transfection. After washing once with PBS (2.000 rpm 2 min), the cells were lysed in 1 ml IP buffer. GFP-fusion (or

GFP) protein pull down was performed using GFP binding protein (GBP) beads (GFP Nanotrap) as previously described (Rothbauer *et al.*, 2008).

2.2.22 Filter assay for testing the activity of recombinant farnesyltransferase

100 nM ^3H -FPP, 5 μM protein and 2 nM FT were mixed in HK farnesylation buffer and incubated for 1 h at 30 °C in a thermomixer. 0,4 ml of 1:10 HCl in EtOH solution was added to the reaction, and the samples were incubated for 1 h at RT. 0,4 ml EtOH was added to the mixture, which was subsequently transferred on filters and after addition of scintillation liquid the samples were counted for incorporation of the radioactive substrate using a scintillation counter.

2.2.23 Imaging

A Zeiss Axiovert 200 M PerkinElmer Ultra-View Spinning Disc confocal microscope (100 \times NA 1.4 oil) was used for timelapse recordings of NIH-3T3 cells and for imaging of yeast cells (flatfield capture mode). For timelapse recordings z-stacks of 7 images covering a distance of 8 μm were recorded and the layers were subsequently fused. Fluorescent images of immunostained embryos and Kc167 cells were obtained using a Leica confocal microscope (DMIRE2, HCX PL APO 63 \times NA 1.4 oil, laser at 405, 488, 568, 633 nm). Fluorescent images of liposomes, NIH-3T3 and S2 cells were obtained using a Zeiss Axioplan 2 (100x / 1.30 oil) (Carl Zeiss). Images were processed with ImageJ and Adobe Photoshop.

2.2.24 Electron Microscopy

Liposome samples were prepared the same way as for fluorescence microscopy and loaded on Pioloform/ carbon coated grids (100 mesh). The samples were negatively stained using 0.5 % Uranyl Acetate. EM data were obtained by A. Hellwig using a ZEISS EM 10 CR (Carl Zeiss). Measurements of tubule length were performed using the “measure” tool of ImageJ.

2.2.25 DamID

Kc167 *Drosophila* cells transfected with the appropriate pNDam-fusion construct or the pNDam control plasmid were collected 24 h after transfection, centrifuged and the pellet was frozen in liquid nitrogen, in aliquots of 10^7 cells. Genomic DNA (gDNA) was extracted from one cell pellet using the DNeasy Tissue kit according to the manufacturer’s protocol. 2,5 μg of gDNA were EtOH precipitated and digested with DpnI. Part of the DpnI digestion reaction was checked on an agarose gel. 1,25 μg of DpnI treated gDNA were used for ligation of the double stranded adaptor oligo (AdR) to the DpnI cleaved ends. (AdR was prepared by annealing the oligos Adt

[CTAATACGACTCACTATAGGGCAGCGTGGTCGCGGCCGAGGA, 5' not phosphorylated)] and Adb [TCCTCGGCCG, 5' not phosphorylated].) Digestion with DpnII followed in order to remove unmethylated GATCs and exclude them from PCR amplification. The methylated fragments were selectively amplified by PCR using the complementary to AdR oligo AdPCR, (GGTCGCGGCCGAGGATC) and Advantage cDNA PCR mix. The PCR products were cleaned using the QiaQuick PCR purification kit. 7 µg of PCR products were labeled and hybridized to GeneChip Drosophila Tiling 2.0R Arrays (Affymetrix). Labeling, hybridization and scanning of arrays were performed by the DNA Microarray Facility of the University of Göttingen. Analysis of microarray data was performed by M. Fornerod.

3. Results

3.1 The farnesylated nuclear proteins Kugelkern and Lamin Dm0 affect nuclear morphology by directly interacting with the nuclear membrane

3.1.1 The extra nuclear membrane structures formed upon Kuk overexpression show an asymmetric composition

Nuclei overexpressing Kuk or La Δ 50 are characterized by abnormal morphology, with intranuclear structures and NM blebs (Goldman *et al.*, 2004; Brandt *et al.*, 2006; Brandt *et al.*, 2008; Scaffidi and Misteli 2006). In fibroblasts expressing La Δ 50 the nuclear membrane protrusions contain La Δ 50 but not lamin B, showing a differential composition than the NM of the main body of the nucleus (Goldman *et al.*, 2004). Here, the composition of the extra membrane structures formed upon Kuk overexpression was examined in cultured cells and in the fly embryo. It has already been shown that increasing Kuk levels in the *Drosophila* embryo induce changes in nuclear morphology, in a dose dependent manner (Brandt *et al.*, 2008). In cellularizing embryos with six genomic copies of *kuk*, where the cortical nuclei show pronounced apical ruffling, an asymmetry was observed in the composition of the NM invaginations. While in these nuclei Kuk generally colocalized with lamin Dm0 at the nuclear envelope, the intranuclear membrane invaginations showed Kuk staining but much less if any lamin Dm0 staining (Figure 6A, arrows).

Similar asymmetry in the composition of the extra NM structures formed upon Kuk overexpression was also observed in cultured cells. Kuk affected nuclear shape in transiently transfected *Drosophila* S2 cells, as shown in Figure 6D. The bleb formed in the Kuk transfected cell shows less Nup50 staining than the NM of the main body of the nucleus. In Kuk transfected mouse fibroblasts, where no endogenous Kuk is present, formation of large and abnormal nuclei was observed as previously described (Brandt *et al.*, 2008). The nuclei of the transfected cells showed blebs and extensive intranuclear membrane structures (Figure 6B and C). Similarly as in the *6xkuk Drosophila* embryo, the blebs showed differential staining pattern, with less Lamin A/C (Figure 6B, arrows), and less nuclear pores (Figure 6C, mAb414) than the main body of the nucleus. In addition, the blebs generally contained less DNA, as shown by the DAPI staining (Figure 6C, DAPI).

The results obtained from overexpression of Kuk in the fly embryo and in cultured cells indicate that Kuk behaves similarly to La Δ 50, with respect to the formation of NM abnormalities of a defined composition that differs from the NM composition of the main body of the nucleus.

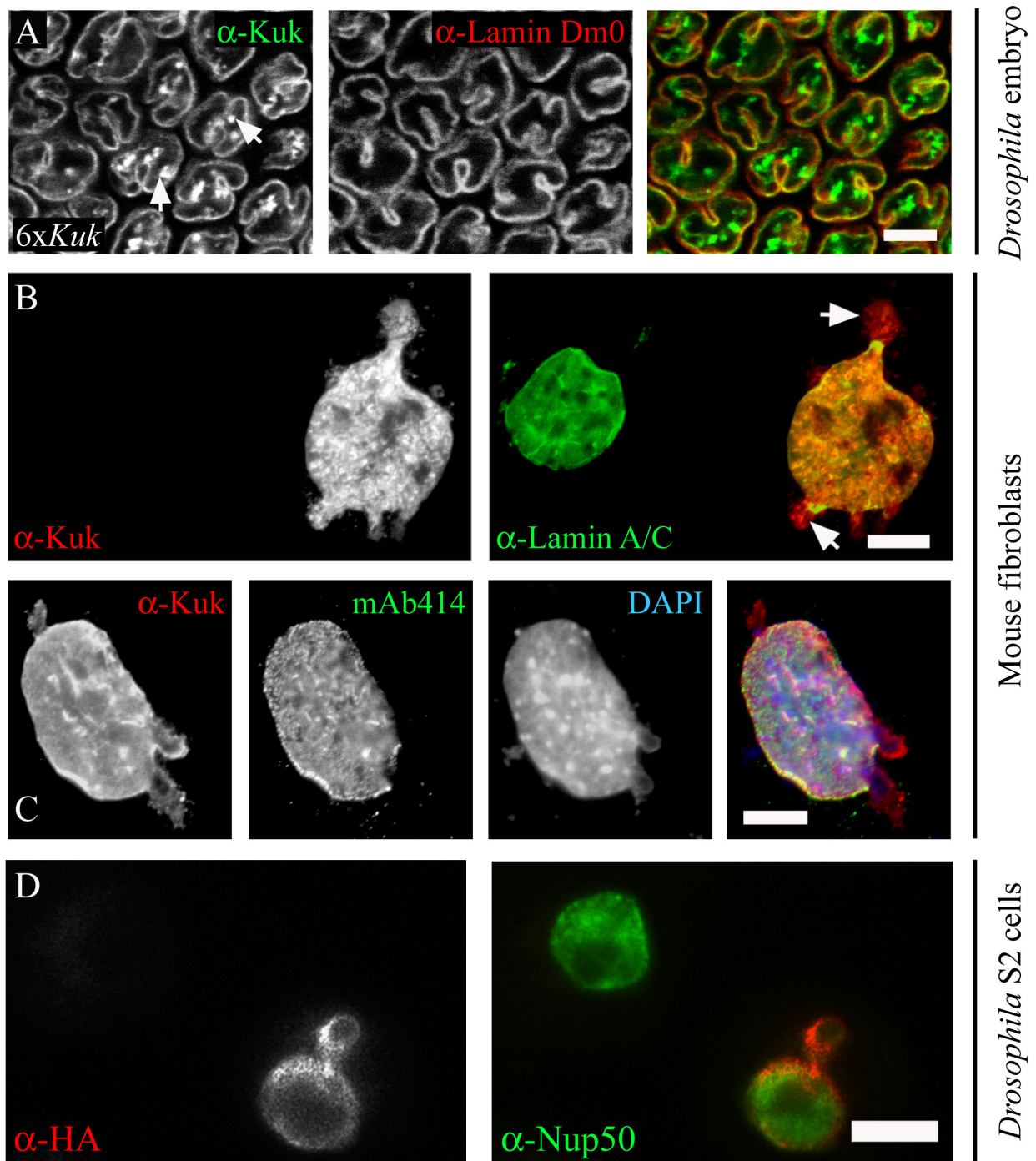


Figure 6: Asymmetric composition of the extra NM structures in Kuk overexpressing cells. A: Surface view of a *Drosophila* embryo with six genomic copies of *kuk*, in late cellularization. The differential staining of the intranuclear membrane structures is indicated by arrows. Lamin Dm0 (red) is used as a marker of the NM. Kuk staining is shown in green. Scale bar: 10 μ m. B-C: Nuclear morphology upon Kuk overexpression in NIH-3T3 cells. B: Nucleus of a transiently transfected NIH-3T3 cell expressing Kuk (red), compared to the nucleus of a non transfected cell. Lamin A/C (green) marks the NM. The differential staining of the NM blebs is indicated by arrows. C: A Kuk-transfected NIH-3T3 cell stained for Kuk (red), nuclear pores (green) and DNA (DAPI staining is shown in blue). Scale bar B-C: 5 μ m. D: Nucleus of a transiently transfected *Drosophila* S2 cell expressing HA-Kuk (red), compared to the nucleus of a non transfected cell. Nup50 (green) marks the nucleoplasm and the NPCs on the NM. Scale bar: 5 μ m.

3.1.2 The nuclear membrane blebs formed upon Kuk overexpression are highly dynamic

Since the NM blebs formed upon Kuk overexpression were found to show a differential composition, the dynamics of these blebs were analyzed by timelapse movies of transiently transfected mouse fibroblasts. When GFP-Kuk and GFP-Kuk- Δ 353-404 (Kuk deletion construct, described in Figure 10) were compared in NIH-3T3 cells, they showed similar behavior. Due to the higher frequency of blebbed nuclei that was observed in GFP-Kuk- Δ 353-404 transfected cells, this construct was chosen for the timelapse experiments. In GFP-Kuk- Δ 353-404 transfected fibroblasts, a differential behavior was observed for the blebs and the intranuclear structures (Figure 7). While the intranuclear structures were found to be quite stable, as previously shown using cells expressing GFP tagged lamin A variants (Broers *et al.*, 1999) and remained unchanged throughout the 94 min of timelapse recording, the nuclear blebs were found to be highly dynamic, forming and disappearing fast, within a few minutes (Figure 7, arrows). Therefore, the nuclear blebs do not differ from the intranuclear membrane structures only in respect to their NM composition, but also in their dynamic behavior during interphase.

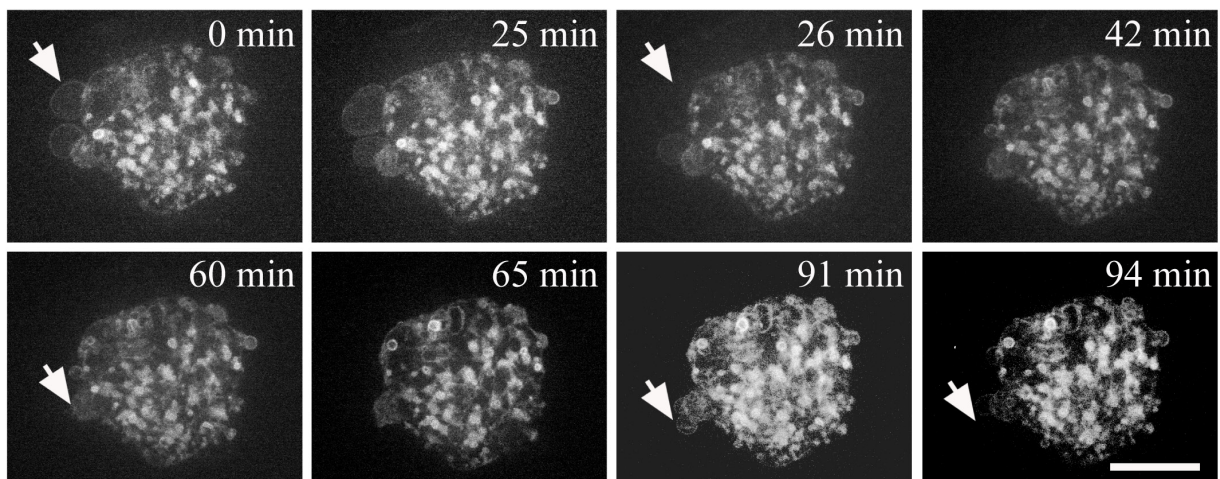


Figure 7: Dynamics of the blebs and intranuclear structures in transiently transfected NIH-3T3 cells. The figure was assembled from selected timepoints of a timelapse movie, showing a NIH-3T3 cell transiently transfected with GFP-Kuk- Δ 353-404. The NM blebs formed upon GFP-Kuk- Δ 353-404 expression show a very dynamic behavior. Arrows indicate examples of blebs growing and disappearing. Scale bar: 7 μ m.

3.1.3 Kuk and lamin Dm0 constructs used in the study

In this work, a number of Kuk and lamin Dm0 constructs (shown in Figure 10) were used in different *in vivo* and *in vitro* assays. The Kuk constructs were designed in order to provide information concerning the function of the different Kuk domains. Kuk-C567S serves as a non farnesylatable control construct. Kuk- Δ N185 lacks the putative coiled coil motif of Kuk (aa 137-185). In order to gain further insight in the role of the putative coiled coil motif of Kuk, the coiled coil motif of the GCN4 leucine zipper (Harbury *et al.*, 1993; Yuan *et al.*, 2003) was added

<i>A.aegypti</i>	-----MSLQVSSQPTSGRRTPQIYQNLG--STTPATTPPTNGNSG	40
<i>A.gambiae</i>	-----MSLQVSNQTTSGRRTPQVYQGFNMPAGAATTPATNGSG	40
<i>D.melanogaster</i>	MLSKMASNTSGGGTTSQGTGTGRRRLPLSLSG--GSTVTRLQOQSS--GSN	45
<i>D.grimshawi</i>	---MAQNTVGGGGSGSAAAGRRVPLSLSGAGAGSSLARLQOAAAAAGSN	47
	. . . * * * . . . : . . . : *	
<i>A.aegypti</i>	KSAS-----KLSLKS-----KQSPVVEH	60
<i>A.gambiae</i>	TTGAGGSGRAAKGGGAKQSQIPVAIGSGGGFGTPGNDGTVPQTAVVYPG	90
<i>D.melanogaster</i>	GRSNPQN--GNKKITES--FLPVKKS-----NQPRTTSTG	77
<i>D.grimshawi</i>	GRSKSPQKKNETNIANSQPFVVVKKSSS-----NQHRISAS	85
	. : . : *	
<i>A.aegypti</i>	TTEPTTP----KDVHKTTTNVAVAVTKLE-----KTPTGAASS	94
<i>A.gambiae</i>	TAGATDG----SSGQKQVQSDHMYGMKQ-----QQQQPAASA	124
<i>D.melanogaster</i>	STGSSQNGVSKPTNGKDKSQNGSSTGKDQKVEKSKDKLPEKKAKEVGAEN	127
<i>D.grimshawi</i>	SSSSSSS----KDDDKKTQNGVS-----KSSSHGNSK	113
	:: :	
	Predicted Coiled coil motif	
<i>A.aegypti</i>	PSKTDKGKEEKKAASNGASNGTHSEKETNGKQ--ETPKAASETPKKDQ	142
<i>A.gambiae</i>	NSATNRSATNGSOLAAVEKNGTSORKNSTGSGAKKTETAAASOQOQOQ	174
<i>D.melanogaster</i>	KDKDGAEMTDMEVVVENKQKEVVSENKQNEVVSENKEVVSENKEVVSEN	177
<i>D.grimshawi</i>	AAQNGSSSIP--VAVVVKEQOK---SKEKQS---AEKKEASLEA--AAAA	154
 : : :	
<i>A.aegypti</i>	AEKVAKESPRASPRSTPQKQ-QAESIPVEQVKTPESTSKTKESPMVTPV	191
<i>A.gambiae</i>	QPSVPAEAGTAKVRDPSRSSGRAQKQKQVVEEAGPANKTMTSQPKSE-K	223
<i>D.melanogaster</i>	KEVASEKVVVAEVPSDKDDNGETKKDDATVESTAPASQTPADAAVIID	227
<i>D.grimshawi</i>	DEAKPAKKEITEITQPTAGDNKTEAVADADAIAAVSDNELKNESAVVVPA	204
	. . . : :	
<i>A.aegypti</i>	AAKVDEPKANEKAVKACPAEGDEMESLVVEPSEYEDSPMPPTGGKTKLL	241
<i>A.gambiae</i>	TTNLESSLLTEKTLKGFSSDGEEMESLLELPWDMEEGATPSRSSAAKSK	273
<i>D.melanogaster</i>	VVFIPDLSTPTKDRKSTRKSGSQKQSP--ISKASNASPVQIKTEAVSSST	276
<i>D.grimshawi</i>	TS----STPTAERKSSRRSATQOKSPGKQPQSKESVQTKQETETLQAA	250
	. . . * . . . : *	
<i>A.aegypti</i>	KYSGAPPTRARISPFVRK-----ETTANASTIVNLSTVS	275
<i>A.gambiae</i>	MPKAAPQAQARVSPFKASGKTQPKPSSGTATAEPEQTAGSPNKKAAAA	323
<i>D.melanogaster</i>	SGSLTPQEDVDMEPLQVDASPIRSVHGN---LNAVPTATSTPGRSLFSFR	323
<i>D.grimshawi</i>	A-----VEDVEMEPLTVDASPIRSVAS-----SAQPTATSTPGRNLFQ	290
	. . . * : * * : .	
<i>A.aegypti</i>	EGQDSGSKDTSLSDSQVPA--LGV---RPLRAISGRRGMRPITDIQ-	318
<i>A.gambiae</i>	AAGDESEKNRSKVDAPSTPT--AGESLIGRPLRSISGRRSTRPISDIK-	370
<i>D.melanogaster</i>	GSN-KQSTEVELAAQTSSSPAGTP----ARTFAQISGRRSIRPIDSLTP	367
<i>D.grimshawi</i>	SSVSKQANEVELTSQQSISPAVAV----ARNFSQISGRRSIRPAAIQTP	335
	. . . : . . . : * : * : * * * * . * *	
<i>A.aegypti</i>	-----FTYRKSTELN---DSASSLNVTVGSEIHNDSLRTPAPG-STRKRK	359
<i>A.gambiae</i>	-----FTHPRRSTADPHNDSISSMNVTVGSEIGSDSMLLRTPGSATRKRK	415
<i>D.melanogaster</i>	SKIGTYRCGN--SDLDTNCTNASMNATVGSEIPNSSSFSFSFFGRGRKRE	416
<i>D.grimshawi</i>	GRMGNRYRCLNTELDTSQNTSMNATVGSEIPNSSSFSFSFFGRGRKRE	385
	. : . : : : : *	
	NLS	
<i>A.aegypti</i>	AMTP----ESTSDALDVKEIVDSPKRRLDFSGFLGIVASPVMTMLKNRSL	405
<i>A.gambiae</i>	DMTP----ESTSD---EPVIDSPKRARLDFSGFLGMVATPVMTMLKNRSL	457
<i>D.melanogaster</i>	RTPPPLTASQSTSDLGHDVMSHPKRARFDLFSLN--LASPFSLRSRFS	464
<i>D.grimshawi</i>	RTPPPLSGSQSANDLAQDVEMSHPKRARFELFSMS--LASPFSLRSRFS	433
	. * *	
<i>A.aegypti</i>	RVRLQSSTPVAKRSFDEEDPTKCVQAEATTTTANISGE-----GAKMDVD	450
<i>A.gambiae</i>	RVKLQSTP--RALAVDEEDASKVVTAEATTTTASVTPQKEADGAGAMDVD	505
<i>D.melanogaster</i>	KATIGTP---TRLRLEPNS--SGVEEQHLNLTSTGVPEEVDVEEQP----	506
<i>D.grimshawi</i>	KATISTPS--SRKQLDQTPPTGDDEEDGGVGVQNVSGIIIQEEDDQLNR	481
	:: : : :	
<i>A.aegypti</i>	PAADATNDKVVEVEK--AKGDTEGQTTDLPSEEDASKVVEGSGDASESPV	498
<i>A.gambiae</i>	VVAGKGAEKSDDATAPVADGQKEGAEGQQQQQESSSSVAED--DEVEVKI	554
<i>D.melanogaster</i>	----AEDVTVGQEAQAEIIPAKKDVEDKNVNGQDGDKESSDGENIDPVV	551
<i>D.grimshawi</i>	SASNSEDVTVAKEAG--LETPKKCGTTPKEQNGEQNKKKVGDDEEQAE---	527
	. : . : . : . : . : . : . : . : . : . : . : . : . : . : . : . : . : . : .	
<i>A.aegypti</i>	EVKDVS----NKRFQCVVM	513
<i>A.gambiae</i>	VTDQPQ----QPKQWCSIM	569
<i>D.melanogaster</i>	EVADVAVAEAGRSICSIM	570
<i>D.grimshawi</i>	-----	

Figure 8: Sequence alignment of Kuk with homologous sequences from *A.aegypti*, *A.gambiae* and *D.grimshawi*.

The coiled coil motif of Kuk and the NLS of Kuk and the respective sequences from the other species are shown in the black boxes. The red box indicates the CaaX box (not present in the *D.grimshawi* sequence). In the light blue boxes are shown the two sequences (aa 353-404 and aa 453-473) that were found to be more conserved in comparison to the rest of the protein sequence. Stars indicate identical aa, two dots indicate conserved aa substitutions and one dot indicates semi conserved aa substitutions. The sequence alignment was performed using ClustaIW2 (Larkin *et al.*, 2007).

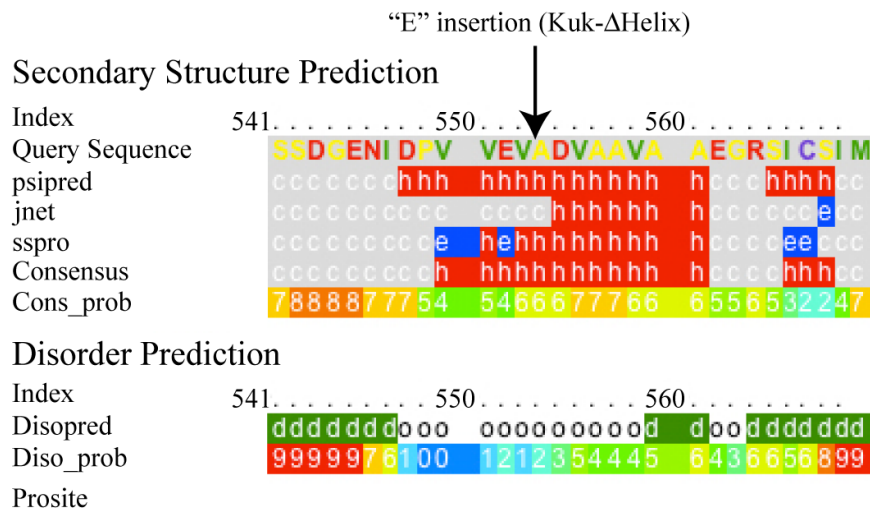


Figure 9: An α -helix is located at the C-terminus of Kuk, as predicted by PHYRE.

The PHYRE automatic fold recognition server predicted a helical structure in the C-terminal part of Kuk (aa 548-561). Red horizontal bars indicate predicted α -helices. The colored numbers in the “Cons_prob” line indicate the confidence of the prediction at each position from 0 (low) to 9 (high). In Kuk- Δ Helix an E was inserted before aa 554, in order to disturb the formation of the helix.

to Kuk- Δ N185 and the Kuk-cc+ Δ N185 construct was generated. Kuk- Δ 353-404 and Kuk- Δ 453-473, lacking the two amino acid sequences that were found to show the highest degree of conservation by alignment of sequences from different mosquito and *Drosophila* species (Figure 8), were generated in order to examine the role of the two motifs. An in silico analysis of Kuk using the Protein Homology/AnalogY Recognition Engine (PHYRE) (Kelley and Sternberg, 2009), shown in Figure 9, predicted the formation of a small α -helix in the C-terminal part of Kuk (aa 548-561). In Kuk- Δ Helix the helix was destroyed by insertion of a “helix breaker” Glutamate (E), before aa 554. The construct was generated in order to test whether this predicted structured domain plays a role for the activity of Kuk. Kuk- Δ C328 lacking the C-terminal part including the NLS and Kuk- Δ N136 lacking the N-terminal part until the coiled coil motif were used as control constructs.

For lamin Dm0, apart from the full length construct, the truncated LaminDm0 Δ N construct that lacks the N-terminal part including the filament forming rod domain was used in order to focus on the function of the C-terminal farnesylated globular part of the protein. Similar lamin constructs, containing only the globular C-terminal part, have already been shown to be able to affect nuclear shape (Prüfert *et al.*, 2004; Ralle *et al.*, 2004). Additional constructs used were the short GFP-NLS-C-term construct in which the globular domain of the C-terminal part of lamin Dm0 has been removed and the GFP-NLS-CaaX construct, in which the NLS and the CaaX motif of lamin Dm0 have been fused to GFP.

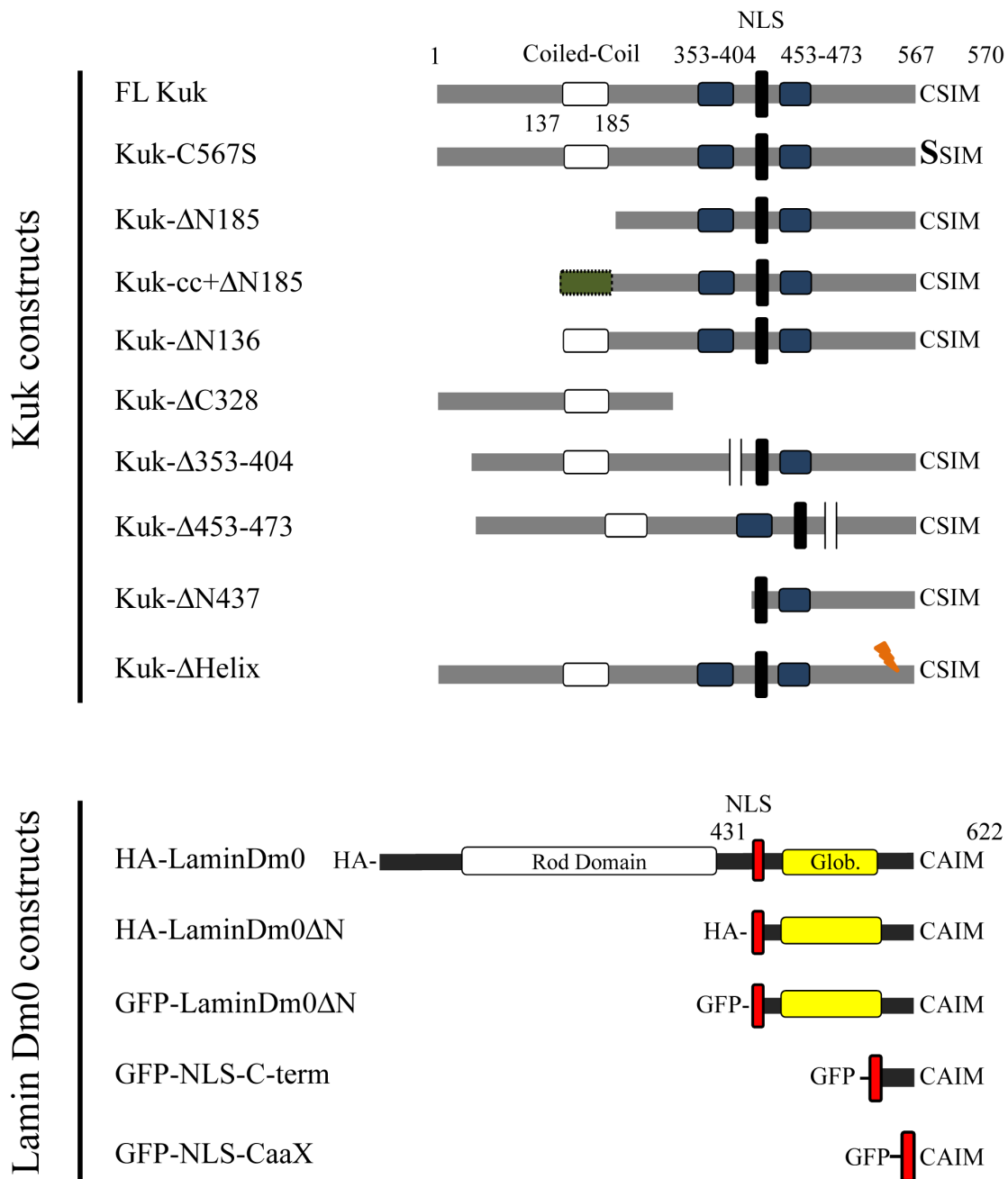


Figure 10: Constructs used in this study.

The structure of Kuk and lamin Dm0 constructs used in this study is schematically shown. The putative coiled coil motif of Kuk (aa 137-185) is shown in white. The two conserved aa sequences 353-404 and 453-473 are shown in blue and the NLS in black. In Kuk-C567S, the C of the CaaX motif has been changed to S. In Kuk- Δ N185, the putative coiled coil motif of Kuk has been deleted. In Kuk-cc+ Δ N185 the coiled coil of the GCN4 leucine zipper protein (Harbury *et al.*, 1993) that has been added to Kuk- Δ N185 is shown in green. In Kuk- Δ Helix, the predicted C-terminal helix has been destroyed (see Figure 9). In the lamin Dm0 constructs the NLS is shown in red, the rod domain in white and the C-terminal globular domain in yellow. In LaminDm0 Δ N the N-terminal part consisting of aa 1-430 including the rod domain has been deleted. HA-LaminDm0 Δ N was used for the transient transfections and GFP-LaminDm0 Δ N recombinant protein was used in the biochemical assays. GFP-NLS-C-term contains the NLS of lamin Dm0 fused to the very C-terminal part of the protein (aa 570-622). GFP-NLS-CaaX consists of GFP fused to the NLS of lamin Dm0 followed by the CaaX motif of lamin Dm0.

3.1.4 Expression of Kuk and lamin Dm0 constructs in mouse fibroblasts

Kuk and lamin Dm0 constructs used in the different *in vivo* and *in vitro* assays described in this work, were first transiently transfected in mouse fibroblasts in order to be tested for their localization and their activity on nuclear shape. The expression of the constructs was under the control of a CMV promoter. The results obtained for all Kuk constructs are shown in Figure 11 and summarized in Table 4. FL-Kuk localized at the NM, and induced formation of abnormally shaped nuclei (Figure 11A). The non-farnesylatable C567S mutant remained nucleoplasmic and did not alter nuclear shape (Figure 11B). Kuk- Δ N185, lacking the coiled coil, localized in intranuclear punctate structures and had no activity on nuclear shape (Figure 11C). In Kuk-cc+ Δ N185, the substitution of the deleted coiled coil restored the NM localization but not the activity of the protein (Figure 11D). This indicates that the properties of the endogenous Kuk coiled coil are required for its activity on nuclear shape and cannot be substituted by the coiled coil of GCN4. Kuk- Δ C328 did not have any effect on nuclear morphology, and showed cytoplasmic localization but without being completely excluded from the nucleus (Figure 11F). The partial import of Kuk in the nucleus can either be explained by the two additional predicted NLSs (aa 116-122 and aa 237-243), still present in the Kuk- Δ C328 construct or by the fact that its 39 kDa MW is in the range of the permeability barrier of the nuclear pore. Kuk- Δ N437 formed punctate cytoplasmic structures (Figure 11I). In order to examine whether the construct is retained in the ER, a co-staining with the ER marker Hsp47 was performed. The Kuk- Δ N437 structures did not show colocalization with the ER marker (Figure 12), with the exception of a small number of dots (Figure 12, arrows). Kuk- Δ N136, Kuk- Δ 453-473, Kuk- Δ 353-404 and Kuk- Δ Helix all showed the same behavior as FL-Kuk, concerning both their NM localization and activity on nuclear shape (Figure 11E, G, H and J). Blebbed nuclei appeared at high frequency in Kuk- Δ 353-404 transfected cells, therefore the construct was chosen for studying the dynamics of the blebs in timelapse movies (Figure 7). The fact that Kuk localization and activity on nuclear shape is not impaired by the deletion of the aa sequences 353-404 and 453-473 indicated that the two motifs are not required for the activity of Kuk in mouse fibroblasts under overexpression conditions. Concerning the activity of the Kuk- Δ Helix construct, there are several explanations. The first explanation could be that the C-terminal predicted helix is not required for Kuk localization and activity on the NM. Nevertheless, since the existence of the helix is not supported by structural data but is only based on the prediction of the *in silico* analysis, it is not certain whether the structure is really present in the protein. Another complication is that even if Kuk contains the predicted helix, one cannot simply assume that the glutamate insertion disturbed the structure. The helix might still be formed despite the aa insertion. Therefore the

data obtained using fibroblasts transfected with the Kuk- Δ Helix construct do not provide conclusive results.

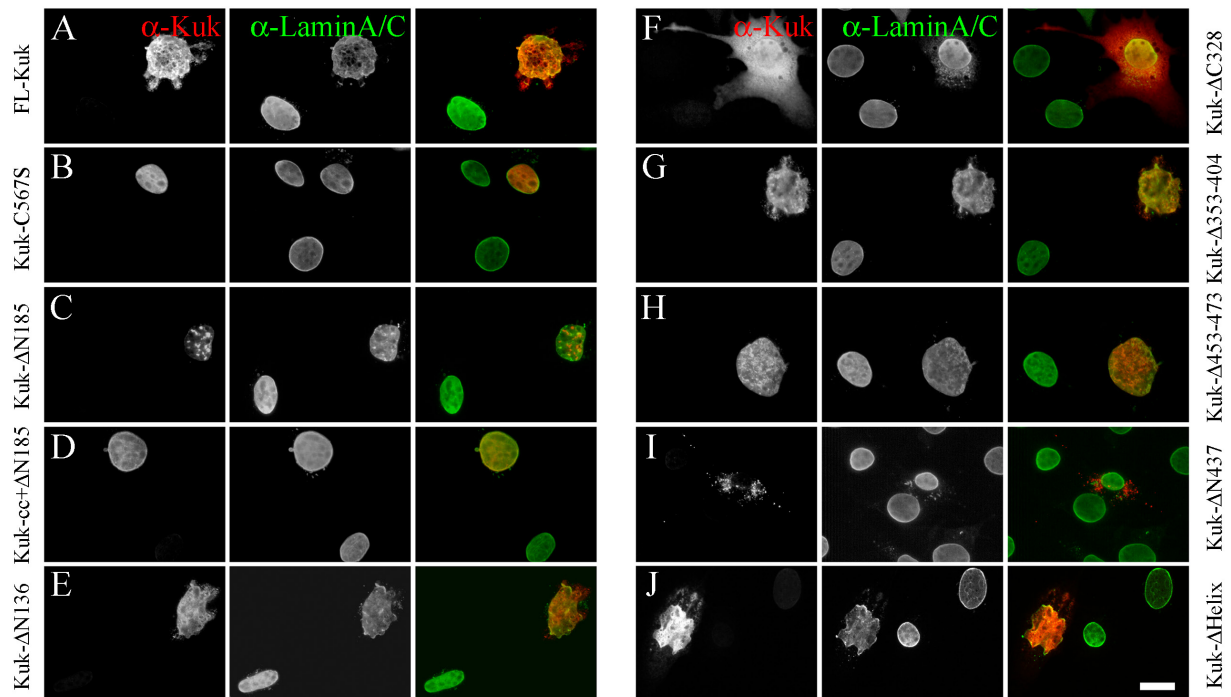


Figure 11: Localization and activity on nuclear shape of Kuk constructs in NIH-3T3 cells. NIH-3T3 cells, transiently transfected with: FL-Kuk (A), Kuk-C567S (B), Kuk- Δ N185 (C), Kuk-cc+ Δ N185 (D), Kuk- Δ N136 (E), Kuk- Δ C328 (F), Kuk- Δ 353-404 (G), Kuk- Δ 453-473 (H), Kuk- Δ N437 (I) and Kuk- Δ Helix (J). Lamin A/C staining in green is used as a marker of the NM and Kuk staining is shown in red. Scale bar: 10 μ m.

Table 4: Summary of the structure-function analysis of Kuk in mouse fibroblasts.

	NM Localization	Activity on nuclear shape
FL- Kuk	+	+
Kuk-C567S	-	-
Kuk- Δ N185	-	-
Kuk-cc+ Δ N185	+	-
Kuk- Δ N136	+	+
Kuk- Δ C328	-	-
Kuk- Δ 353-404	+	+
Kuk- Δ 453-473	+	+
Kuk- Δ N437	-	-
Kuk- Δ Helix	+	+

To sum up, the results from the transient transfection of Kuk constructs in NIH-3T3 cells, confirm that both the coiled coil motif and the CaaX motif of Kuk are required for NM

localization and activity on nuclear shape as previously shown by Brandt *et al.*, 2006. Furthermore it was shown that deletion of the two conserved aa sequences 353-404 and 453-473 did not change the behavior of Kuk in mouse fibroblasts.

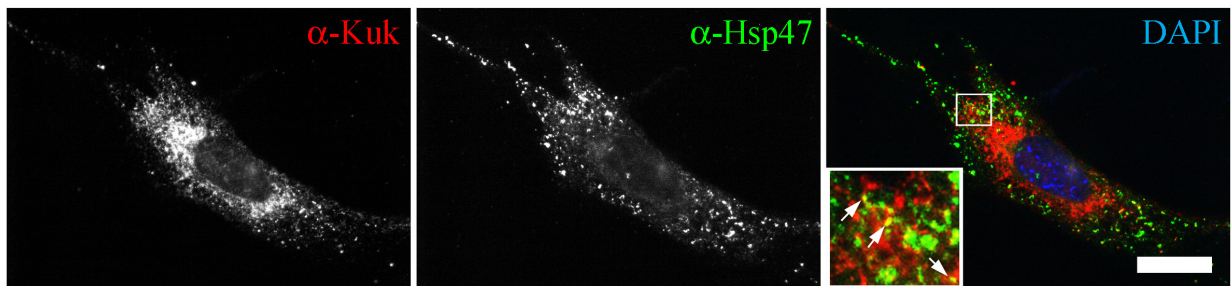


Figure 12: Kuk- Δ N437 structures do not colocalize with the ER marker Hsp47. NIH-3T3 cell, transiently transfected with Kuk- Δ N437. Kuk staining is shown in red and staining for the ER marker Hsp47 in green. DAPI staining (in blue) marks the nucleus. In the right panel, the area in the white square is shown magnified and the arrows indicate dots of colocalization of Kuk and the Hsp47 (yellow). Scale bar: 10 μ m.

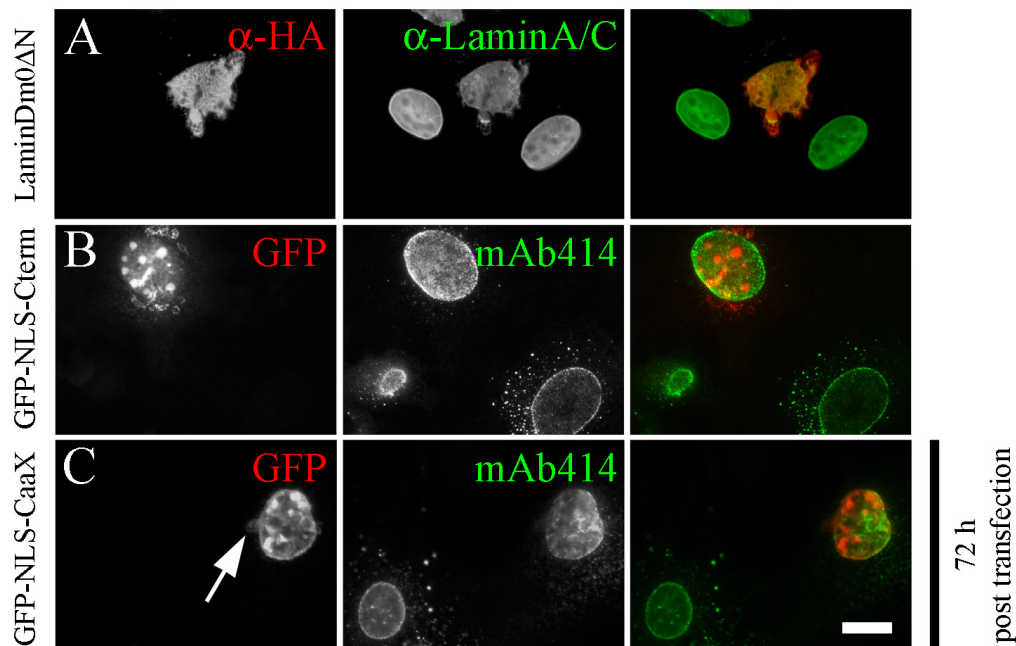


Figure 13: Localization and activity on nuclear shape of lamin Dm0 constructs in NIH-3T3 cells. NIH-3T3 cells, transiently transfected with: LaminDm0 Δ N (A), GFP-NLS-C-term (B) and GFP-NLS-CaaX (C). Lamin A/C (in green) is used as a marker of the NM. The transfected cells are marked by HA (A) or GFP (B,C), shown in red. The arrow in C indicates a NM bleb. Scale bar: 10 μ m.

The lamin Dm0 constructs used in yeast and in the biochemical assays were also transfected in NIH-3T3 cells in order to test their activity on nuclear shape. HA-LaminDm0 Δ N showed NM localization and induced abnormal nuclear shapes in the transfected cells (Figure 13A). The result is in agreement with previous studies, where the globular domain of lamins was shown to be sufficient to induce nuclear membrane overproliferation in cultured cells (Prüfert *et al.*, 2004; Ralle *et al.*, 2004). GFP-NLS-C-term also localized at the NM and affected nuclear shape

(Figure 13B). The construct was less active than HA-LaminDm0 Δ N, since the number of nuclei with abnormal shapes was lower than when HA-LaminDm0 Δ N was used. This indicates that the globular part of lamin Dm0 that is still present in HA-LaminDm0 Δ N, might contribute to the activity of the protein on nuclear shape. GFP-NLS-CaaX was targeted to the NM and showed activity on nuclear shape (Figure 13C), in agreement to the results of Ralle et al., 2004, where a construct with similar structure to GFP-NLS-CaaX, was shown to induce formation of intranuclear membrane structures in HeLa cells. Nevertheless, the GFP-NLS-CaaX construct used in the present study, showed the lowest activity on nuclear shape among all the constructs used. Abnormal nuclei were only observed 72 h post transfection (as indicated in Figure 13C), while for all other lamin Dm0 and Kuk constructs, 24 h were sufficient for inducing nuclear shape abnormalities.

3.1.5 Structure-function analysis of Kuk in the cellularizing *Drosophila* embryo

Information concerning the role of the coiled coil and CaaX motif of Kuk was obtained from experiments in A6 cells (Brandt *et al.*, 2006) and in NIH-3T3 cells (this study), two systems in which the developmental function of Kuk cannot be addressed. In order to identify the role of the different Kuk domains concerning the function of Kuk during cellularization, an mRNA injection assay was employed in the early fly embryo. mRNA from different Kuk constructs was injected into *kuk* deficient embryos. The role of the putative coiled coil motif, the CaaX box and the two conserved aa sequences 353-404 and 453-473 were examined using this assay. Early blastoderm stage embryos were injected with mRNA in their posterior part and the nuclear morphology at late cellularization stage was compared to wt nuclei (Figure 14B). The different constructs were tested for NM localization and for their ability to induce and maintain nuclear elongation and apical ruffling (rescue of the Kuk phenotype, shown in Figure 14A).

The results of the injection experiments are shown in Figure 15 and are summarized in Table 5. FL-Kuk localized to the NM, rescued the Kuk phenotype and induced apical ruffling of the nuclei (Fig. 15A, A', Table 5), while a differential staining of the extra membrane structures was observed (Fig. 15A') like in the *6xkuk* embryos (Figure 6A). Kuk- Δ C328, similarly as in mouse fibroblasts, was found to be uniformly distributed between the cytoplasm and the nucleoplasm (Figure 15B) due to the lack of the main NLS, and not functional (Figure 15B'). The non-farnesylatable Kuk-C567S mutant showed nucleoplasmic localization and was unable to restore nuclear elongation or induce apical ruffling (Figure 15C, C', Table 5). Kuk- Δ N185 accumulated in the nucleoplasm where it formed punctate structures (Figure 15D) and showed no activity on nuclear shape (Figure 15D', Table 5). Kuk-cc+ Δ N185 was able to localize at the NM but could

not rescue the mutant phenotype (Figure 15E, E', Table 5). In agreement to what was observed for Kuk-cc+ Δ N185 in mouse fibroblasts, the behavior of the construct in the embryo indicates that the endogenous coiled coil motif of Kuk is necessary for its activity on nuclear shape.

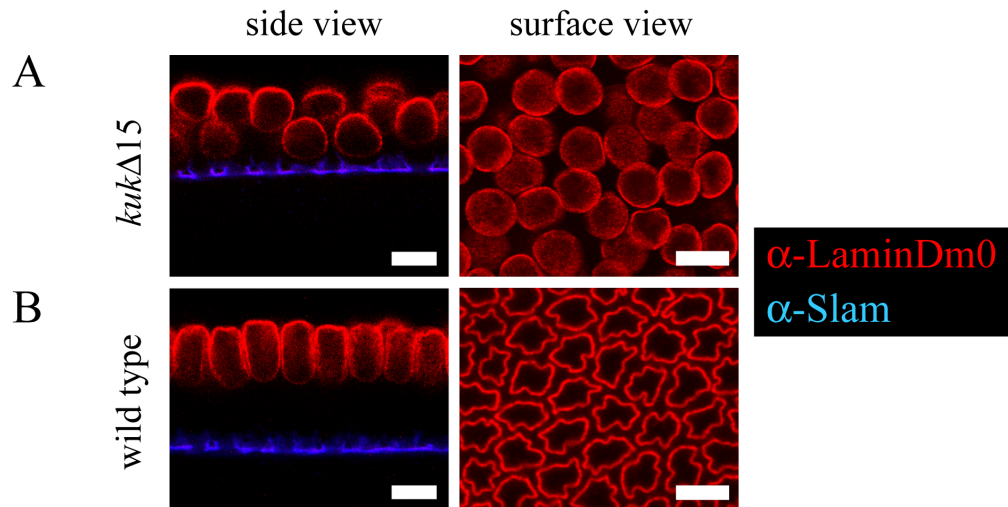


Figure 14: Nuclear morphology in the *kukΔ15* embryo and the wt embryo in late cellularization. Side view of a *kukΔ15* (A) and a wt *Drosophila* embryo (B) in late cellularization. Lamin Dm0 (red) marks the NM and Slam (blue) marks the invaginating membrane. Scale bar: 10 μ m.

Kuk- Δ 453-473 showed the same localization and activity as FL-Kuk (Figure 15G, G', Table 5), indicating that this conserved region is not required for Kuk function. On the other hand when Kuk- Δ 353-404 was injected, even though it localized at the NM and induced nuclear membrane ruffling (Figure 15F'), it was unable to rescue the mutant phenotype (Figure 15F, Table 5). This suggests that the domain is specifically required for nuclear elongation. The construct induced formation of intranuclear structures (Figure 15F'), similar to the ones observed upon Kuk overexpression and also nuclear membrane blebs (Figure 16, arrows). Such blebs were never observed upon injection of FL-Kuk or in 6x *kuk* embryos (Figure 6A).

Table 5: Summary of the structure-function analysis of Kuk in the fly embryo.

	NM Localization	Activity on nuclear shape (apical ruffling)	Rescue of the <i>kuk</i> phenotype (nuclear elongation)
FL- Kuk	+	+	+
Kuk- Δ C328	-	-	-
Kuk-C567S	-	-	-
Kuk- Δ N185	-	-	-
Kuk-cc+ Δ N185	+	-	-
Kuk- Δ 353-404	+	+	-
Kuk- Δ 453-473	+	+	+
HA-LaminDm0	+	-	-

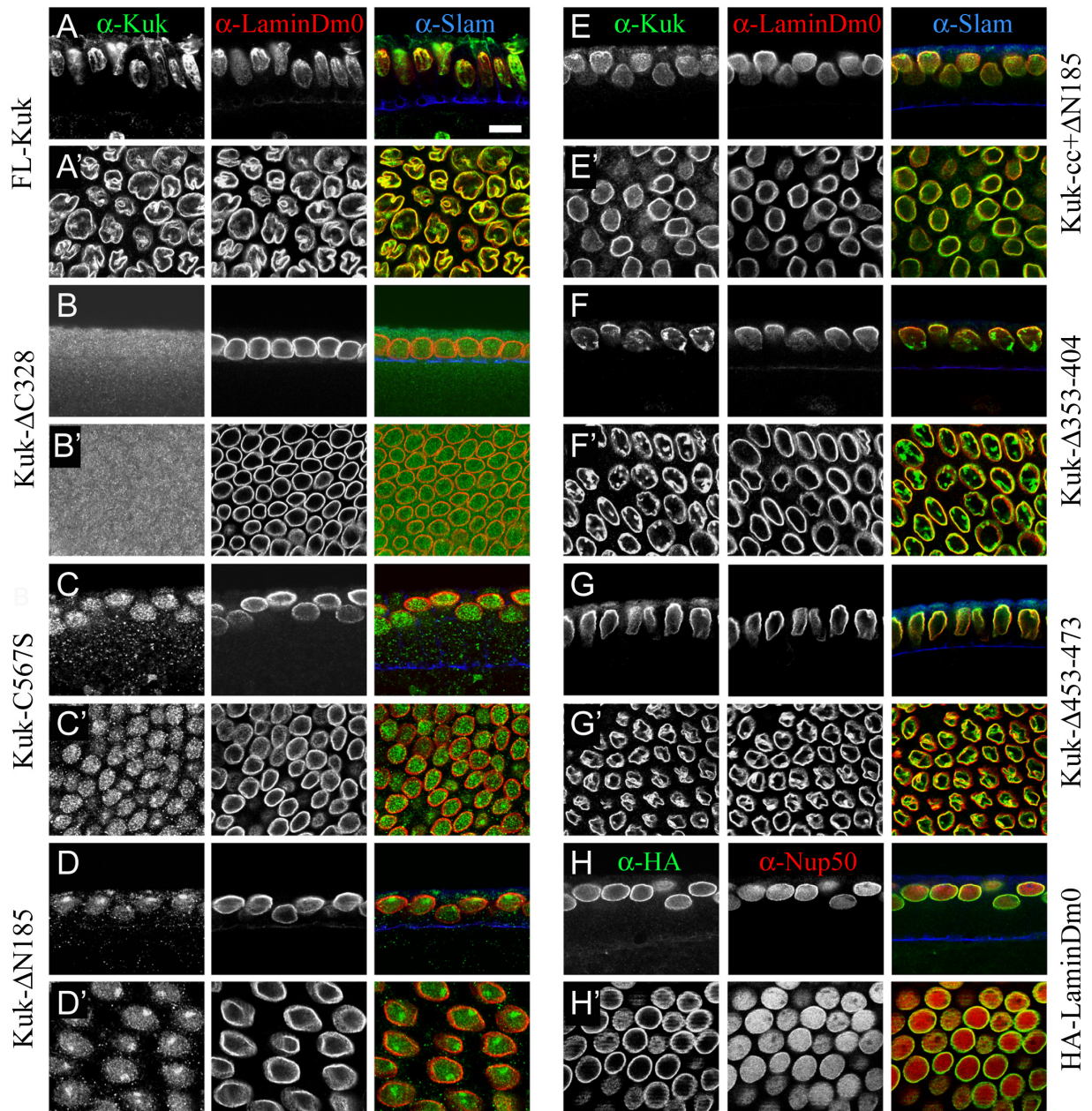


Figure 15: Structure-function analysis of Kuk in the cellularizing *Drosophila* embryo.

Nuclear morphology of *kuk* Δ 15 embryos injected with mRNA of different constructs. All embryos are in late cellularization stage. The invaginating membrane is stained by Slam (blue). Lamin Dm0 (red, A-G') marks the NM and Nup-50 (red, H,H') marks the nucleoplasm and the NPCs of the NM. A: FL-Kuk injected embryo, side view. A': Surface view. B: Kuk- Δ C328 injected embryo, side view. B': Surface view. C: Kuk-C567S injected embryo, side view. C': Surface view. D: Kuk- Δ N185 injected embryo, side view. D': Surface view. E: Kuk-cc+ Δ N185 injected embryo, side view. E': Surface view. F: Kuk- Δ 353-404 injected embryo, side view. F': Surface view. G: Kuk- Δ 453-473 injected embryo, side view. G': Surface view. H: HA-LaminDm0 injected embryo, side view. H': Surface view. Scale bar: 10 μ m.

In addition, it was tested whether the *kuk* phenotype in the blastoderm embryo could be rescued by overexpressing the other farnesylated protein of the INM, lamin Dm0. When HA-LaminDm0 was injected in *kuk* deficient embryos, even though it properly localized at the NM, the nuclei were neither elongated nor apically ruffled in late cellularization (Figure 15H, H',

Table 5). Therefore it seems that the activity of Kuk in elongating the cortical nuclei is specific and cannot be complemented by additional lamin Dm0.

In conclusion, this analysis led to the identification of a conserved aa sequence (aa 353-404) that is required for the function of Kuk in nuclear elongation. The inability of Kuk- Δ 353-404 to rescue the mutant phenotype suggests that this conserved motif is specifically required for maintaining nuclear elongation during cellularization, while it does not seem to play a role in NM localization and induction of apical ruffling of the nuclei. Kuk- Δ 353-404 was the only construct tested where the function of Kuk on nuclear elongation could be separated from its effect on apical ruffling. Furthermore, the results from Kuk- Δ 353-404 and Kuk-cc+ Δ N185 suggest that NM localization of Kuk is not sufficient for the function of the protein.

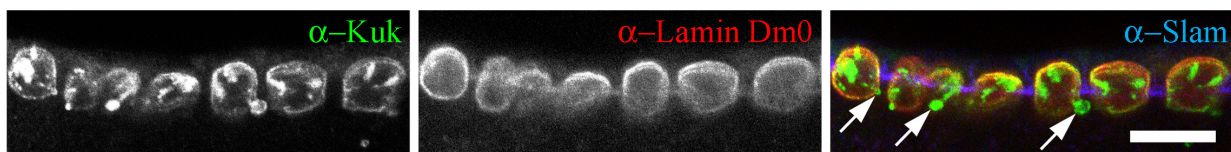


Figure 16: Nuclear membrane blebs in the Kuk- Δ 353-404 injected embryo.

Kuk deficient embryo, injected with Kuk- Δ 353-404 mRNA, in mid cellularization. Lamin Dm0 in red marks the NM and Kuk staining is shown in green. Slam in blue, marks the invaginating membrane. The arrows indicate NM blebs. Scale bar: 10 μ m.

3.1.6 Maternally provided *kuk* is required for nuclear elongation during cellularization

Kuk expression is moderate during the first thirteen division cycles and is greatly increased in early interphase of the fourteenth cycle, thus showing a zygotic peak. Nevertheless, the fact that embryos from *kuk* deficient females show the *kuk* mutant phenotype implies that maternally provided *kuk* is important for nuclear elongation during cellularization. A series of experiments was performed in order to clarify whether the effect of *kuk* on nuclear elongation is maternal or zygotic. Embryos with different number of maternally or zygotically provided copies of *kuk* were obtained by performing the crosses shown in Figure 17.

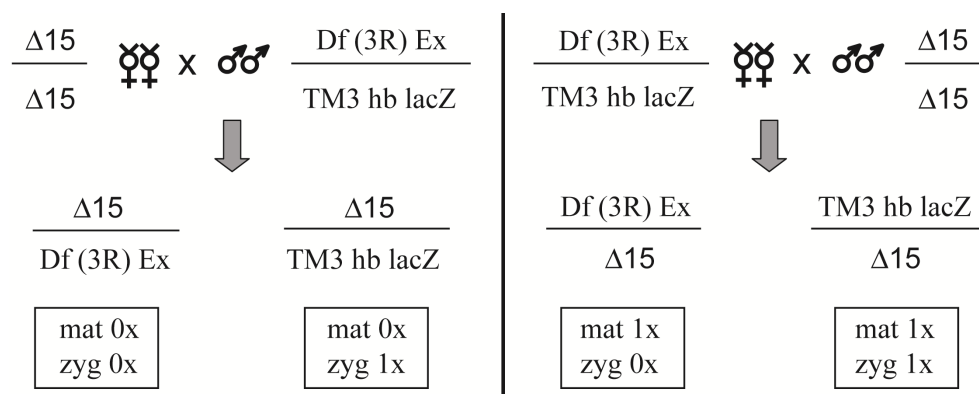


Figure 17: Crossing scheme used for obtaining embryos with different number of maternally and zygotically provided copies of *kuk* (mat= maternally provided, zyg= zygotically provided).

The nuclear morphology of the different categories of embryos in late cellularization was compared to the one of the wild-type embryo (Figure 14B). In embryos where no maternally provided *kuk* was present, the nuclei remained round by the end of cellularization, regardless of the expression of zygotic *kuk* (Figure 18A, left). Embryos with one maternally provided copy showed nuclear elongation, even though the nuclei were shorter than the wt nuclei. The embryos arising from the crosses shown in Figure 17 contain maximum one copy of zygotically provided *kuk*, which corresponds to half the copy number found in the wt embryo. In order to examine whether the reduced number of genomic copies of *kuk* is the reason for the defect in nuclear elongation, the nuclear morphology of maternally null embryos, but with two copies of zygotically provided *kuk* was examined. These embryos also failed to show nuclear elongation and apica ruffling (Figure 18B). Therefore it seems that maternally provided *kuk* is required for nuclear elongation during cellularization in the *Drosophila* embryo.

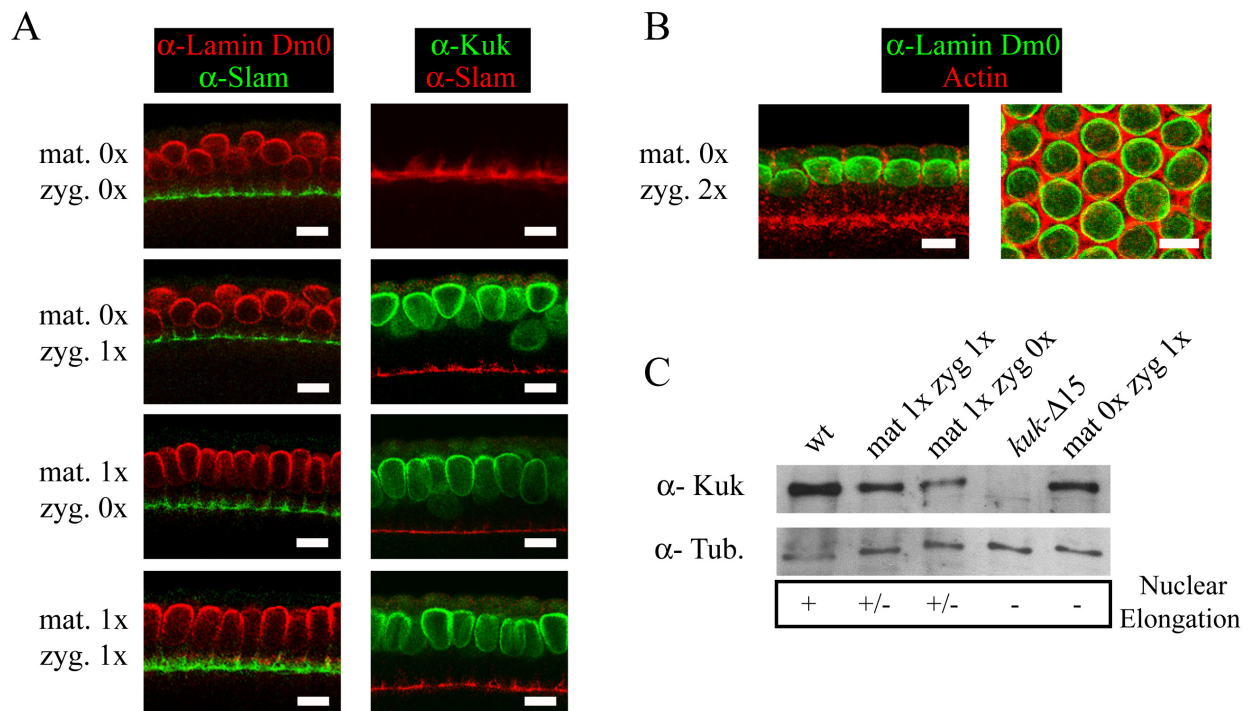


Figure 18: Nuclear morphology and Kuk protein levels in embryos with different number of maternally and zygotically provided copies of *kuk*.

A: Late cellularizing embryos with 0x or 1x copies of maternally provided *kuk* and 0x or 1x copies of zygotically provided *kuk* stained for lamin Dm0 (red, left panel) or Kuk (green, right panel). Slam (in green, left panel and in red, right panel) marks the invaginating membrane. B: Late cellularizing embryo with no maternally provided *kuk* and 2x copies of zygotically provided *kuk* stained for lamin Dm0 (green) and actin (red). Left panel: side view. Right panel: surface view. C: α -Kuk western blot from lysates of single embryos with different genotypes. α -Tubulin is shown as a loading control. The nuclear elongation for the embryos of the different genotypes is indicated by: + (wt elongation), - (no elongation), +/- (the nuclei elongate, but not fully, they remain shorter than the nuclei in the wt embryo).

By Kuk immunostaining of embryos of the different genotypes, it was found that Kuk protein is expressed in all the embryos with at least one copy of *kuk* (Figure 18A, right). When

the Kuk protein levels were compared among the different categories of embryos no difference was observed, indicating that the effect of maternally provided *kuk* is not related to upregulation of protein expression (Figure 18C).

Considering the fact that there are two different *kuk* transcripts (*Kuk-RA* and *Kuk-RB*) that produce the same protein (Figure 19A), RT-PCR experiments were performed in order to examine whether the maternal transcript is different than the zygotic transcript. For the RT-PCR experiments, lysates from embryos in late cellularization were used. Embryos with no maternally provided *kuk* and two zygotic *kuk* copies (obtained from crossing *kuk-Δ15* x *4xkuk* flies) were compared to early cellularizing wt embryos containing only maternally provided *kuk* and late wt embryos containing both maternally and zygotically provided copies. *Kuk-Δ15* embryos were used as a negative control. RT-PCR for *bottleneck* was performed as a control for the embryonic stage, since the gene is expressed only after onset of zygotic transcription (Schejter and Wieschaus, 1993). By this experiment, it was found that *Kuk-RB* is exclusively transcribed zygotically, while *Kuk-RA* is transcribed both maternally and zygotically (Figure 19B).

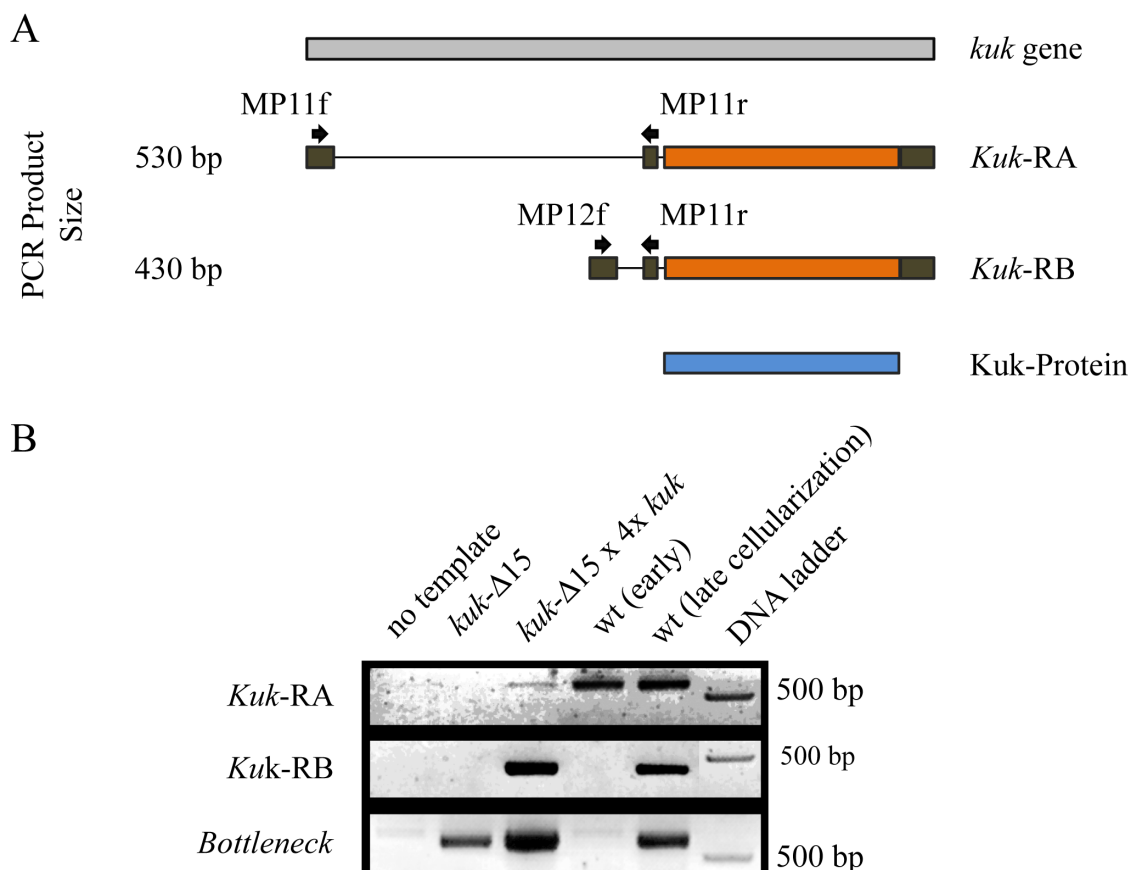


Figure 19: Maternally and zygotically provided *kuk* transcripts.

A: Schematic representation of the two different *kuk* transcripts *Kuk-RA* and *Kuk-RB*, which when translated give rise to the same protein (shown in blue). The primers used to amplify the cDNA generated from the two different transcripts, and the size of the resulting PCR products are shown on the scheme. B: RT-PCR products made using as template total cDNA prepared from single embryos in late cellularization. RT-PCR for *bottleneck* is shown as a control for the embryonic stage.

Since the levels of Kuk protein expression do not seem to depend on maternally provided *kuk*, the question is why is maternally provided *kuk* essential for inducing nuclear elongation during cellularization. One explanation could be that the protein arising from the maternally provided *kuk* bears unique postranslational modifications, essential for the function of the protein. However, this hypothesis seems quite unlikely since both maternal and zygotic Kuk proteins show identical electrophoretic behaviour on SDS-PAGE. Another explanation might be that it is essential for the *Kuk* mRNA to be present in the embryo from an early time point in embryonic development, in order for nuclear elongation to take place. This hypothesis is supported by the fact that *Kuk* mRNA can rescue nuclear elongation when injected in *kuk* mutant embryos in preblastoderm stage but not when injected in embryos in cycle 13 (data not shown). This hypothesis can also explain the difference between the maternal and the zygotic *Kuk* transcripts, which differ only in their 5'-UTR. It is possible that *Kuk*-RA is more stable than *Kuk*-RB. If this is the case, it could explain why only *Kuk*-RA is found as a maternal transcript, since the presumably increased stability of the transcript can ensure that the mRNA will not be degraded until the onset of cellularization when it starts being translated.

3.1.7 Inhibition of farnesylation affects the localization of ectopically expressed and endogenous Kuk

Farnesylation renders proteins lipophilic, resulting in their association to membranes. To further analyze the role of farnesylation in the localization and the activity of farnesylated NM proteins on nuclear shape, the behavior of selected Kuk constructs and LaminDm0 Δ N was examined in the presence of the FTI ABT-100, in transiently transfected fibroblasts. Deletion of the N-terminal part of Kuk results in proteins that behave differently compared to FL-Kuk, as described in 3.1.3. Kuk- Δ N185 lacking the coiled coil motif and Kuk- Δ N437 lacking the entire N-terminal part, formed punctate structures in the nucleoplasm and the cytoplasm respectively (Figure 20B and C). This shows that deletion of the N-terminal part of Kuk has a different effect than the deletion of the N-terminal part of lamin Dm0. LaminDm0 Δ N was found to properly localize and induce NM overproliferation in cultured cells (Figure 13A and 20D).

In the presence of the FTI ABT-100, FL-Kuk and LaminDm0 Δ N were found to localize in the nucleoplasm and they did not show any activity on nuclear shape (Figure 20A' and D'). The two constructs behaved similarly as the non farnesylatable Kuk-C567S (Figure 11B). Farnesylation seems to be an absolute requirement for the NM localization and NM deforming activity of Kuk and LaminDm0 Δ N, since treatment with the FTI completely dissociated the proteins from the NM and abolished their activity on nuclear shape. In addition, the FTI was

found to promote the nucleoplasmic localization of the constructs Kuk- Δ N185 and Kuk- Δ N437 (Figure 20B' and C').

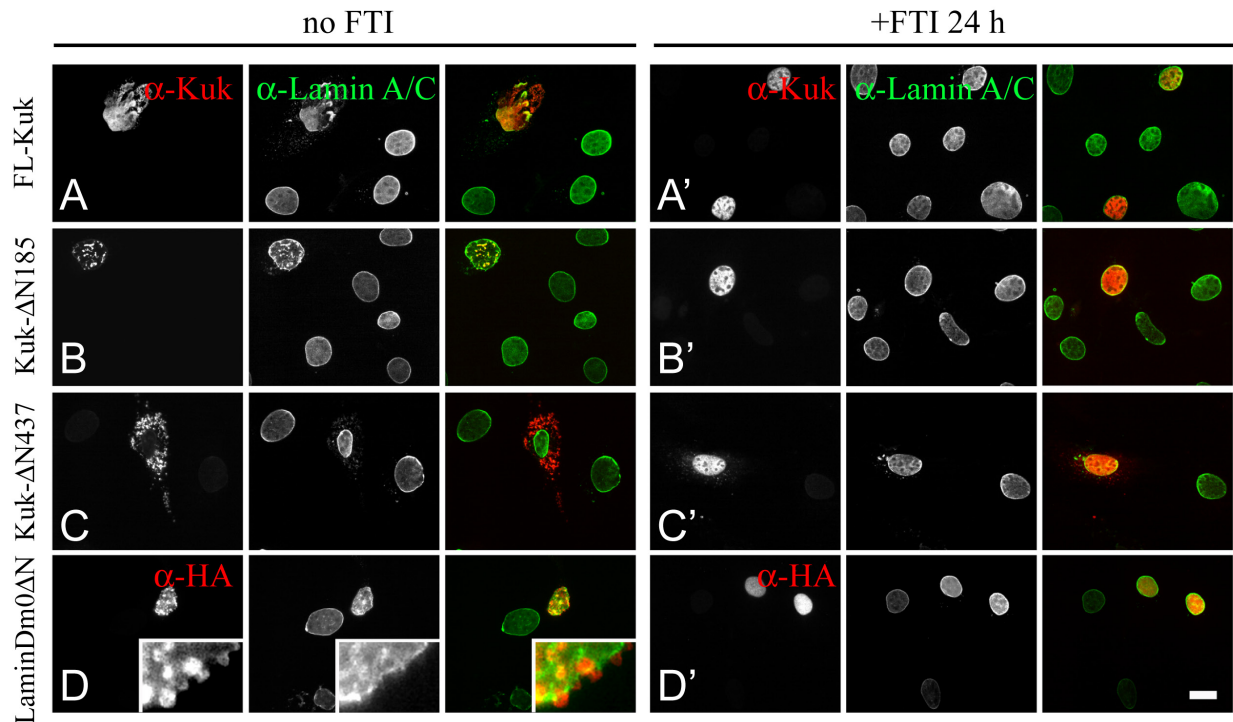


Figure 20: FTI treatment promotes nucleoplasmic localization and impairs the activity of Kuk constructs and LaminDm0 Δ N in transiently transfected mouse fibroblasts.

A-D: NIH-3T3 cells transiently transfected with different Kuk constructs and LaminDm0 Δ N under control conditions (no FTI added). The cells were fixed and stained 24 h post transfection. In D, a part of the transfected nucleus is shown magnified in order to visualize the NM blebs formed upon LaminDm0 Δ N overexpression. A'-D': Transiently transfected NIH-3T3 cells, treated with the FTI ABT-100 for 24 h. Lamin A/C staining (green) marks the NM (A-D'). Transfected cells are marked by Kuk staining in A-C' (in red) and HA staining in D and D' (in red). Scale bar: 10 μ m.

After showing that localization of ectopically expressed Kuk is affected by the FTI, it was tested whether endogenous Kuk could also be affected by such a treatment. Indeed it was observed that the FTI ABT-100 promoted nucleoplasmic localization of endogenous Kuk in *Drosophila* S2 cells (Figure 21A, Kuk staining). The inhibitor failed to affect the NM localization of endogenous lamin Dm0 (Figure 21A, lamin Dm0 staining). This was not entirely surprising, since lamin Dm0 is expected to have a slow turnover as indicated by photobleaching experiments using GFP-Lamin fusion proteins (Broers *et al.*, 1999). The inhibition of Kuk farnesylation was confirmed by WB (Figure 21B). After treatment with the FTI the amount of farnesylated Kuk, represented by a ~120 kDa band, was found to be significantly reduced. A second band of ~110 kDa corresponding to non farnesylated Kuk was predominantly detected in the FTI-treated sample. The shift in Kuk MW induced by the FTI treatment corresponds to the size difference between *in vitro* farnesylated recombinant Kuk and the non farnesylatable Kuk-C567S mutant (Figure 21C).

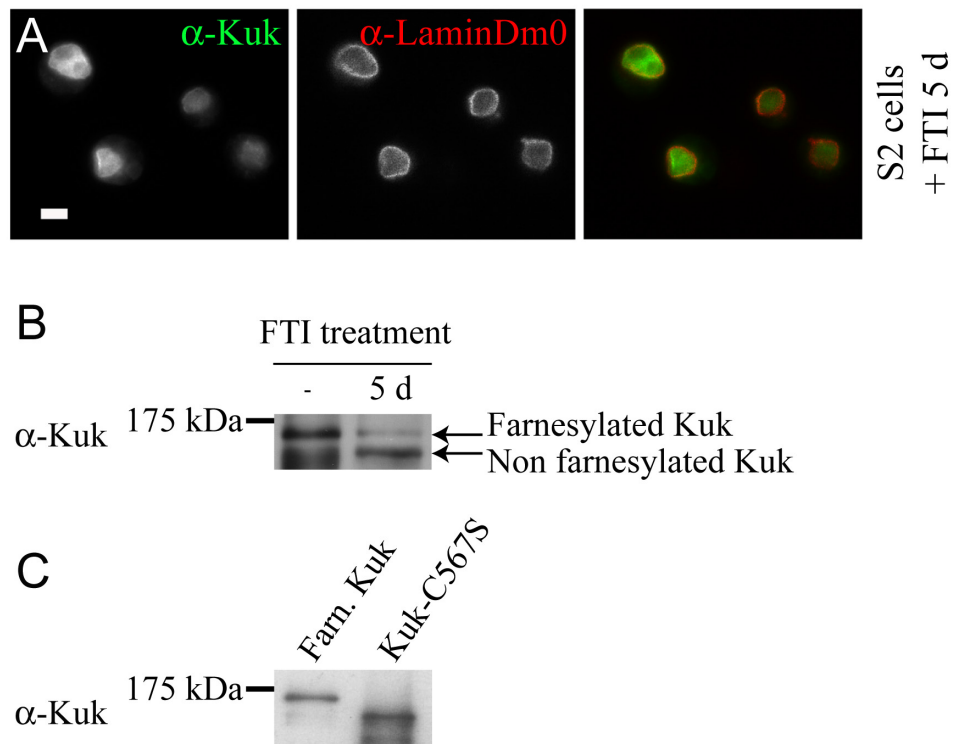


Figure 21: FTI treatment promotes nucleoplasmic localization of endogenous Kuk in S2 cells. A: S2 cells treated with the FTI ABT-100 for 5 d. Lamin Dm0 staining is shown in red and Kuk staining in green. Scale bar: 5 μ m. B: FTI treatment increases the electrophoretic mobility of Kuk. In total extract of non treated S2 cells a band of \sim 120 kDa, corresponding to farnesylated Kuk is detected. In the total extract of FTI treated cells the intensity of the \sim 120 kDa band is reduced and a \sim 110 kDa band representing non farnesylated Kuk is additionally detected. Kuk runs at a significantly higher MW than predicted (Brandt *et al.*, 2006). C: Western blot showing farnesylated recombinant Kuk and the non farnesylatable Kuk-C567S mutant.

In conclusion, farnesylation was found to be essential for protein targeting to the NM or in case of Kuk- Δ N185 and Kuk- Δ N437 for accumulation in nucleoplasmic or cytoplasmic structures. This may simply be due to the increased lipophilicity of the proteins after farnesylation. Another possibility is that association of the farnesylated C-terminus with the NM has specific effects, such as orienting the protein towards the lipid bilayer or positioning the protein in a way that it can participate in protein-protein interactions.

3.1.8 Kuk and lamin Dm0 localize at the INM independently of a group of selected INM proteins

Farnesylated proteins normally only have a weak affinity for membranes. In some cases this affinity becomes higher by a second modification i.e. in the case of Ras by palmitoylation (Hancock *et al.*, 1990; Wright and Philips, 2006). Since a second modification following farnesylation has not been described for Kuk and lamin Dm0, it was examined in this work whether the two proteins are stabilized at the NM with the contribution of other lamina or INM proteins. For this purpose selected lamina and INM proteins were depleted by RNAi in

Drosophila S2 cells. Kuk and lamin Dm0 localization did not seem to depend on one another (Figure 22A and O), as previously shown (Brandt *et al.*, 2006). When LBR, dMAN1 or lamin C were downregulated, localization of neither lamin Dm0 nor Kuk was affected (Figure 22B, M and N). On the other hand, otefin localization was found to be dependent on lamin Dm0 (Figure 22E) as previously described (Wagner *et al.*, 2004).

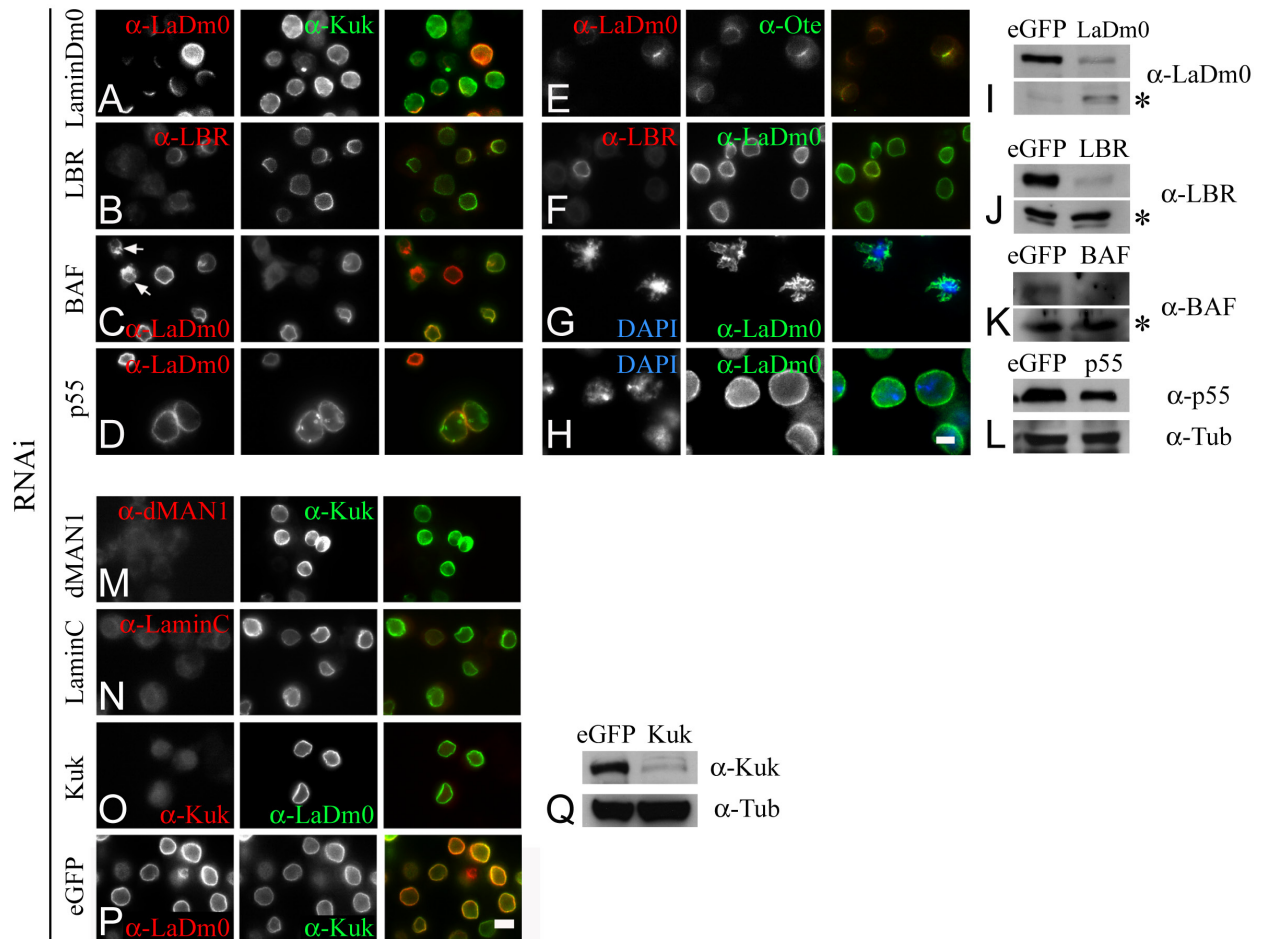


Figure 22: Kuk and lamin Dm0 localize at the NM independently of selected INM proteins. Localization of Kuk and lamin Dm0 after depletion of different INM proteins by RNAi in *Drosophila* S2 cells. A-D: Kuk staining (green) shows Kuk localization in RNAi treated cells. In red, the staining for the respective depleted protein is shown. Arrows in C indicate deformed nuclei, due to BAF depletion. E: Otefin (green) localization in lamin Dm0 (red) RNAi treated cells. F: Lamin Dm0 (green) localization in LBR (red) RNAi treated cells. G: Deformed nuclei after depletion of BAF (blue: DNA, green: lamin Dm0). H: Enlarged nuclei after p55 depletion (blue: DNA, green: lamin Dm0). M-N: Kuk staining (green) shows Kuk localization in RNAi treated cells. In red, the staining for the respective depleted protein is shown (dMAN1 in M, Lamin C in N). O: Lamin Dm0 (green) localization in Kuk RNAi treated cells. Kuk staining is shown in red. P: S2 cells treated with control RNAi against eGFP. Lamin Dm0 staining is shown in red and Kuk staining in green. Scale bar: 5 μ m. I-L, Q: Western blots from total cell extracts, showing the reduced amounts of the respective RNAi depleted proteins. Cells treated with RNAi against eGFP were used as control samples. Asterisks in I-K indicate cross-reacting bands used as a loading control. In L and Q, the immunoblot against α -Tubulin is shown as a control for equal loading.

Surprisingly, under the experimental conditions that were used, the NM localization of Kuk but not of lamin Dm0 was dependent on the chromatin binding protein BAF and on the

chromatin remodelling complex component p55. Kuk failed to localize at the NM when BAF was depleted (Figure 22C, arrows). Upon downregulation of p55, Kuk localized at the NM, but it additionally formed intranuclear structures where no lamin Dm0 was detected by immunostaining (Figure 22D). In the nuclei that were severely deformed due to the depletion of BAF, lamin Dm0 localization was affected, but not as much as Kuk localization (Figure 22C, arrows and G). This observation comes in agreement with the data obtained using BAF RNAi treated *C.elegans* embryos, in which Ce-Lamin and three nuclear membrane proteins fail to assemble properly (Margalit *et al.*, 2005). Altered lamin Dm0 distribution has also been found to correlate with the loss of detectable BAF amounts in fly imaginal discs (Furukawa *et al.*, 2003).

Another finding of the RNAi experiment was that downregulation of both BAF and p55 severely affected nuclear morphology, potentially due to indirect effects. In the case of BAF, severely deformed nuclei were observed (Figure 22C, arrows and G). Upon downregulation of p55 the nuclei were found to be particularly enlarged (Figure 22D and H). While depletion of BAF has already been described to result in NE distortion (Furukawa *et al.*, 2003), nothing has been so far reported about an effect of p55 on nuclear morphology.

The RNAi experiments reveal an unexpected function of chromatin-interacting proteins for the NM localization of Kuk and might suggest that the interaction of chromatin with components of the nuclear envelope is involved in proper organization of the INM and lamina. In addition, the results indicate a lamina independent mechanism of activity for lamin Dm0 and Kuk.

3.1.9 Kuk and LaminDm0 Δ N affect nuclear morphology even in the absence of a classical nuclear lamina

Since Kuk and lamin Dm0 do not seem to depend on candidate lamina and INM proteins for their NM localization it was examined whether they would also be able to localize at the NM in the complete absence of the nuclear lamina. For this purpose Kuk and LaminDm0 Δ N were expressed in yeast, which does not have a classical nuclear lamina (Hattier *et al.*, 2007). The expression was driven by the GalI, galactose inducible promoter. Ectopically expressed human lamin B has been shown to localize at the nuclear envelope of *S.cerevisiae* (Smith and Blobel, 1994), but an activity on nuclear shape has not been reported. The nuclei of *S.cerevisiae* cells in log phase are generally round, as observed in a yeast strain expressing mCherry-Nup133, which marks the NM (Figure 23A). Inducible GFP-Kuk expression resulted in the formation of abnormally shaped, lobulated nuclei (Figure 23B). Abnormally shaped nuclei were also formed upon inducible expression of the non filament forming construct GFP-LaminDm0 Δ N (Figure 23C). In contrast to GFP-Kuk that appeared to localize exclusively at the NM, GFP-

LaminDm0 Δ N could partially be found in the cytoplasm as it was also observed when the construct is expressed in mammalian or *Drosophila* cells (data not shown).

The activity of the truncated GFP-LaminDm0 Δ N construct indicates that the C-terminal farnesylated part of NM proteins is sufficient for inducing nuclear shape changes in yeast, while filament formation does not seem to be required. Overall, the observations in yeast, suggest that the farnesylated proteins Kuk and lamin Dm0 exert their activity on NMs independently of intermediate filament formation and regardless of the absence of lamina proteins.

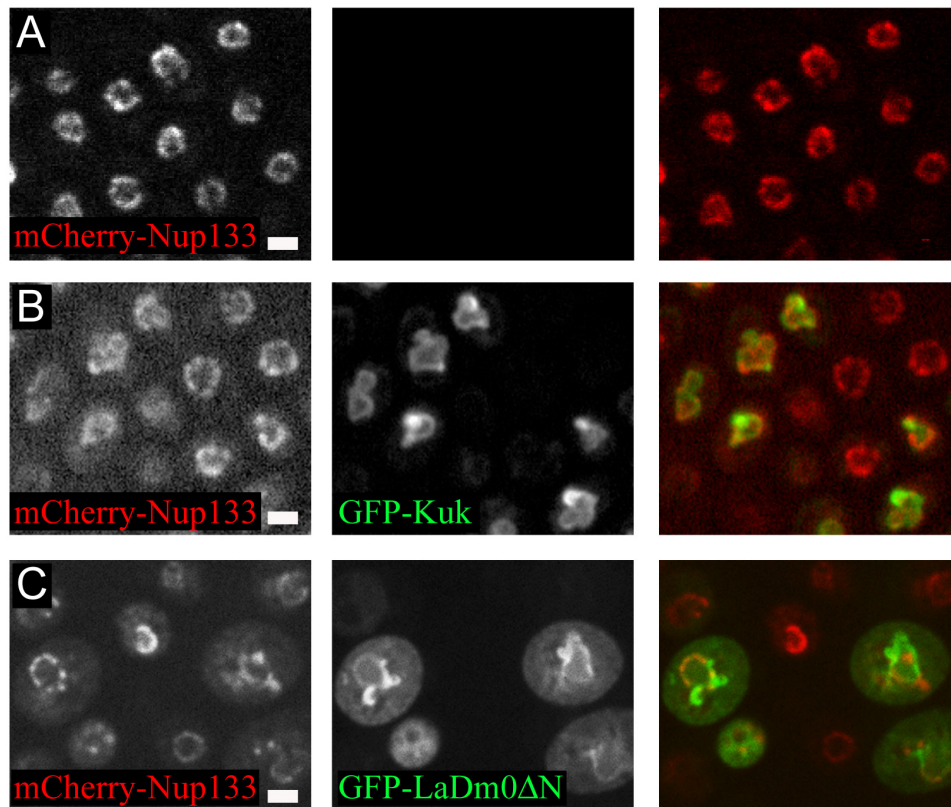


Figure 23: Nuclear morphology of *S.cerevisiae* cells in mid-log phase.

A: Non transformed yeast cells. B: GFP-Kuk expressing *S.cerevisiae*. C: GFP-LaminDm0 Δ N expressing *S.cerevisiae*. In A-C, mCherry-Nup133 marks the NM and GFP-Kuk and GFP-LaminDm0 Δ N are shown in green. Scale bar: 2,5 μ m.

3.1.10 Farnesylation is not an absolute requirement for the binding of Kuk and lamin Dm0 constructs to protein free liposomes

Since the results from the yeast and the RNAi experiments indicate a lamina independent mechanism of activity for lamin Dm0 and Kuk, it was tested whether the two farnesylated proteins could directly affect the structure of the lipid bilayer of the NM. If the proteins were asymmetrically incorporated in the lipid bilayer, this would lead to the expansion of the surface area of the inner layer of the membrane thus leading to abnormal nuclear shapes. To address this possibility, liposome binding assays were performed. Protein free liposomes were prepared using Folch I fraction of total bovine brain extract (mainly consisting of PI and PS), supplemented with

3% v/v Rhodamine coupled PE. The net charge based on the lipid composition was expected to be negative. The liposomes were prepared by extrusion and their expected average diameter was 100 nm.

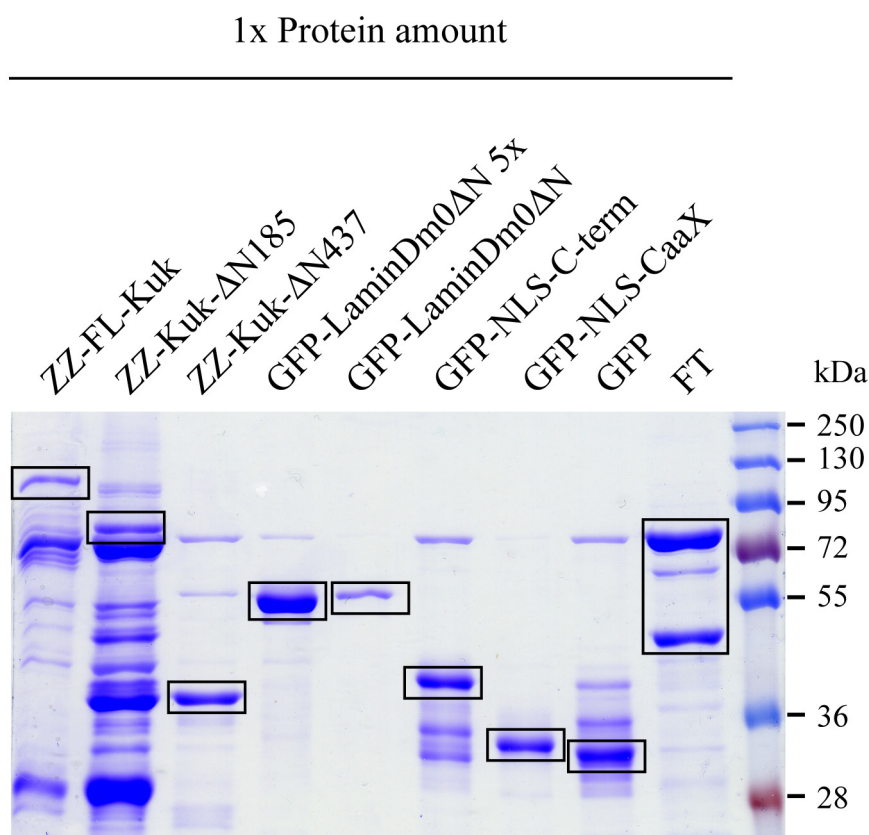


Figure 24: Protein amounts of the constructs used for the liposome assays.

A: Coomassie blue stained SDS-gel showing the protein amounts used for the liposome deformation assays. Approximately 2 μg of protein were loaded for each construct. The bands representing the corresponding proteins are indicated by black boxes. The amounts shown here refer to the 1x protein amount described in Table 6. Considering that the 1x protein amount was 2 μg and taking into account the MW of each protein, the protein concentration in the final liposome-protein mixture was estimated to be approximately 1-4 μM . For GFP-LaminDm0 ΔN a 5x amount, corresponding to the protein amount used for the EM analysis of liposome deformation, was also loaded on the gel. For the Kuk constructs the protein amount shown here was the highest protein amount that could be used for the liposome assays, due to the low protein concentration of the samples. For FT the two subunits of the enzyme, 75 kDa (GST-tagged large subunit) and 45 kDa (His-tagged small subunit) respectively can be visualized in the last lane of the gel.

Recombinant FL-Kuk, Kuk- $\Delta\text{N}185$, Kuk- $\Delta\text{N}437$, LaminDm0- ΔN , GFP-NLS-C-term and GFP-NLS-CaaX purified from *E.coli* extracts were used for the binding assays. A protein gel showing the purity and the amounts of the proteins used is shown in Figure 24. Since in *E.coli* there is no farnesyltransferase (FT), all the purified recombinant proteins were not farnesylated. In order to farnesylate them for the liposome assay, recombinant rat FT was used. The activity of the FT was first tested by *in vitro* farnesylation assays using radioactively labeled ^3H -farnesyl-pyrophosphate (^3H -FPP) (Figure 25A). FL-Kuk, Kuk- $\Delta\text{N}185$ and LaminDm0 ΔN were used in

this assay. Ras (purified recombinant protein provided by M.P. Mayer) was used as a positive control and the non farnesylatable Kuk-C567S mutant as a negative control. As shown in Figure 25A, the control protein Ras and all tested constructs except Kuk-C567S can incorporate the radioactive ^3H -FPP when incubated in the presence of the FT. As observed in the coomassie blue stained SDS gels shown in Figure 25B and C, farnesylation decreased the electrophoretic mobility of Kuk and increased the one of lamin. The reason why the two farnesylated proteins behaved differently in respect to their electrophoretic mobility is not known. The shift in the MW of the farnesylated proteins can also be observed in Figure 26.

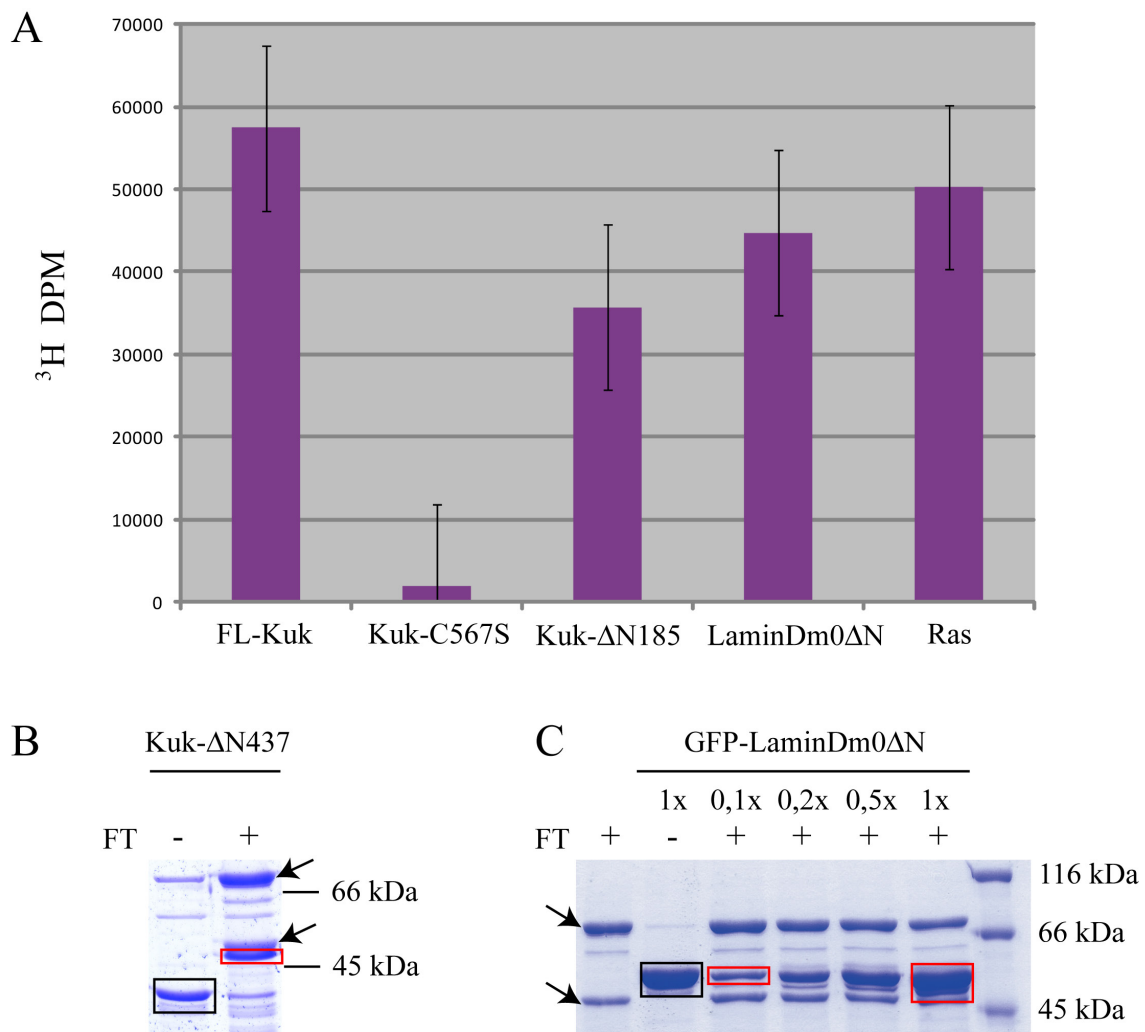


Figure 25: Test of the recombinant rat FT activity.

A: Graph showing the ^3H -FPP incorporation after incubation of FL-Kuk, Kuk-C567S, Kuk- $\Delta\text{N}185$, LaminDm0 ΔN and Ras, with the radioactive substrate and FT. The incorporation was counted using a scintillation counter (measurement in dpm). B-C: Kuk- $\Delta\text{N}437$ and LaminDm0 ΔN are shown as representative examples of the MW shift upon farnesylation B: Coomassie stained SDS-gel showing Kuk- $\Delta\text{N}437$ without and with addition of FT and FPP. The black square indicates non farnesylated protein and the red square farnesylated protein. The arrows indicate the two FT subunits. C: Coomassie stained SDS-gel showing LaminDm0 ΔN without and with addition of FT and FPP. Different amounts of protein ranging from 0,1x to 1x were used for the different samples. The black square indicates non farnesylated protein and the red squares farnesylated protein. The arrows indicate the two FT subunits in the lane where only FT was loaded.

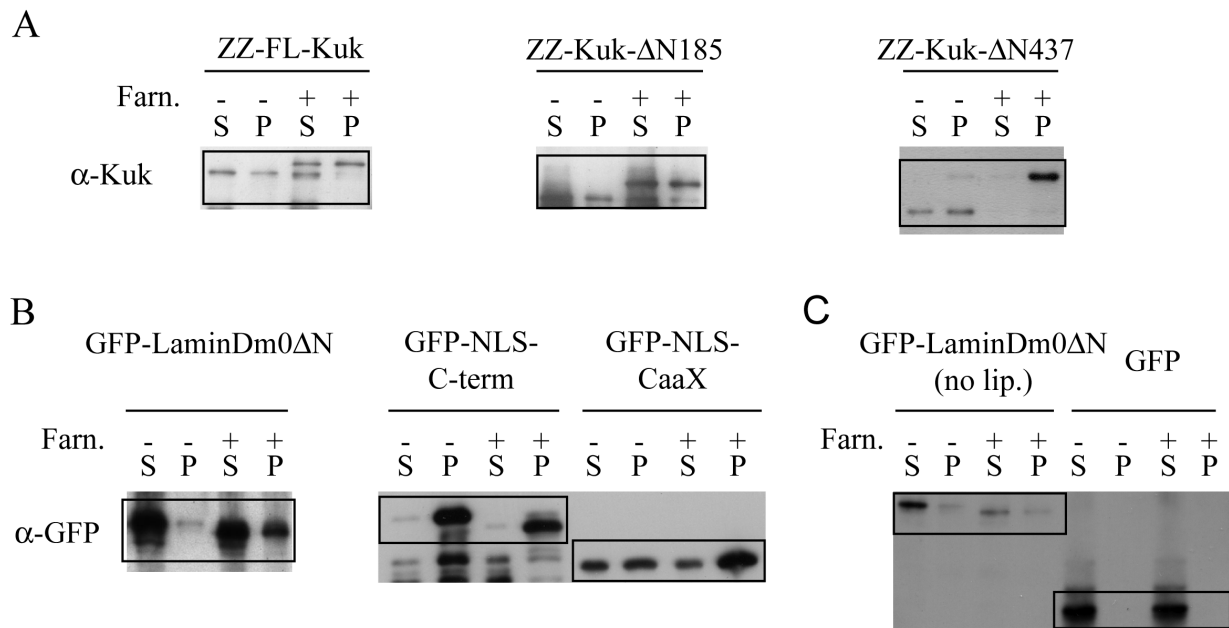


Figure 26: Binding of Kuk and LaminDm0 constructs to protein free liposomes.

WBs showing the results of the lipid binding assay. Lanes labelled by – correspond to the samples with non farnesylated proteins, where no FPP was added. Samples labelled by + show the samples where all the components of the farnesylation reaction were added. (FT enzyme was added to all samples, in order to keep the total protein concentration equal between – and + samples.) S= supernatant or unbound protein fraction. P= pellet or bound protein fraction. A: α-Kuk WB showing the distribution of FL-Kuk, Kuk-ΔN185 and Kuk-ΔN437 between supernatant and pellet depending on farnesylation. B: α-GFP WB showing the distribution of GFP-LaminDm0ΔN, GFP-NLS-C-term and GFP-NLS-CaaX between supernatant and pellet depending on farnesylation. C: α-GFP WB showing the distribution of GFP-LaminDm0ΔN between supernatant and pellet when no liposomes were added to the sample. The distribution of the control GFP protein, which cannot be farnesylated is shown in the right half of panel C.

In the liposome binding assays, the protein free liposomes were incubated with farnesylated or non farnesylated recombinant proteins and the distribution of the proteins between the liposomes and the soluble fraction was examined by WB. The results of the binding assay shown in Figure 26 are in agreement with what has been described for the binding of small farnesylated peptides to liposomes. According to previous studies (Silvius and l'Heureux, 1994; Rowat *et al.*, 2004) even though farnesylated peptides are lipophilic, they are not quantitatively bound to the lipid vesicles. A part of the total peptide amount remains in the aqueous phase. As shown in Figure 26A, farnesylation slightly improved liposome binding of FL-Kuk and Kuk-ΔN185. The same was observed for LaminDm0ΔN and GFP-NLS-CaaX (Figure 26B). The control protein GFP (Figure 26C) remained in the supernatant regardless of the addition of farnesylation reaction components. Kuk-ΔN437 shifted almost exclusively to the bound fraction when it was farnesylated (Figure 26A). GFP-NLS-C-term bound to the liposomes regardless of farnesylation (Figure 26B). This unusual behavior of GFP-NLS-C-term might be due to the positively charged NLS motif binding to the negatively charged liposomes. The fact that even the non farnesylated proteins were able to partially bind to the liposomes, implies that there might be other parts of

the protein that mediate lipid binding in addition to the farnesylated C-terminus. The increased amounts of protein found in the bound fraction (liposome pellet) were not due to protein precipitation as it can be seen in the samples where no liposomes were added (Figure 26C). Farnesylation of Kuk constructs induced a shift to higher MW, as also shown in Figure 25C. Farnesylation of LaminDm0ΔN, GFP-NLS-C-term and GFP-NLS-CaaX increased the electrophoretic mobility of the proteins, in agreement with what has been shown for LaΔ50 (Capell *et al.*, 2005).

3.1.11 Farnesylated Kuk and lamin Dm0 constructs deform protein free liposomes

Interestingly, the farnesylated recombinant protein constructs changed the morphology of the liposomes, as it was observed by incubation of the liposomes with the proteins, followed by fluorescence microscopy. The morphology of the spherical liposomes (Figure 29A) was not affected by the addition of non farnesylated LaminDm0ΔN (Figure 27A) or other non farnesylated proteins (Figure 29A), despite the fact that they were able to bind to the liposomes as shown by the binding assay. Addition of farnesylated LaminDm0ΔN resulted in the formation of large lipid structures (Figure 27A'), morphologically different from the protein free liposomes. In these large liposome structures, accumulation of GFP-LaminDm0ΔN could be observed (Figure 27B).

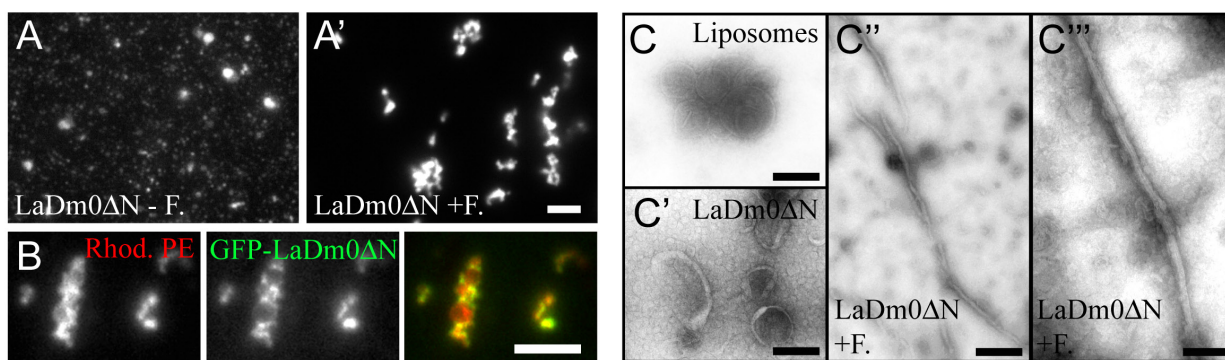


Figure 27: Farnesylated LaminDm0ΔN induces morphological changes in protein free liposomes. A-B: Liposome morphology as observed by fluorescence microscopy. A: Liposomes upon addition of non farnesylated GFP-LaminDm0ΔN. A': Liposomes upon addition of farnesylated GFP-LaminDm0ΔN. B: Colocalization of farnesylated GFP-LaminDm0ΔN (green) and Rhodamine-PE labelled liposomes (red). Scale bar A-B: 15 μm. C-C''': EM analysis of liposome morphology (performed by A. Hellwig). Scale bar: 100 nm.

Since the resolution of fluorescence microscopy was not sufficient for analyzing in detail the structural changes in the liposomes, the lipid deformation assay was performed using 5x LaminDm0ΔN protein amounts (SDS-PAGE shown in Figure 24) and the samples were analyzed by electron microscopy (EM). The EM analysis of the negatively stained samples (performed by A. Hellwig), showed that a part of the spherical liposomes formed tubules when

incubated with farnesylated LaminDm0ΔN (Figure 27C'' and C'''). The elongated structures corresponded to less than 5% of the total area of the sample, in non randomly taken pictures. Even though the morphological changes in the liposomes were found to be very pronounced when examined by fluorescence microscopy, not many structures showing an altered morphology could be observed by EM. This might be due the unstable attachment of the morphologically altered liposome structures on the grid during preparation of the EM samples.

Generally, if a sphere of a given diameter is deformed in a way that it gives rise to a cylindrical shape, the length of the cylinder depends on the diameter of the sphere, since the volume of the shape is not expected to change. The diameter of the liposomes used in these experiments was 100 nm, therefore according to this rationale the average length of the tubules formed upon their deformation should be ~300 nm, if the diameter of the tubules was ~30 nm. When the average length of the tubules formed by the deformation of the spherical liposomes was measured, it was found to be ~400 nm (Figure 28), which is close to the theoretically expected length.

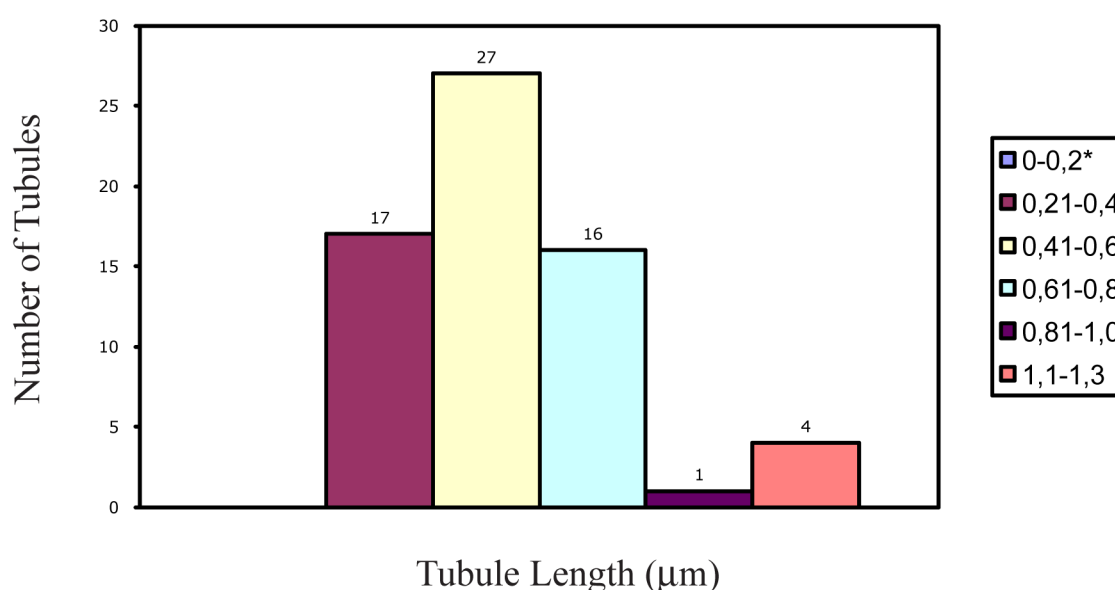


Figure 28: Quantification of tubule length in liposomes incubated with farnesylated LaminDm0ΔN. The tubule length was measured and plotted against the number of liposomes showing this length. Structures with a length up to 200 nm (indicated by the * in the table) were excluded from the measurements, since they might represent collapsed liposomes. The majority of the tubules had an average length of 400 nm. When a sphere of a given diameter is deformed so as to give rise to a cylindrical shape, the length of the cylinder depends on the diameter of the sphere, since the volume of the shape is not expected to change. The volume of the sphere ($\frac{4}{3}\pi r^3$) would theoretically be equal to the volume of the cylinder ($\pi r'^2 l$) (r = radius of the sphere and r' = radius of the cylinder). The expected length of the transformation of a 100 nm spherical liposome to a tubule with a diameter of ~30nm according to the above calculations is ~300 nm. Therefore the measured average tubule length is close to the theoretically expected length. (Only tubules with a diameter of ~30 nm were counted and included in the quantification.) The tubules were measured using the “measure” tool in Image J.

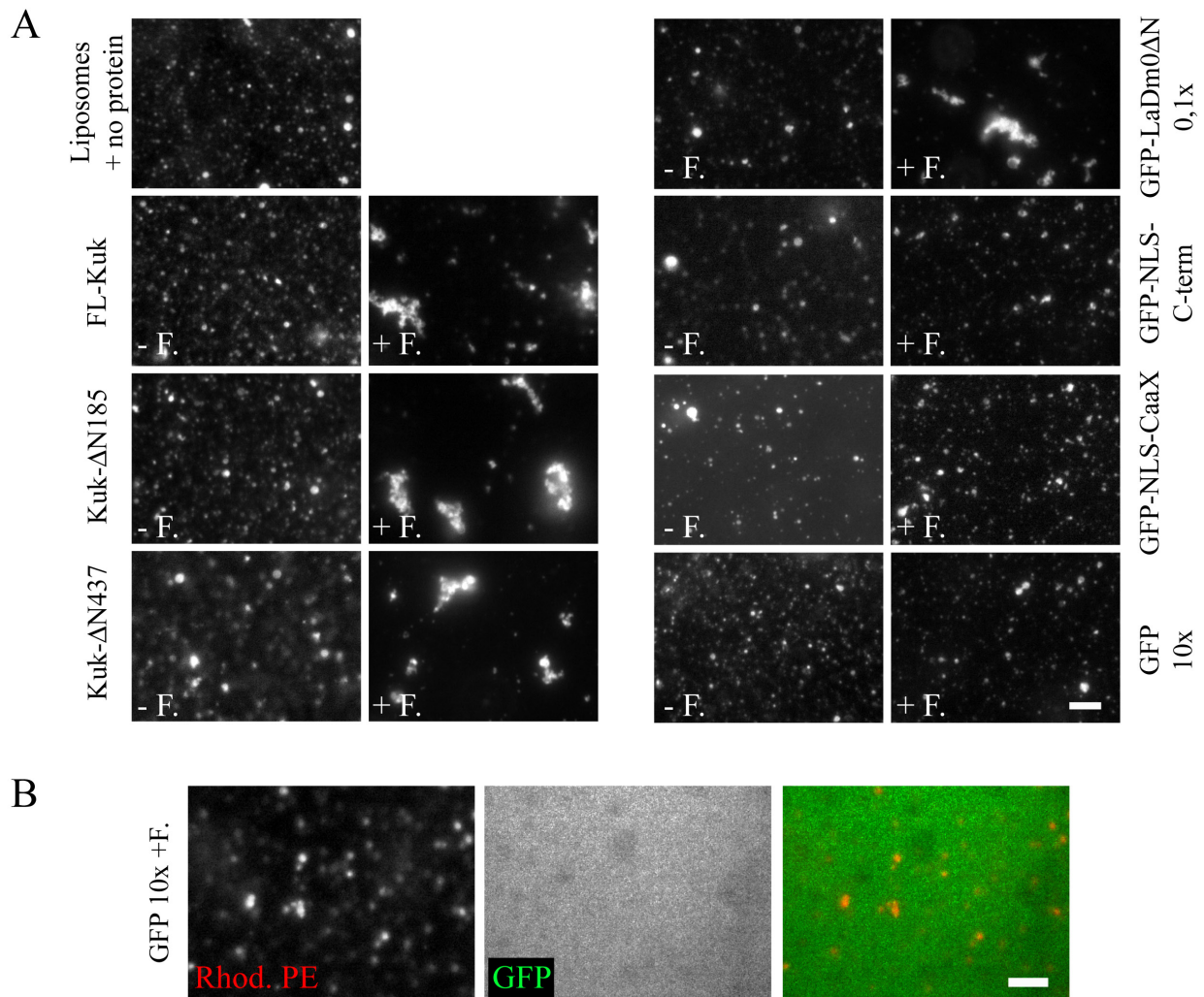


Figure 29: Liposome morphology upon addition of different proteins.

A: Fluorescence microscopy images showing the morphology of liposomes upon addition of different protein constructs. The results shown in this figure are summarized in Table 6. -F= no addition of FPP. +F= FPP was added to the mixture of liposome and proteins (FT was added to all the samples). The protein amount used was 1x for all constructs except LaminDm0ΔN (0,1x) and GFP (10x). B: Liposome morphology upon addition of 10x GFP protein together with the components of the farnesylation reaction. Rhodamine-PE labels the liposomes. The GFP panel shows that there is no colocalization of protein and liposomes. Scale bar throughout the figure: 15 μm.

Apart from LaminDm0ΔN, for which the highest protein concentration was obtained, the effect of all other farnesylated recombinant proteins on liposome morphology was examined by fluorescence microscopy. The results are shown in Figure 29 and are summarized in Table 6. All Kuk constructs could induce liposome deformation when farnesylated (Figure 29A, left panel), even though the effect was weaker than the effect of LaminDm0ΔN (Table 6), probably due to the lower protein concentration of the constructs (Figure 24). GFP-NLS-C-term and GFP-NLS-CaaX showed activity on liposome morphology, even though this activity was noticeable only at 10x higher protein amounts than LaminDm0ΔN (Figure 29A and Table 6). As mentioned above, the two constructs also showed lower activity than LaminDm0ΔN when expressed in mouse

fibroblasts (Figure 13B and C). These observations suggest that the C-terminal globular part of lamin Dm0 might have a role in deforming membranes. In addition, these experiments indicate that binding to the liposomes, which was observed for all the constructs upon farnesylation, is not sufficient for deforming the liposomes, at least when the 1x protein amount is used.

The control protein GFP did not induce any morphological changes to the liposomes and did not show any accumulation on them regardless of its high concentration and of the addition of the farnesylation reaction components (Figure 29B). Overall, the morphological changes observed in the liposome assays indicate that farnesylated NM proteins could have a direct activity on the lipid bilayer of the NM, which would result in the observed nuclear shape changes.

Table 6: Summary of the results obtained by the liposome deformation experiments.

The table summarizes the results shown in Figures 27 and 29. The effect of the respective constructs on the liposome morphology is shown by +++ (very strong), + (strong), or – (no effect). The proteins were used in 0,1x, 1x or 10x amounts, except for the three Kuk constructs for which a 10x amount was not possible to obtain (NA). All the results shown in this table refer to the samples where the components of the farnesylation reaction were added to the liposome-protein mix. The second column shows the μM concentration for each of the proteins in the mixture of protein-liposomes (final volume 20 μl), where 1x protein amount was used. The 1x protein amount refers to the amount shown on the Coomassie blue stained SDS-gel in Figure 24.

Recombinant Protein +Farn.	Deformation of Liposomes		
	0,1x protein (~ 0,1-0,4 μM)	1x protein (~ 1-4 μM)	10x protein (~ 10-40 μM)
zz-Kuk	-	+	NA
zz-Kuk- ΔN185	-	+	NA
zz-Kuk- ΔN437	-	+	NA
GFP-Lamin ΔN	+	+	+++
GFP-NLS-Cterm	-	-	+
GFP-NLS-CaaX	-	-	+
GFP	No effect & no colocalization with liposomes	No effect& no colocalization with liposomes	No effect & no colocalization with liposomes

3.2 Interplay between Kuk and chromatin

3.2.1 The GFP-Kuk HeLa s/a stable cell line: a system for studying ageing related cellular phenotypes

3.2.1.1 Characterization of the GFP-Kuk HeLa s/a cell line

Ectopic expression of Kuk in mouse fibroblasts by transient transfection has been shown to induce HGPS related cellular phenotypes, such as abnormal nuclear shapes, NPC clustering, DNA damage and loss of the heterochromatin markers HP1 and tri-me-H3K9 (Brandt *et al.*, 2008). Since all these defects are also observed upon La Δ 50 overexpression, in HGPS patients and physiological ageing (Scaffidi and Misteli, 2006), an *in vitro* system with cultured cells expressing Kuk would be adequate for studying ageing-related cellular phenotypes. So far, data related to Kuk overexpression were obtained from transiently transfected mouse fibroblasts. Among the complications of using transiently transfected cells are that one cannot take for granted that Kuk expression levels are comparable in all the transfected cells and that since transfection efficiency is never 100%, quantification of the obtained results has to be performed by analyzing different markers in individual cells and is therefore time consuming and error-prone.

In order to overcome these problems, an inducible stable cell line expressing GFP-Kuk was generated. For generating the GFP-Kuk cell line, the HeLa s/a (silent but activatable), tetracycline controlled system was used (Weidenfeld *et al.*, 2009). The advantage of the HeLa s/a cell line is that the transgene is integrated in a defined genomic locus, in which the tetracycline induced expression is tightly controlled. For obtaining the most suitable GFP-Kuk expressing cell line, fifteen single clones were selected and amplified. All fifteen clones showed doxycycline (dox) inducible Kuk expression, as observed by WB. The clones were induced for 2 d and the nuclear shape was examined by fluorescence microscopy in order to identify the clone with the most prominent nuclear shape changes. The results obtained from two clones, clone 11 and clone 15 are shown as representative examples in Figure 30. In both clones, abnormal nuclear shapes can be observed after 2 d of dox induction (Figure 30A). Clone 15 showed slightly higher Kuk protein expression levels (Figure 30B) and pronounced nuclear shape abnormalities at higher frequency, therefore it was chosen for conducting all the experiments described in this chapter.

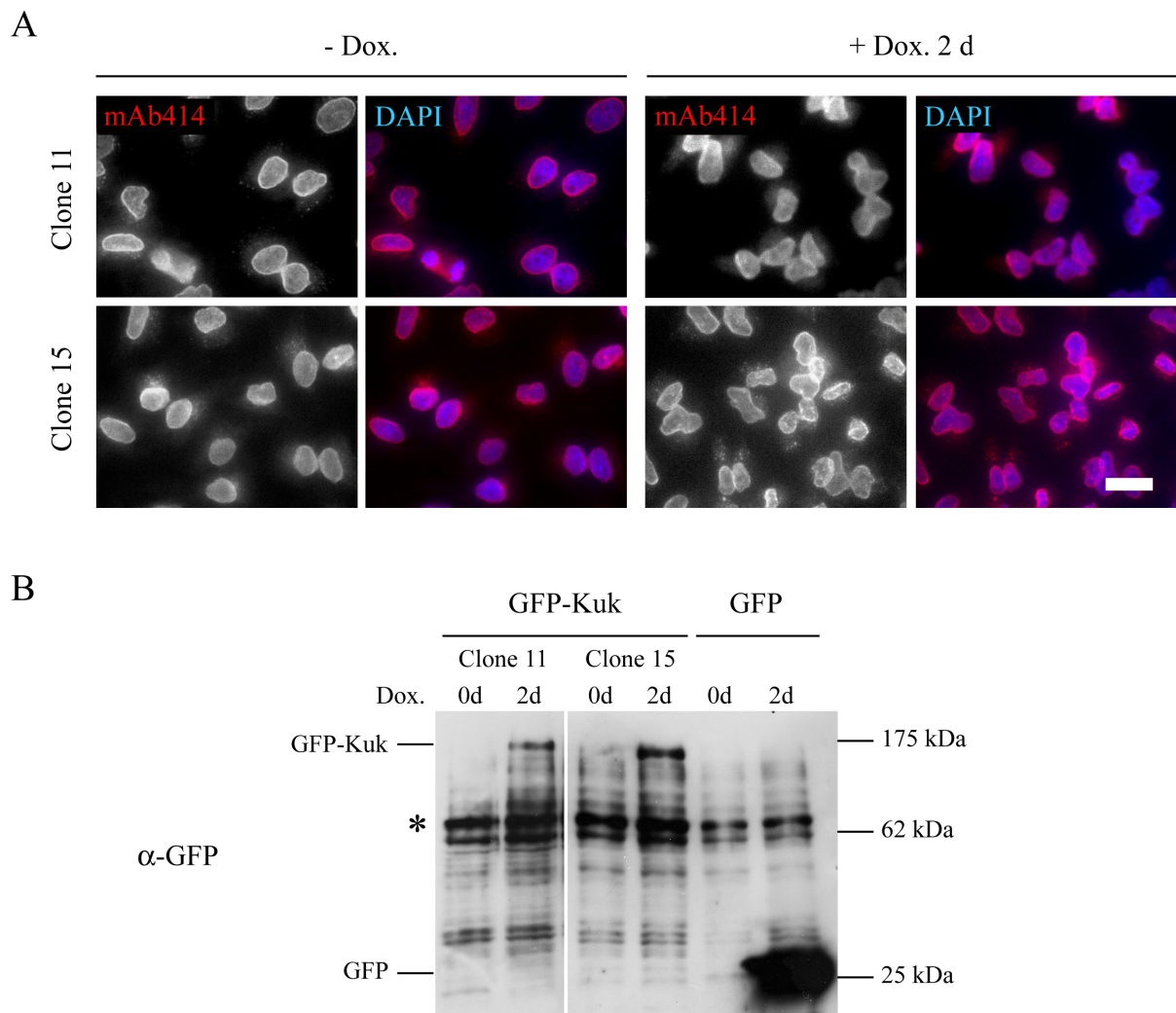


Figure 30: Nuclear morphology in dox induced GFP-Kuk HeLa s/a clones 11 and 15.

A: Uninduced cells (left panel) and cells induced with dox for 2 d (right panel) stained for nuclear pores (mAb414, in red) and DNA (DAPI staining, in blue). Scale bar: 15 μ m. B: α -GFP WB showing the expression of GFP in the GFP-HeLa s/a cell line and of GFP-Kuk in clones 11 and 15 of the GFP-Kuk HeLa s/a cell line, before (0 d) and after dox induction (2 d). A crossreacting band used for comparing total protein levels is indicated by the asterisk.

3.2.1.2 Analysis of ageing related cellular phenotypes in the induced GFP-Kuk HeLa s/a cell line

The GFP-Kuk HeLa s/a cell line was induced by addition of dox for 7 d and a series of stainings and WB for different proteins were performed in order to analyze the ageing related phenotypes arising due to the GFP-Kuk expression. A WB for Kuk showed that already after 1 d of dox induction Kuk protein shows detectable expression levels (Figure 31B). No detectable amounts of protein could be observed in the uninduced cells, confirming the tight regulation of inducible gene expression. The amount of Kuk protein is found increased by day 2, and remains quite stable until day 7. Two bands showing a slight MW difference are detected by the α -Kuk WB. The lower MW band might represent non farnesylated GFP-Kuk or Kuk after proteolytic cleavage of the GFP. The size difference of the two bands mostly supports the first hypothesis. It

is possible that the farnesylation machinery of the cell is not capable of quantitatively farnesylating the increasing amounts of GFP-Kuk protein.

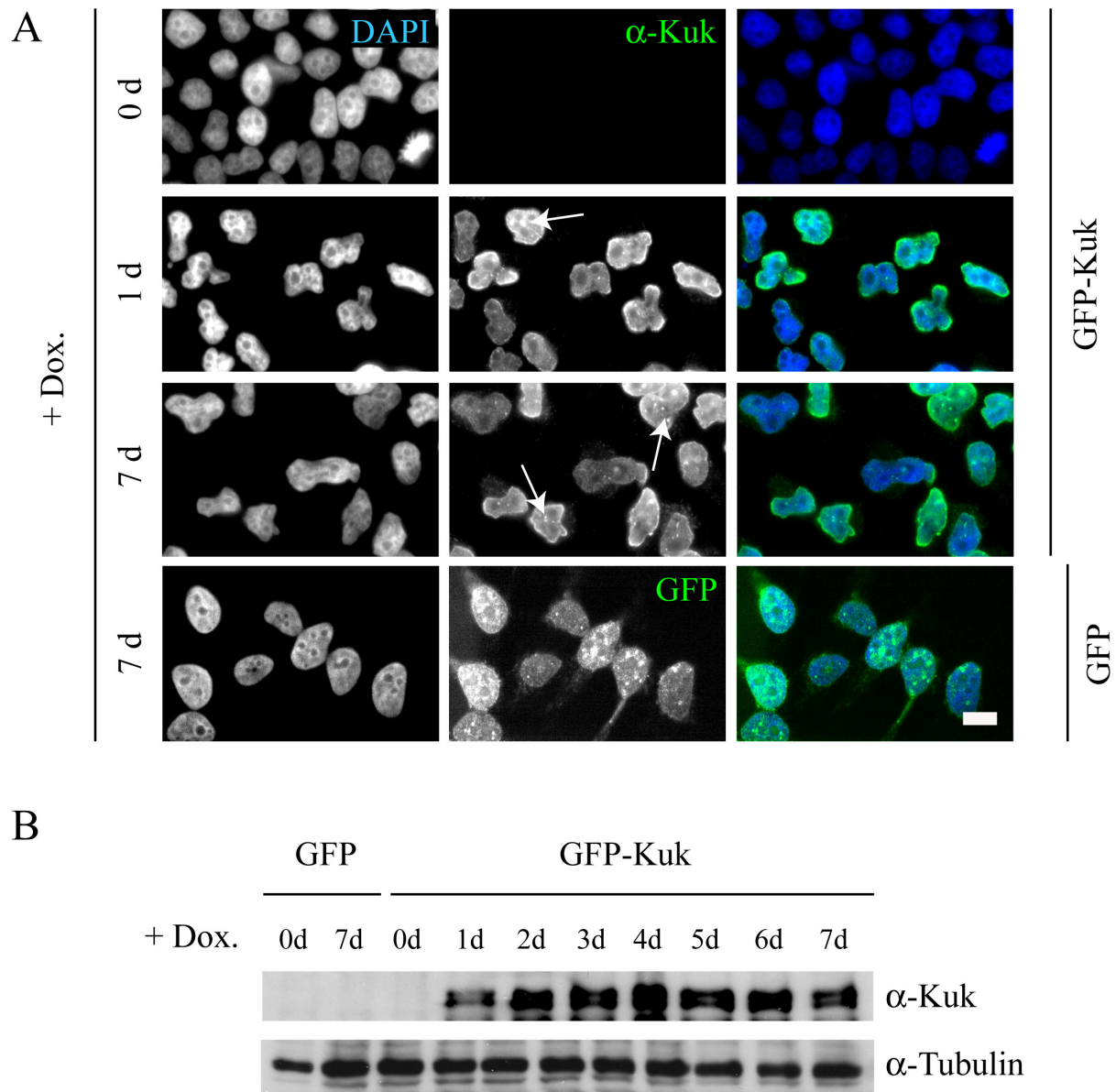


Figure 31: Abnormally shaped nuclei and GFP-Kuk protein levels during a 7 d dox induction. A: Abnormally shaped nuclei are already observed 1 d after induction and the effect lasts throughout the 7 d of dox treatment. Intranuclear structures are indicated by arrows. Non induced cells (0 d) and induced GFP HeLa s/a cells are shown as controls. DAPI in blue marks the nuclei and Kuk and GFP are shown in green. Scale bar: 7 μ m. B: α -Kuk WB showing the increasing GFP-Kuk protein levels during a 7 d long dox induction. The second band (lower MW) might represent non farnesylated GFP-Kuk. WB against α -Tubulin is shown as loading control.

When the cells were stained for Kuk, no staining could be observed in the uninduced cells. In the dox induced cells GFP-Kuk was found to localize at the NM as expected. Induction of GFP-Kuk expression led to the formation of abnormally shaped nuclei, with intranuclear structures showing Kuk staining (Figure 31A, arrows). The frequency and the number of the intranuclear structures were found to be increased after long induction times (5-7 d). Abnormally

shaped nuclei were observed throughout the 7 d long induction. The nuclei of the control line GFP HeLa s/a, expressing GFP protein, were found to be normally shaped even after 7 d of dox induction (Figure 31A), indicating that the nuclear shape defects are due to the GFP-Kuk expression and are not caused by non specific effects of the dox induction.

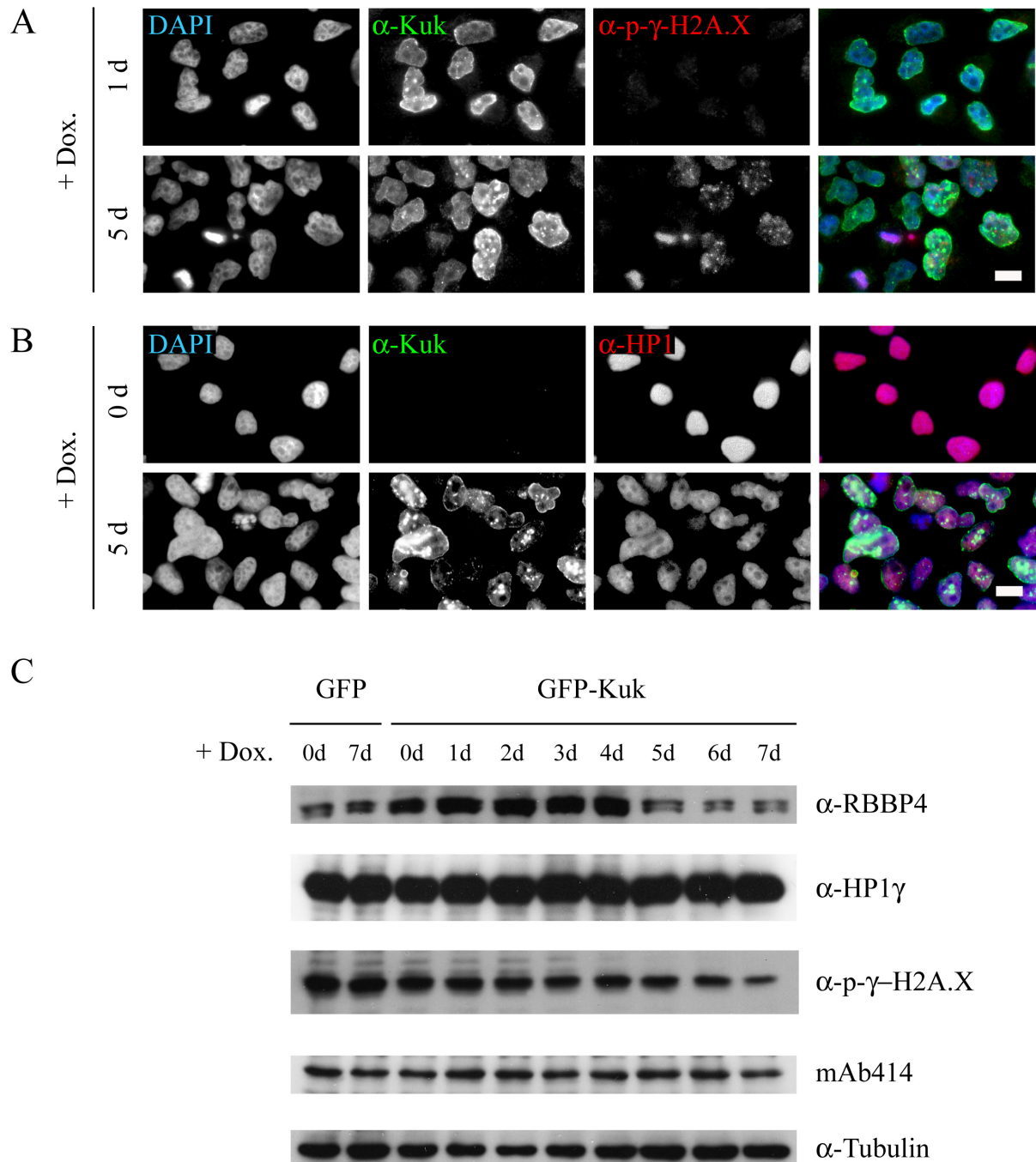


Figure 32: GFP-Kuk expression induces increased DNA damage and heterochromatin loss in the GFP-Kuk HeLa s/a cell line.

A: p-γ-H2A.X staining (red) showing the resulting DNA damage after 5d of GFP-Kuk expression. Kuk staining is shown in green and DAPI staining in blue. B: HP1-γ staining (red) showing the loss of heterochromatin observed upon GFP-Kuk expression. Kuk staining is shown in green and DAPI staining in blue. Scale bar: 7 μm. C: Western blot showing protein levels of RBBP4, HP1-γ and p-γ-H2A.X during the 7 d of dox induction. mAb414 detects NPC proteins. α-Tubulin WB is shown as a loading control. Samples from uninduced (0 d) and 7 d induced GFP HeLa s/a cells are shown as controls.

The induced cells were also stained for markers that are generally used for monitoring DNA damage and heterochromatin loss phenotypes. When the cells were stained for the DNA damage marker p- γ -H2A.X, foci of this histone variant could be observed in the induced cells expressing GFP-Kuk. After 5 d of dox induction, the cell number with DNA-damage foci was high, with more than two cells per image frame bearing the foci (Figure 32A). The number of the foci was not quantified. When a WB for p- γ -H2A.X was performed, increased protein levels could not be observed for the DNA-damage related histone variant (Figure 32C). A complication in the use of p- γ -H2A.X as a DNA damage marker arises from the fact that phosphorylation of H2A.X has been reported to take place during cell cycle under physiological conditions in HeLa cells, even in the absence of DNA damage (Ichijima *et al.*, 2005). Therefore, the total amounts of p- γ -H2A.X detected by WB are affected by the mitotic rate of the cells. This indicates that while p- γ -H2A.X is a good marker for detecting double strand break foci by immunostaining, it is not suitable for quantifying DNA damage by WB under the conditions used in this study.

Immunostaining of HP1- γ was found to be reduced after 5 d of dox induction in GFP-Kuk expressing cells, compared to non induced control cells (Figure 32B). The reduction in HP1- γ staining indicates heterochromatin loss and comes in agreement to what has been previously shown in fibroblasts where La Δ 50 or Kuk are overexpressed (Scaffidi and Misteli, 2006; Brandt *et al.*, 2008). Nevertheless, the levels of HP1- γ were not found to be reduced by WB (Figure 32C). The observed reduction of HP1- γ staining might be due to altered protein distribution, while the total protein amount is not influenced.

In addition to HP1- γ , another heterochromatin marker, RBBP4 was tested in GFP-Kuk expressing cells. RBBP4 is a component of the nucleosome remodeling and deacetylase (NURD) complex and it is also the p48 subunit of the chromatin assembly factor (CAF-1) complex. RBBP4 has been shown to be reduced in La Δ 50 expressing cells and in cells from aged individuals (Pegoraro *et al.*, 2009). RBBP4 levels were also found to be reduced in the GFP-Kuk HeLa s/a line, after 5 d of induction (Figure 32C). Together with the reduced HP1- γ staining, the lower RBBP4 protein amounts further confirm the loss of heterochromatin in the GFP-Kuk expressing cells.

Since it has been described that Kuk expressing fibroblasts show nuclear pore clustering (Brandt *et al.*, 2008), it was examined here whether a difference in the total number of nuclear pores could be observed. WB with mAb414, recognizing NPC proteins showed that the levels of nuclear pore proteins do not appear to be changed (Figure 32C).

Overall, the experiments using the GFP-Kuk HeLa s/a cell line showed that induction of GFP-Kuk expression promotes ageing related cellular phenotypes such as abnormal nuclear

shapes, loss of heterochromatin and DNA damage. Therefore, the cell line can be used as an *in vitro* system for further analyzing these phenotypes in a quantitative way i.e. by examining the levels of other protein markers. In addition, the cell line can be used for testing chemical compounds for their ability to ameliorate or even completely reverse the ageing related defects.

3.2.1.3 The FTI ABT-100 reverses the ageing related cellular phenotypes observed in the induced GFP-Kuk HeLa s/a cell line

Interfering with farnesylation by using FTIs has been shown to block the targeting of La Δ 50 to the NM, resulting in improvement of the nuclear shape abnormalities in cultured cells (Glynn and Glover, 2005; Toth *et al.*, 2005; Yang *et al.*, 2005). Apart from decreasing the frequency of nuclear shape defects, the nucleoplasmic localization of non farnesylated La Δ 50 was accompanied by restoration of the heterochromatin defects, as observed by using different heterochromatin markers (Columbaro *et al.*, 2005). Nevertheless, DNA damage accumulation does not seem to be corrected by the FTI treatment, indicating that the abnormal nuclear shapes and increased DNA damage that are observed due to the accumulation of La Δ 50 are independent phenotypes (Liu *et al.*, 2006).

In order to investigate whether the GFP-Kuk HeLa s/a cell line is suitable for testing the efficacy of chemical compounds in ameliorating ageing related phenotypes, the cells were induced by dox in the presence of the FTI ABT-100 (Rozema *et al.*, 2005) and the ageing related nuclear phenotypes were examined using appropriate markers. Treatment with ABT-100 blocked GFP-Kuk farnesylation, as indicated by the shift in the MW of GFP-Kuk observed by WB (Figure 33B). GFP-Kuk was almost exclusively detected by a band of lower MW (non farnesylated protein) after 1-3 d of FTI treatment. Nevertheless, after 4-7 d of FTI treatment, farnesylated Kuk (band of higher MW) could also be detected in the cell lysates. The observed inhibition of GFP-Kuk farnesylation resulted in its nucleoplasmic localization (Figure 33A). After 5-7 d of dox induction in the presence of the FTI, GFP-Kuk was also detected at the NM (a representative picture is shown in Figure 33A, 7 d), in agreement with the detectable levels of farnesylated GFP-Kuk observed by WB. Localization of GFP was not affected by the FTI treatment (Figure 33A). Treatment with the FTI prevented the formation of abnormal nuclear shapes in the GFP-Kuk expressing cells (Figure 33A), in agreement with what has previously been described concerning the correction of the nuclear shape phenotype by FTIs.

In addition to the nuclear shape defects, the loss of heterochromatin phenotype was examined in the presence of the FTI. Since it was shown that RBBP4 could successfully be used as a marker for quantitative analysis of heterochromatin loss, RBBP4 protein levels were examined by WB in lysates from GFP-Kuk HeLa s/a cells induced by dox in the presence of the

inhibitor. The levels of RBBP4 were found to be almost completely unaffected when GFP-Kuk farnesylation was blocked (Figure 33B). The small reduction in the RBBP4 protein amount observed at 6-7 d of induction might be due to the fact that after 5 d, farnesylated GFP-Kuk starts accumulating in the nucleus.

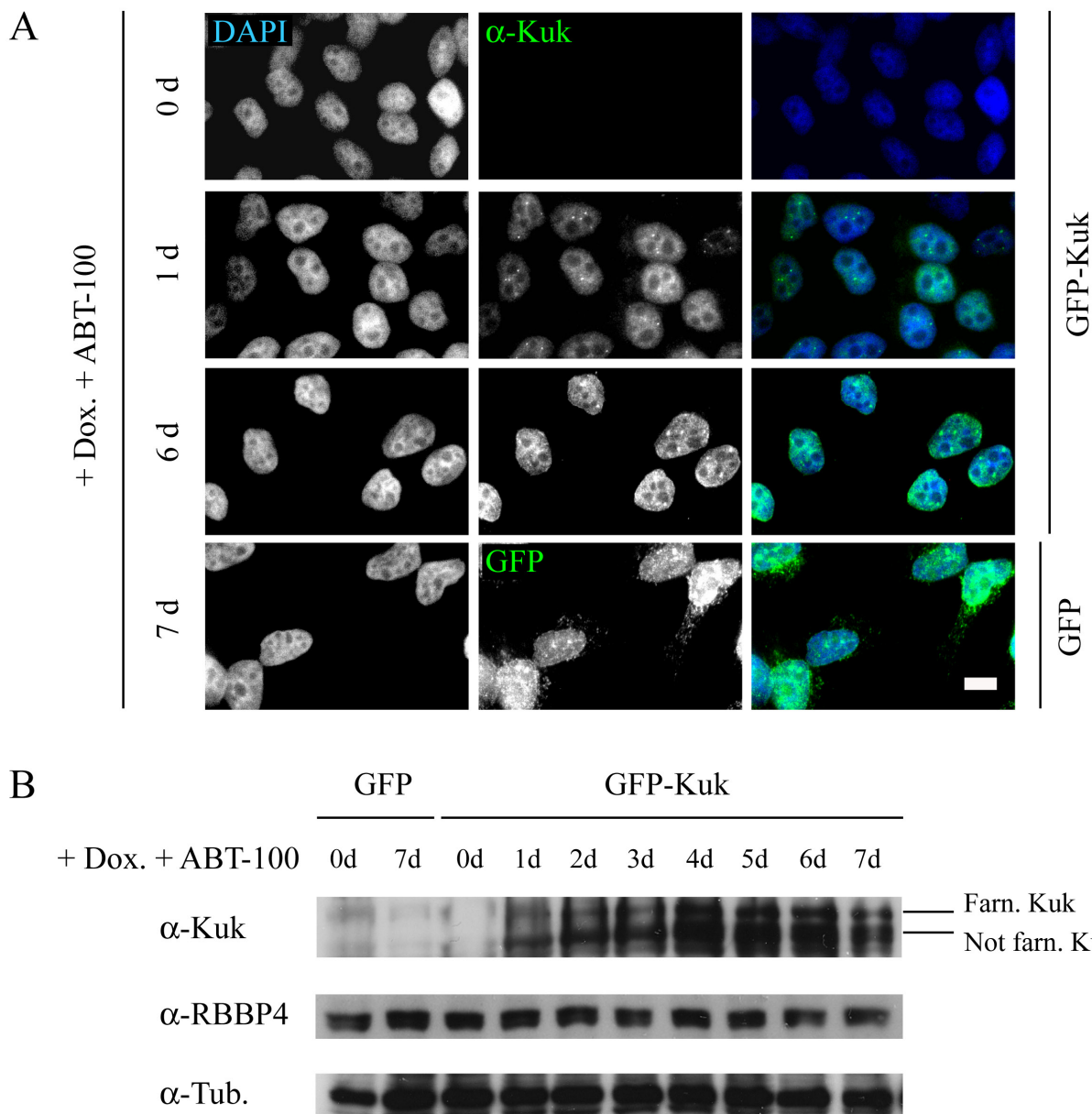


Figure 33: The FTI ABT-100 prevents nuclear shape and heterochromatin defects in GFP-Kuk expressing HeLa *s/a* cells.

A: GFP-Kuk expressing cells in the presence of the FTI. Uninduced GFP-Kuk HeLa *s/a* cells (0 d) and induced GFP HeLa *s/a* cells are shown as controls. GFP-Kuk and GFP are shown in green and DAPI in blue. Scale bar: 7 μ m. B: α -Kuk WB showing the inhibition of Kuk farnesylation due to the presence of the FTI. The higher MW band represents farnesylated GFP-Kuk and the lower MW band represents non farnesylated GFP-Kuk. RBBP4 is used as a heterochromatin marker and α -Tubulin as a loading control.

Collectively, the results of the FTI treatment of GFP-Kuk HeLa *s/a* cells indicate that the cell line is suitable for testing FTIs and other chemical compounds for their ability to prevent

ageing related nuclear phenotypes caused by GFP-Kuk accumulation. Apart from nuclear shape defects and loss of heterochromatin, other cellular defects that have previously been described to correlate with accumulation of farnesylated lamin A variants, such as DNA damage (Liu *et al.*, 2006; Scaffidi and Misteli, 2006), impaired DNA repair (Manju *et al.*, 2006), hyperproliferative behavior and apoptosis (Bridger and Kill, 2004), mitosis and cell cycle progression alterations (Cao *et al.*, 2007; Dechat *et al.*, 2007) and altered Notch signaling (Scaffidi and Misteli, 2008), can also be examined using this cell line. Suitable markers need to be selected in order to address each of the above mentioned phenotypes. In addition to the different FTIs, other chemical compounds and drugs, such as the already tested trichostatin A (Columbaro *et al.*, 2005), can be used alone or in different combinations in order to attempt to reverse ageing-related cellular phenotypes.

3.2.2 Identification of Kuk interacting proteins

3.2.2.1 IgG pull down of ZZ-Kuk followed by mass spectrometry

Despite the fact that the results obtained from GFP-Kuk expression in yeast and from the *in vitro* experiments using protein free liposomes indicate that the effect of Kuk on nuclear shape is achieved by direct interaction of Kuk with the lipid bilayer of the NM, the involvement of Kuk-interacting proteins cannot be excluded. Interaction of Kuk with lamina components, NM proteins or chromatin binding proteins could not only provide insight on how Kuk regulates nuclear shape changes during cellularization, but it could also help elucidating how Kuk affects heterochromatin.

In order to identify potential Kuk interacting partners, IgG pull down assays using the ZZ-Kuk fusion protein were performed. ZZ-Kuk was expressed in *kukΔ15 Drosophila* embryos under the control of a heat shock promoter. Kuk deficient embryos were chosen so that there is no competition between the fusion protein and the endogenous Kuk protein for binding to the Kuk interacting proteins. The expression of the fusion protein was induced in 0-12 h old embryos (overnight collections) by a 45 min long heat shock at 37°C. After the heat shock the embryos were incubated at 25°C for 30 min in order to recover from the heat shock. As a control, heat-shocked *kukΔ15* embryos without the *zz-kuk* transgene were used. Nuclei were isolated from the embryonic lysate, in order to enrich for nuclear proteins. The nuclear lysate was incubated with IgG-coupled beads, the bound proteins were eluted using two different salt concentrations and the eluates were subjected to mass spectrometric analysis.

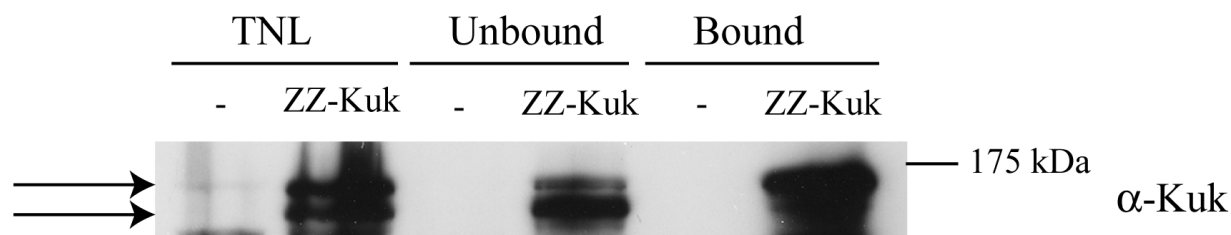


Figure 34: ZZ-Kuk binds to IgG beads.

WB against Kuk, showing the ZZ-Kuk amounts in the total nuclear lysate (TNL), in the supernatant after incubation with the IgG beads (unbound) and on the IgG beads (bound). Two bands, indicated by arrows are detected. Protein amounts loaded: TNL= equivalent of 20 embryos, Unbound= equivalent of 20 embryos, Bound= equivalent of 350 embryos. - indicates samples from *kuk* Δ 15 (control) embryos. ZZ-Kuk indicates samples from embryos expressing ZZ-Kuk.

Initially, the pull down assay was tested using 1 g of embryos and the samples were analysed by WB in order to confirm that ZZ-Kuk can bind to the IgG beads. As shown in Figure 34, two bands (indicated by arrows) representing ZZ-Kuk are detectable in the total nuclear lysate (TNL). The lower band, which is not enriched in the bound fraction but remains mostly in the unbound fraction, could either represent non farnesylated ZZ-Kuk or Kuk from which the ZZ tag has been cleaved. The latter is more probable; since it would be unexpected that non farnesylated ZZ-Kuk would show reduced binding to the IgG beads. A ~120 kDa band representing ZZ-Kuk was specifically enriched in the bound fraction of the nuclear lysate prepared from embryos with the *zz-kuk* transgene.

After confirming by WB that ZZ-Kuk could bind to the IgG beads, the experiment was scaled up. 3 g of embryos were lysed, the IgG pull down procedure followed as described in 2.2.19 and the eluates were loaded on an SDS-gel which was subjected to silver staining. As shown in Figure 35 (bound fraction, ZZ-Kuk), the fusion protein was found to remain bound on the beads even after elution with 1,5 M MgCl₂, due to the stable binding of the ZZ-tag to the IgG moiety. 300 mM of NaCl were used in the IP buffer in this experiment, in order to create stringent conditions and obtain a low background on the SDS-PAGE so that the ZZ-Kuk band would be better distinguishable.

The IgG pull down assay was finally performed using 5 g of embryos, which were lysed in IP buffer containing 150 mM NaCl. This rather low salt concentration was chosen in order to not disturb weak protein-protein interactions. The eluates after treatment with 1 M NaCl and 1,5 M MgCl₂ were loaded on SDS-PAGE and analyzed by mass spectrometry (performed by H. Urlaub). Instead of cutting out the bands that were selectively found in the ZZ-Kuk sample, the whole lanes corresponding to the control and the ZZ-Kuk samples were cut out and analyzed by mass spectrometry. The samples eluted with 1,5 M MgCl₂ were not taken into account for

identifying candidate interacting partners since they contained only a very small number of proteins, among which none were found to be relevant to the function of Kuk.

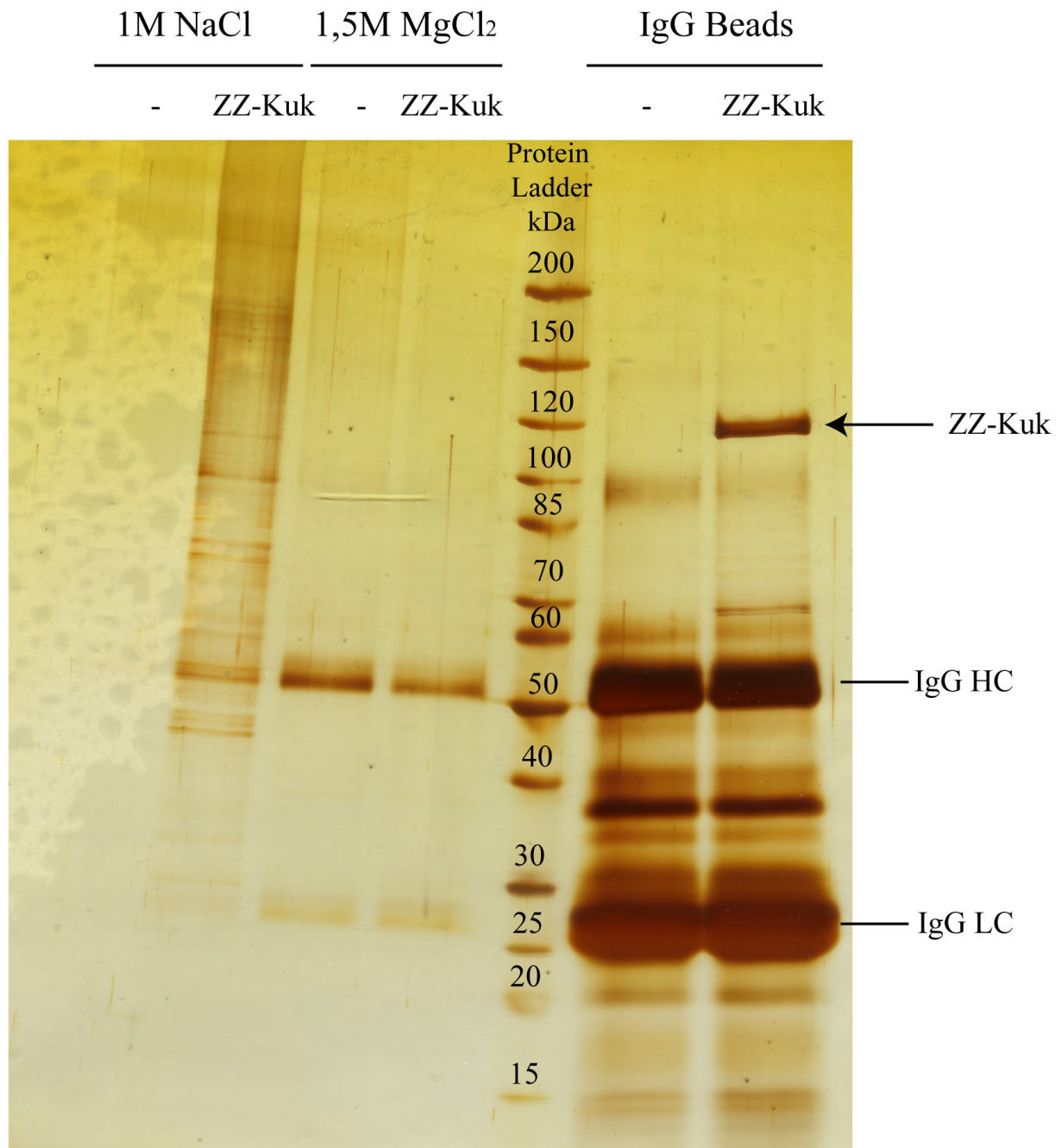


Figure 35: ZZ-Kuk remains bound to the IgG beads after elution with increasing salt concentrations. Silver stained SDS-PAGE (5-17% gradient gel). The eluates after binding of the cleared nuclear lysate to IgG beads are shown. ZZ-kuk is not eluted by the increasing salt concentration and is found bound to the beads (band indicated by the arrow). The IgG heavy chain (HC) and light chain (LC) are also visible on the lanes where the beads were loaded. - indicates samples from *kuk* Δ 15 (control) embryos. ZZ-Kuk indicates samples from embryos expressing ZZ-Kuk.

Table 7: Selected proteins identified by mass spectrometry in the 1M NaCl eluate of the IgG pull down assay.

Proteins with a score above 80 and relevant in respect to Kuk function in nuclear elongation and interaction with chromatin were selected from the full list. Proteins in bold italics represent nuclear import related proteins. Kuk was also found in the sample and is shown in bold red. Information about the different candidates was obtained from FlyBase unless otherwise indicated.

Hit No	GI No	Protein Description	Suggested Protein functions-Related Molecular processes
14	gi 555821	<i>pendulin (NLS-receptor)</i>	Transport
19	gi 45550830	<i>Nup358 [Drosophila melanogaster]</i>	Transport
21	gi 17137782	<i>female sterile (2) ketel [Drosophila melanogaster]</i>	Transport
41	gi 5734514	drosophila dodeca-satellite protein 1 (Dp1) [Drosophila melanogaster]	Heterochromatin formation, chromosome condensation
43	gi 24647601	kugelkern, isoform A [Drosophila melanogaster]	Nucleus organization
58	gi 156759	actin	Cytoskeletal protein
84	gi 2982720	CtBP [Drosophila melanogaster]	Transcription factor binding, transcription corepressor and coactivator activity
89	gi 17647135	actin 57B, isoform A [Drosophila melanogaster]	Cytoskeletal protein, import of NFAT transcription factor
100	gi 2947310	<i>nucleoporin [Drosophila melanogaster]</i>	Transport
112	gi 3309275	<i>karyopherin alpha 3 [Drosophila melanogaster]</i>	Transport, import of NFAT transcription factor
136	gi 19921114	<i>Nup107 [Drosophila melanogaster]</i>	Transport
164	gi 21358125	pontin [Drosophila melanogaster]	TATA-binding, DNA helicase
169	gi 161076460	Not1, isoform C [Drosophila melanogaster]	Basal transcriptional repressor
176	gi 24647046	suppressor of variegation 3-9, isoform B [Drosophila melanogaster]	Histone methyltransferase activity, chromosome organization
194	gi 17737463	imitation SWI, isoform A [Drosophila melanogaster]	Chromatin organization
201	gi 1072120	nucleosome assembly protein NAP-1 [Drosophila melanogaster]	Histone binding, transcription regulation, nucleosome assembly
205	gi 3869123	DREF transcription factor [Drosophila melanogaster]	Transcription factor, regulation of transcription from RNA polymerase II promoter
209	gi 17737635	reptin [Drosophila melanogaster]	Chromatin silencing, DNA helicase activity
228	gi 45549037	abnormal wing discs (awg) [Drosophila melanogaster]	Microtubule binding
279	gi 4325130	dMi-2 protein [Drosophila melanogaster]	Transcription repression activity, nucleosome binding
281	gi 1004223	centrosome-associated zinc finger protein [Drosophila melanogaster]	Component of the gypsy insulator complex (UniProt)
297	gi 17737759	karyopherin beta 3 [Drosophila melanogaster]	Transport
306	gi 24667974	putzig [Drosophila melanogaster]	Chromosome organization
311	gi 5911472	microtubule associated protein [Drosophila melanogaster]	Microtubule related
316	gi 8314	otefin [Drosophila melanogaster]	Nuclear envelope protein
332	gi 17864514	protein on ecdysone puffs, isoform B [Drosophila melanogaster]	DNA binding, regulation of mRNA splicing
340	gi 1945346	gamma-tubulin (γ -tub)	Centrosome organization, microtubule nucleation
350	gi 62512112	Tousled-like kinase, isoform C [Drosophila melanogaster]	Chromatin organization, histone phosphorylation
385	gi 1401254	nucleoplasmin-like protein-short [Drosophila melanogaster]	Chromatin assembly
387	gi 33088246	adherin Nipped-B [Drosophila melanogaster]	Transcription activator activity
408	gi 4220848	moira [Drosophila melanogaster]	Positive regulator of transcription
416	gi 30059936	*nucleoporin 98-96 (nup98) [Drosophila melanogaster]	Transport, gene regulation in the nucleoplasm (Kalverda <i>et al.</i> , 2010)
445	gi 158332	RNA polymerase II	Transcription from RNA polymerase II promoter

Selected proteins, the function of which could be relevant to Kuk function in respect to nuclear elongation during cellularization and interaction with chromatin, are shown in Table 7. Kuk itself was found in the sample, confirming that the approach worked. A further confirmation that the assay was successful were the several nuclear import related proteins (pendulin, Nup358, Nup107, Nup98, fs(2)Ket, nup, karyopherin α 3 and karyopherin β 3) that were found to be enriched in the ZZ-Kuk sample. Since ZZ-Kuk contains an NLS and is imported in the nucleus, it is expected to interact with components of the NPC. The *Drosophila* INM protein otefin was also detected, but as shown in Figure 36, the interaction could not be demonstrated by WB.

Among the candidate ZZ-Kuk binding proteins, γ -tub, actin isoforms and MT related proteins were found. Interaction of Kuk with γ -tub, a component of the centrosome, could explain the disrupted centrosome-NM interaction observed in *kuk* deficient embryos (Pilot *et al.*, 2006). Interaction with actin or MT binding proteins could play a role in the maintenance of the elongated nuclear shape by Kuk, which may be stabilized by interactions of the NM with cytoskeletal elements. The idea of NM-MT interaction is supported by the fact that in the presence of MT depolymerizing drugs the cortical nuclei fail to elongate (Brandt *et al.*, 2006; Pilot *et al.*, 2006).

Several proteins related to chromatin organization (Dp1, su(var)3-9, ISWI, NAP-1, reptin, dMi-2, putzig, tousled-like kinase, nucleoplasmin-like protein), regulators of transcription (CtBP, pontin, Not1, moira), transcription factors (DREF) and RNA polymerase II were also identified as candidate ZZ-Kuk interacting partners. Since several chromatin binding proteins and transcriptional regulators are associated with lamins (reviewed in Andres and Gonzalez, 2009) it is interesting to investigate whether the above mentioned proteins indeed interact with Kuk. Interestingly, Nup98 which was also in the list of candidates was recently shown to be involved in regulation of gene expression (Kalverda *et al.*, 2010). An interaction of Kuk and Nup98 could provide insight concerning the regulation of gene expression by components of the NM and the NPC.

In conclusion, several interesting potential Kuk interacting proteins were identified in this work. The selected candidates are related to different cellular processes such as transcription, chromatin organization and organization of cytoskeletal elements. Further analysis is required in order to confirm the interactions and address their biological significance.

3.2.2.2 Candidate approach for identifying Kuk interacting proteins

In the context of trying to identify Kuk binding proteins, it was tested by WB whether selected candidate proteins interact with Kuk. The samples from the IgG pull down experiment shown in Figure 34 were analyzed by WB using antibodies against different candidate proteins.

Interaction with otefin was investigated since otefin was found to be a potential interactor by mass spectrometry analysis (Table 7). Nevertheless, no interaction could be detected by WB, where otefin was found in the unbound fraction (Figure 36A). One complication in the experiment could be the fact that the MW of otefin (53 kDa) is very similar to the MW of the IgG HC (50 kDa) and this could result in a non distinguishable otefin band in the bound fraction. The same problem was encountered when p55 (55 kDa) was tested (Figure 36B). p55, which was chosen as a potential interacting partner since its downregulation by RNAi affected Kuk localization (Figure 22), seems to exclusively remain in the unbound fraction. No interaction was detected for dNC2- β (Figure 36D), a regulator of transcription predicted to interact with Kuk by a two hybrid based protein interaction map of *Drosophila* proteins (Giot *et al.*, 2003). ZZ-Kuk interaction with HP1 could not be detected either (Figure 36E). The IgG LC interferes with the detection of the HP1 band (23 kDa), therefore the interaction cannot be completely excluded.

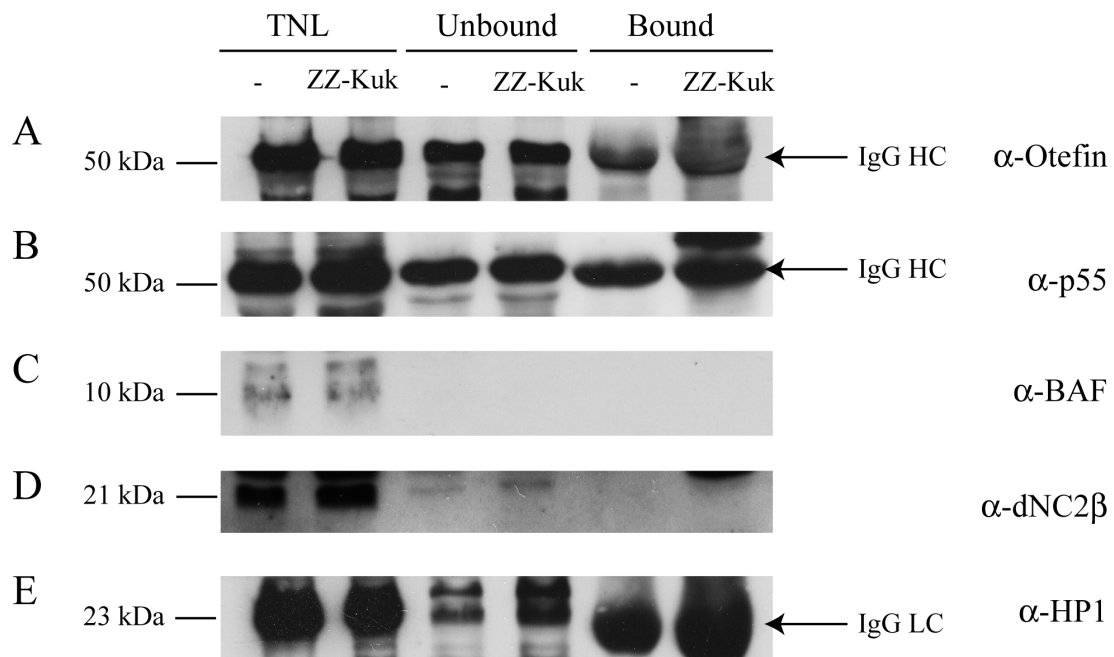


Figure 36: ZZ-Kuk does not interact with endogenous Otefin, p55, BAF, dNC2 β and HP1 in the *Drosophila* embryo.

WB against Otefin, p55, BAF, dNC2 β and HP1 showing the respective protein distribution in the total nuclear lysate (TNL), in the supernatant after incubation with the IgG beads (unbound) and on the IgG beads (bound). Protein amounts loaded: TNL= equivalent of 20 embryos, Unbound= equivalent of 20 embryos, Bound= equivalent of 350 embryos. - indicates samples from *kuk* Δ 15 (control) embryos. ZZ-Kuk indicates samples from embryos expressing ZZ-Kuk. In C and D the absence of the bands from the unbound fraction might be due to protein degradation.

The potential interaction of Kuk with BAF was also examined, since downregulation of BAF in S2 cells was shown to affect Kuk localization (Figure 22). BAF is a conserved 10 kDa DNA binding protein that binds directly to dsDNA, histone variants, transcription factors and LEM domain NM proteins (Margalit *et al.*, 2007). Recently it was also shown that BAF interacts

with mature lamin A, different prelamins A variants and La Δ 50 (Capanni *et al.*, 2010). As shown in Figure 36, ZZ-Kuk does not pull down endogenous BAF. Since it has been reported that BAF is detected at a MW of 20 kDa when in complex with LAP2- α (Dechat *et al.*, 2004), it is required to perform further experiments in order to address the possibility that BAF might be detected at a different MW than 10 kDa when interacting with Kuk. With the experimental conditions used here, the high protein amount in the bound fraction results in a number of non specific bands after WB analysis, therefore it is difficult to decide whether bands of a MW different than the expected BAF MW represent BAF multimers or background bands.

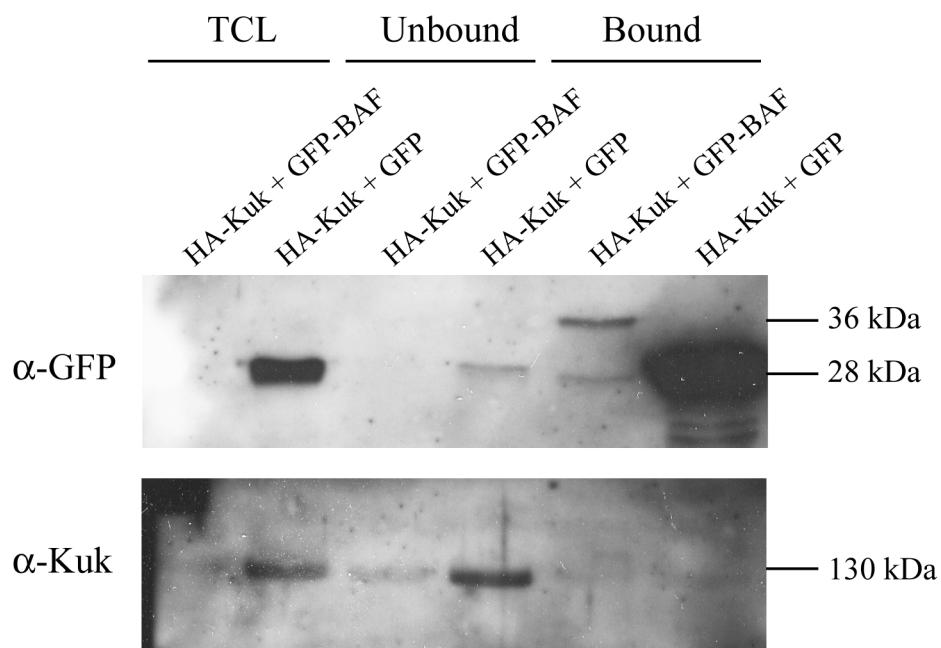


Figure 37: HA-Kuk does not interact with GFP-BAF in transiently transfected NIH-3T3 cells. GFP pull down was performed in total cell lysates (TCL) of NIH-3T3 cells, transfected with HA-Kuk in combination with GFP-BAF or GFP (control transfection). WB against GFP was performed in order to verify the efficiency of the GFP pull down and WB against Kuk for analyzing the presence of HA-Kuk in the different fractions. The unbound fraction represents the supernatant after incubation with the GBP beads and the bound fraction the GBP beads.

The potential interaction of Kuk and BAF was also investigated in NIH-3T3 cells, transiently transfected with HA-Kuk in combination with GFP-BAF or GFP (control sample). GFP binding protein (GBP) beads (GFP-Nanotrap, Rothbauer *et al.*, 2008) were used in order to pull down the GFP-BAF containing complexes (Figure 37). GFP-BAF was not detectable by WB in the total cell lysate (TCL) or in the supernatant but it was found enriched on the GBP beads (Figure 37, bound fraction). GFP, which showed a significantly higher expression than GFP-BAF was almost exclusively found in the bound fraction after incubation with the beads. HA-Kuk was not found in the bound fraction; therefore an interaction with GFP-BAF could not be shown using this assay. Before concluding that there is no interaction between BAF and Kuk

it is necessary to perform a similar experiment and test whether HA-Kuk can coimmunoprecipitate GFP-BAF. Since in the experiments demonstrating the interaction between lamin A and BAF, lamin A efficiently pulled down BAF but lamin A pull down by BAF was rather weak (Capanni *et al.*, 2010) performing the pull down for both proteins separately is necessary for obtaining conclusive results.

3.2.3 Analyzing the interplay of Kuk and chromatin by DamID

3.2.3.1 Identification of Kuk interacting genomic regions

The effect of Kuk on heterochromatin structure is observed both in downregulation and overexpression conditions. In *kuk* deficient embryos, there is impaired chromocenter formation during early embryonic development (Brandt *et al.*, 2006). In addition, when Kuk is overexpressed in mouse fibroblasts, it induces nuclear shape changes and loss of heterochromatin markers (Brandt *et al.*, 2008), similarly as in cases of overexpression of La Δ 50. In both situations, apart from the described loss of general heterochromatin markers, such as HP1, tri-me-H3K9 (Scaffidi and Misteli, 2006; Brandt *et al.*, 2008) and components of the NURD complex (Pegoraro *et al.*, 2009), not so much is known concerning the genomic regions that are affected by the altered heterochromatin structure and it remains unclear whether there is an effect on gene expression. Taking this into account, in this work it was attempted to identify genomic regions that respond to changes in NM/ lamina structure, induced by Kuk overexpression.

For the analysis the DNA adenine methyltransferase identification (DamID) technique was used in *Drosophila* Kc167 cells. DamID is a well characterized method of identifying protein-chromatin interactions and it has been used in *Drosophila* and mammalian cells (Pickersgill *et al.*, 2006; Vogel *et al.*, 2007). The principle of the DamID technique is generating a Dam-“protein of interest” fusion construct, and expressing it in cells thus leading to specific methylation of DNA sequences located near the binding sites of the protein (van Steensel and Henikoff, 2000). By isolating genomic DNA, selectively amplifying the methylated fragments (using a methylation specific PCR protocol) and subsequently performing a microarray analysis, the genomic binding sites of the protein of interest can be identified. In parallel to the Dam-fusion protein DamID experiment, a Dam only experiment is performed as a reference. What is always calculated for each locus is the ratio of Dam-fusion / Dam, in order to normalize for local variability in chromatin accessibility (van Steensel and Henikoff, 2000). For DamID the Dam-fusion expression levels have to be very low, in order to not saturate methylation levels. The Dam constructs used in this study are under the control of a heat shock promoter, but the DamID

experiments were performed without heat shock, using only the basal expression of the constructs. In the experiments performed for testing the expression and subcellular localization of the Dam constructs the cells were heat shocked in order to obtain detectable protein levels for the immunostaining analysis.

Using the DamID technique, a large number of mostly silenced loci was identified to interact with lamin Dm0, the major component of the nuclear lamina in *Drosophila* cells (Pickersgill *et al.*, 2006). In the work presented here, Kuk-DamID was performed in order to identify Kuk interacting genomic regions and compare them with the lamin Dm0 associated regions. For this purpose, Dam-Kuk fusion constructs were generated with the same rationale as described by Pickersgill *et al.* for the lamin Dm0 constructs. One construct is the Dam-Kuk (FL Kuk) that can be targeted to the INM and the second one is the DamKuk-C567S, with a point mutation in the CaaX box (C/S), which prevents farnesylation. The non farnesylatable Dam-Kuk-C567S was designed as a control construct, since it was expected to not be targeted to the INM, but to be dispersed in the nucleoplasm.

The Dam-Kuk constructs were tested for expression and correct localization by immunofluorescence microscopy (Figure 38) and they were compared to the previously described Dam-Lamin constructs that were here used as reference samples. Dam-Kuk was targeted to the NM and in some cells it induced formation of intranuclear structures (Figure 38, arrows). Dam-Kuk-C567S was predominantly found to localize at the NM despite the fact that it is non farnesylatable and it was expected to be dispersed in the nucleoplasm. One explanation might be that Dam-Kuk-C567S interacts with endogenous Kuk and is in this way targeted to the NM. In some cells Dam-Kuk-C567S was found in the nucleoplasm (Figure 38, arrowhead), probably due to lower expression levels of the fusion protein in these cells. The variable localization of Dam-Kuk-C567S rendered the construct not suitable for being used as a control. The two Dam-Lamin constructs behaved as previously described (Pickersgill *et al.*, 2006), with Dam-Lamin localizing at the NM and Dam-Lamin- Δ CaaX which lacks the CaaX motif and is therefore not farnesylatable, showing a nucleoplasmic localization.

After confirming that the Dam-Kuk fusion shows NM localization, similarly as the endogenous Kuk protein, DamID was performed for identifying the Kuk-interacting genomic loci. In the DamID experiments, the methylation by the trace levels of Dam-fusion proteins due to leaky expression was analyzed. The analysis of the microarray data was performed by M. Fornerod. Comparison of the linear maps of Kuk and lamin Dm0 interaction along the chromosomes showed that the two proteins interact with similar genomic regions, since the two maps highly correlated with each other along the whole chromosome. The map for chromosome 2R is shown as a representative example in Appendix 6.1. Similar results were obtained for 2L

and chromosomes 3 and X. Kuk gave stronger peaks than lamin Dm0, which makes it easier to define the borders of the broad genomic domains with which it interacts. The fact that Kuk and lamin Dm0 interact with similar genomic regions was not entirely unexpected, since they are both localized at the nuclear periphery.

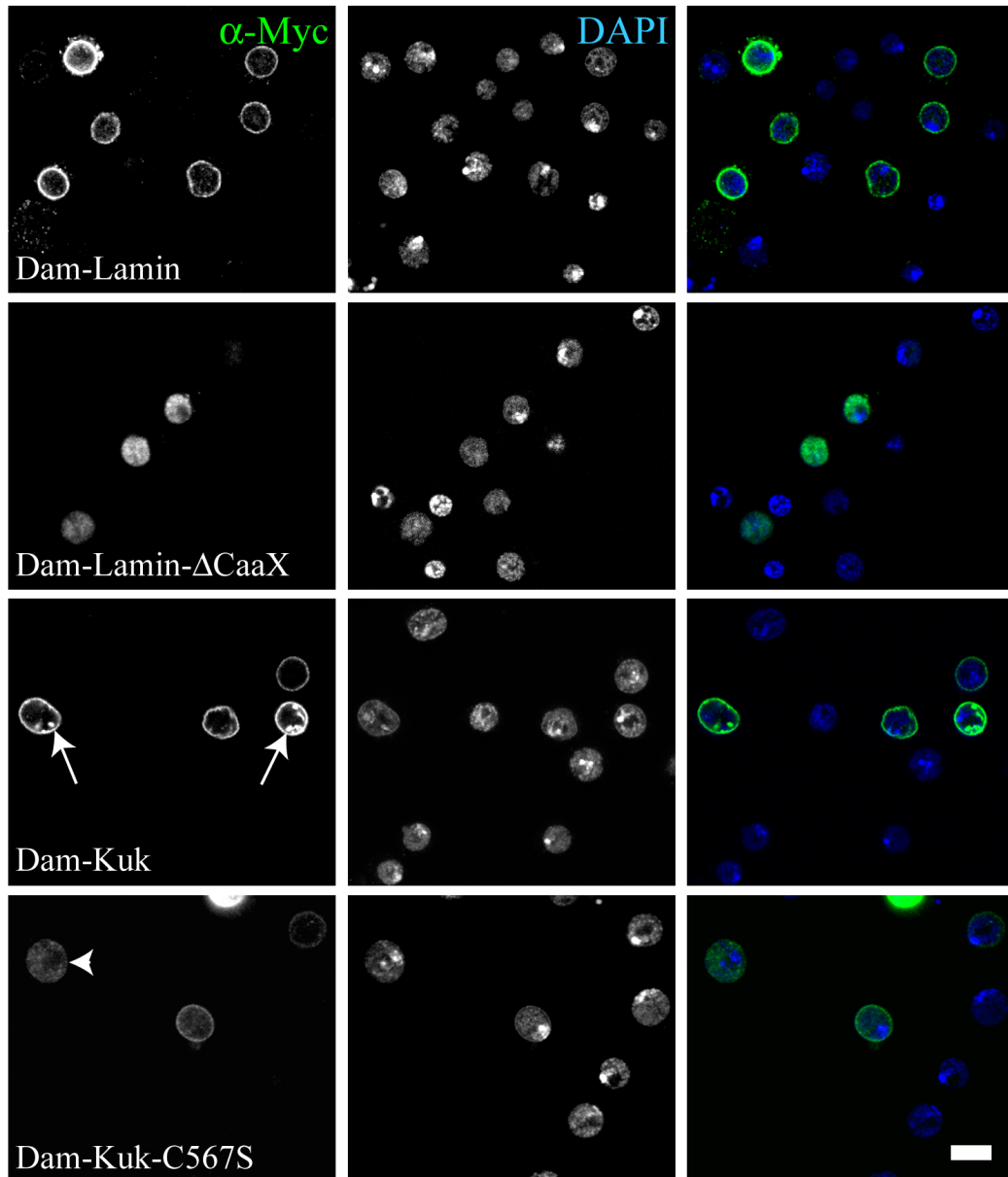


Figure 38: Localization of the Dam fusion constructs in Kc167 cells.

Localization of the transfected Dam fusion constructs, was visualized by α -Myc staining (green). DAPI staining marking the nuclei is shown in blue. The constructs used were: Dam-Lamin, the non farnesylatable Dam-Lamin- Δ CaaX construct, Dam-Kuk and the non farnesylatable Dam-Kuk-C567S construct. Protein expression in the transfected cells was induced by heat shock. Scale bar: 4 μ m.

3.2.3.2 Kuk overexpression increases chromatin accessibility in Kc167 *Drosophila* cells

Taking into account that Kuk overexpression in cultured cells results in changes in chromatin organization as observed by the loss of heterochromatin markers, the DamID technique was used in *Drosophila* Kc167 cells in order to test whether increasing the levels of

Kuk has an influence on the association of genomic regions with the nuclear periphery. For this purpose, DamID for lamin Dm0 was performed under control conditions (cotransfection of empty vector) and under Kuk overexpression conditions (cotransfection of HA-Kuk) and the lamin Dm0 interacting genomic elements identified under the two different conditions were compared. HA-Kuk was expressed under the control of a CMV promoter. The lamin Dm0 sample under Kuk overexpression conditions is referred to as “LaminDm0+Kuk” and the control sample as “LaminDm0”.

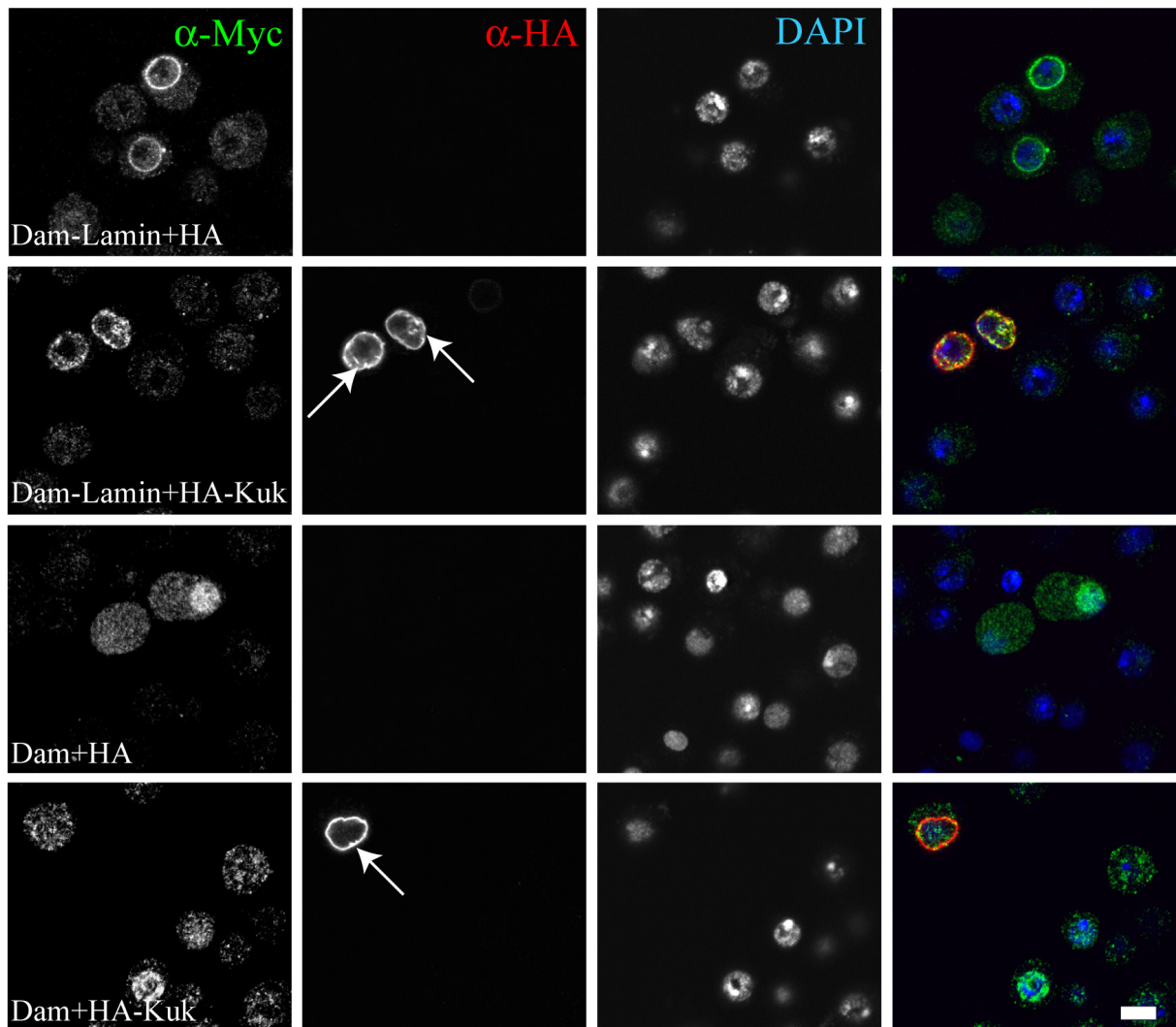


Figure 39: HA-Kuk expression in Kc167 cells cotransfected with Dam-Lamin or Dam. Localization of transfected Dam-Lamin or Dam constructs, visualized by α -Myc staining (green). HA-Kuk is visualized by α -HA staining (red). DAPI staining marking the nuclei is shown in blue. Protein expression in the transfected cells was induced by heat shock. Scale bar: 4 μ m.

Immunofluorescence microscopy was performed using heat-shocked cells in order to test the localization of Dam-LaminDm0 and Dam under the different conditions and confirm the expression and NM targeting of HA-Kuk (Figure 39). Dam-LaminDm0 was targeted to the nuclear periphery as expected, both under control and Kuk overexpression conditions while Dam

was mostly nucleoplasmic (Figure 39, α -myc). HA-Kuk was found to localize at the NM and was able to induce slight NM ruffling and formation of intranuclear structures (Figure 39, α -HA, arrows). The rather weak effect of Kuk overexpression on nuclear shape might be due to the fact that the cells were harvested 36 h after transfection, which is a quite short incubation time for monitoring nuclear shape changes in *Drosophila* cultured cells.

Comparison of the linear maps of LaminDm0 and LaminDm0+Kuk interaction along all chromosomes showed that the two maps generally correlated with each other, with the exception of a defined number of dips. The map for chromosome 2R is shown as a representative example in Appendix 6.2, and the dips are marked by the black box selection. Since the values represent the Dam-Lamin/Dam or Dam-Lamin+Kuk/Dam+Kuk ratio, the dips might be due to a decrease in the Dam-Lamin signal or to an increase of the Dam signal, under Kuk overexpression conditions. In order to distinguish between the two possibilities the maps of Dam-Lamin+Kuk vs Dam-Lamin and Dam+Kuk vs Dam were compared. As shown in Appendix 6.3, the interaction of Dam-Lamin with chromatin does not seem to be affected, in contrast to the interaction of Dam with chromatin, which is found highly increased (peaks marked by the black box selection).

In conclusion, the DamID results under Kuk overexpression conditions indicated that a defined number of genomic loci showed increased accessibility to the Dam. The affected genomic loci are shown in a table, in Appendix 6.4. These genomic regions were not found to be Kuk-interacting regions or LaminDm0-interacting regions, since the binding for both Kuk and LaminDm0 at these regions was found to be rather low. The *pigeon* locus, one of the loci found to be rendered more accessible upon Kuk overexpression is shown as a representative example in Appendix 6.5. Similar results were obtained for the other affected loci.

The genomic regions, the accessibility of which is found increased when Kuk is overexpressed need to be further analyzed. Since most of the affected genomic regions were found to be located in genes, what should be investigated is whether the increased accessibility correlates with increased gene expression. In addition, it would be interesting to examine whether among the genes that are found to be affected there is enrichment in genes represented in certain gene ontology groups.

3.2.4 Identification of a group of nuclear proteins that affect the localization of the X-chromosome in *Drosophila* S2 cells

In species where males and females have different numbers of sex chromosomes, equal levels of expression of sex-linked genes are achieved by a mechanism called dosage compensation. In *Drosophila*, where males have one X chromosome and females two X chromosomes, dosage compensation of the X-linked genes is achieved by hyperactivation of the

X chromosome in males and is regulated by the MSL (male specific lethal) complex (Straub and Becker, 2007). Two components of the NPC, Nup153 and Mtor were recently shown to be involved in transcriptional regulation of dosage compensation in *Drosophila* (Mendjan *et al.*, 2006). In this study it was shown that RNAi depletion of the two NPC components in S2 *Drosophila* cells (male cells), resulted in X chromosome decondensation and loss of MSL staining as well as loss of dosage compensation of X-linked genes as shown by qPCR.

Driven by the observations of Mendjan *et al.*, it was tested in this study whether other components of the NPC, NM proteins, components of chromatin remodelling complexes and other nuclear proteins are involved in peripheral localization and transcriptional regulation of the dosage compensated X chromosome in male cells. For this purpose, an RNAi screen was performed in *Drosophila* S2 cells. The initial experiments were performed by A. Brandt (unpublished results) and they were here confirmed for selected candidates and extended with additional ones. The list of candidates is shown in Appendix 6.6. *Drosophila* S2 cells were treated with RNAi against the different candidates and stained for lamin Dm0 in order to visualize the NM and for the MSL complex component MSL3 for marking the X chromosome. Immunofluorescence microscopy followed in order to examine the localization of the X chromosome in the nuclei of the RNAi treated cells. The two possibilities for X chromosome localization in S2 cells (shown in Figure 40A) are: “peripheral”, where the X is found to be in close proximity to the nuclear periphery (NM) and “detached”, where the X is detached from the nuclear periphery and is found in the interior of the nucleus. When the X chromosome is detached, it frequently shows a more decondensed morphology, observed by the dispersed staining for MSL3. Approximately 200 nuclei were counted for each sample and the percentage of nuclei with detached X chromosome was calculated. Untreated cells were used as a control and RNAi against eGFP was used as control RNAi treatment.

The results of the RNAi screen are shown in Figure 40B. In the untreated control cells and in cells treated with control RNAi ~16% of the nuclei showed detached X chromosome (indicated by the red line on the chart in Figure 40B). RNAi against different nuclear proteins resulted in increased percentage of nuclei with mislocalized X chromosome. In order to make sure that the increased detachment of X chromosome was not due to counting errors, only the samples that showed comparable percentage of detachment to the two control genes Nup153 and Mtor were considered as significantly affected. The X chromosome detachment in these cases was $\geq 40\%$ and the genes, downregulation of which induced this effect, are shown in the green selection box on the chart in Figure 40B. Among the selected genes with the strongest effect on X chromosome localization was Kuk, the chromatin remodeling complex component p55, the

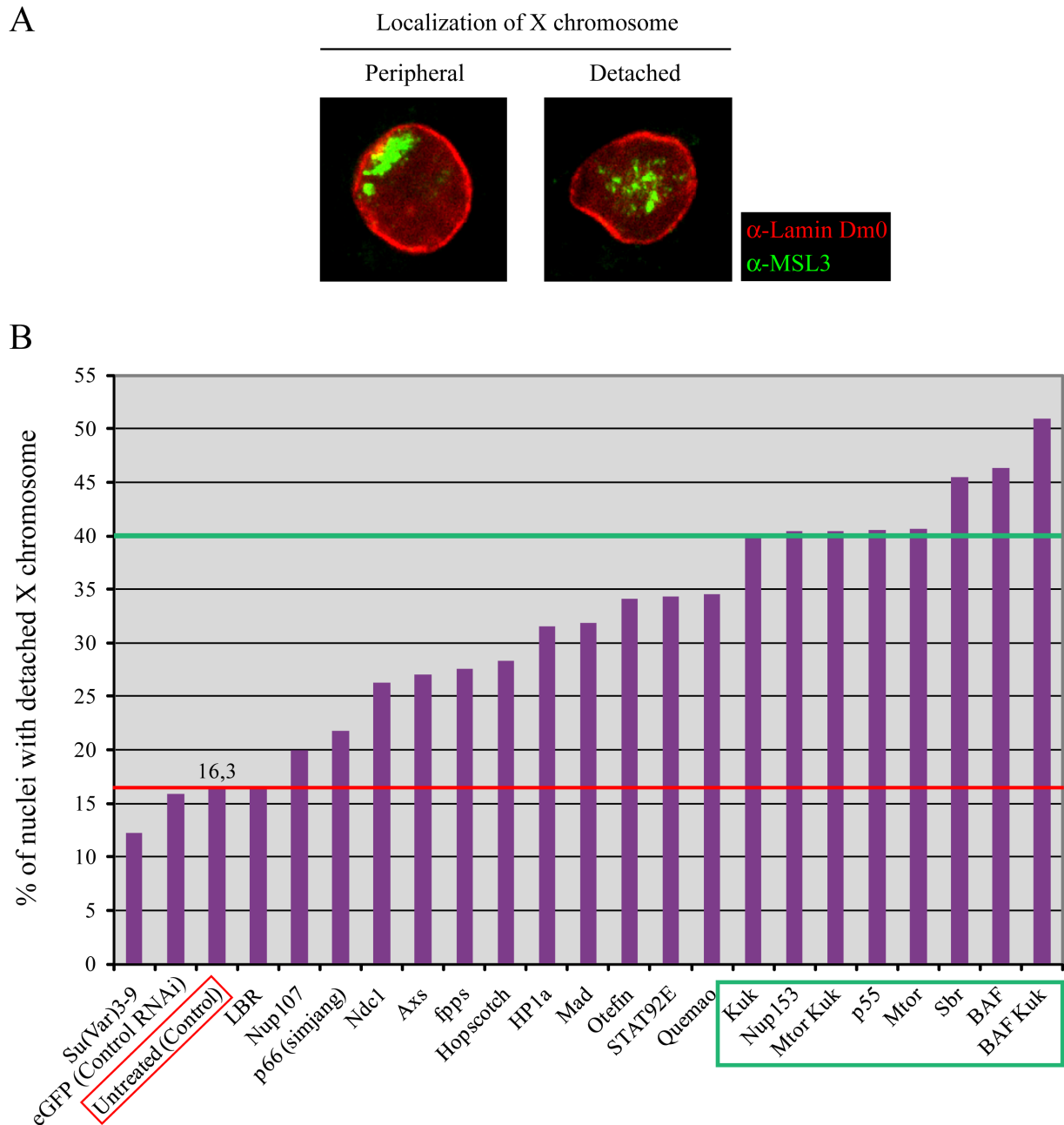


Figure 40: RNAi treatment against a number of nuclear proteins results in mislocalization of the X-chromosome in male *Drosophila* cultured cells.

A: Nuclei of S2 *Drosophila* cells stained for lamin Dm0 (red) marking the NM and MSL3 (green) marking the X chromosome. The two different possibilities of X chromosome localization are “peripheral localization of the chromosome” (left) and “detached chromosome” (right). B: Chart showing the percentage of nuclei with detached X chromosome in cells treated with RNAi against different nuclear proteins, eGFP (control RNAi) and in untreated cells (red square, control sample). 200 nuclei were counted from each sample, with the exception of BAF (123) and BAF-Kuk (106), due to the reduced cell viability after the RNAi treatment. Mtor and Nup153 were used as positive controls, since it has been described that their downregulation affects X chromosome structure and localization (Mendjan *et al.*, 2006). When the nuclear proteins selected in the green box were downregulated, more than 40% of the nuclei showed detachment of the X chromosome. The red line indicates the percentage of nuclei with detached X chromosome in the control sample (16,3 %). Similar number was obtained from the control RNAi sample (eGFP).

mRNA export related factor Sbr and the adaptor protein of INM and chromatin, BAF. When Kuk and Mtor were simultaneously downregulated by double RNAi treatment, the percentage of nuclei with detached X chromosome did not increase. Interestingly, in cells treated with RNAi against BAF and Kuk the percentage of nuclei with mislocalized X chromosome increased, indicating a potential synergistic effect of the two candidates.

After showing that downregulation of selected nuclear proteins resulted in the mislocalization of the X chromosome in cultured cells, it was tested whether the same effect could be observed *in vivo*. For this purpose, the localization of the X chromosome was examined in fixed and stained wt and *kuk* deficient male *Drosophila* stage 10 embryos (extended germband stage). The percentage of nuclei with detached X chromosome in *kuk* deficient embryos was found to be 38% compared to 18% in wt embryos (Figure 41). The numbers are in agreement with what was observed in cultured cells (40% for Kuk RNAi treated cells and ~16% for control cells), which provides further evidence confirming the results obtained in the RNAi screen.

In conclusion, the RNAi screen led to the identification of four nuclear proteins, Kuk, BAF, p55 and Sbr downregulation of which results in mislocalization of the X chromosome in male cells at a similar extent as when the NPC components Nup153 and Mtor are downregulated. What remains to be addressed is whether the mislocalization of the X chromosome is accompanied by loss of dosage compensation of X-linked genes.

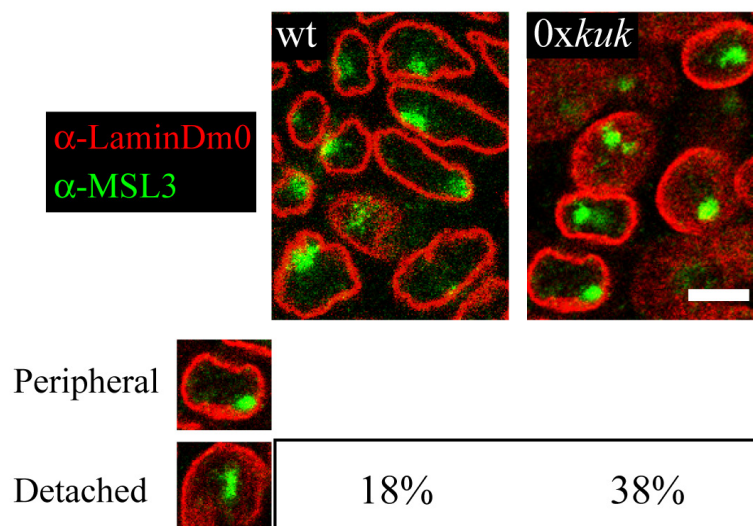


Figure 41: Increased percentage of nuclei with detached X chromosome in *kuk* deficient embryos. Wt and *kuk* deficient stage 10 embryos stained for lamin Dm0 (red) marking the NM and MSL3 (green) marking the X chromosome. Scale bar: 5 μ m. Examples of the two different possibilities of X chromosome localization, peripheral and detached chromosome are shown in the bottom left part of the figure. The percentage of nuclei with detached X chromosome in wt and *kuk* deficient embryos is indicated.

4. Discussion

4.1 The nuclear membrane proteins Kugelkern and Lamin Dm0 affect nuclear shape by directly interacting with the nuclear membrane via their farnesylated C-terminal part

Even though the effect of the farnesylated proteins lamin, La Δ 50 and Kuk on nuclear morphology has been described at the phenotypic level, the mechanism underlying this phenomenon has remained mostly unknown. So far, the analysis of lamin function and activity has been mostly focused on the N-terminal filament forming part of the protein (Wiesel *et al.*, 2008; Ben-Harush *et al.*, 2009; Kapinos *et al.*, 2009). Concerning the farnesylated C-terminal part, it was shown by Ralle *et al.*, 2004 and Prüfert *et al.*, 2004, that it seems to be sufficient for inducing formation of abnormally shaped nuclei, regardless of the presence of the N-terminal part. Triggered by these observations, the interaction of farnesylated NM proteins with the NM and in particular with the phospholipid bilayer of the NM was investigated in this work, focusing on the C-terminal part containing the CaaX motif.

The results of the structure-function analysis of Kuk performed in mouse fibroblasts and in the fly embryo, confirmed that both the coiled coil motif and the CaaX motif are required for Kuk NM localization and activity on nuclear shape, as previously reported (Brandt *et al.*, 2006). Substitution of the putative coiled coil motif of Kuk by the coiled coil of GCN4, results in a construct that localizes at the NM but does not show the wt activity on nuclear shape. This indicates that the properties of the endogenous coiled coil, which is required for Kuk function, cannot be substituted by the coiled coil used. In addition, it was found that the conserved motif consisting of aa 353-404 is required for the nuclear elongation induced by Kuk during cellularization. Kuk- Δ 353-404 localizes at the NM and induces nuclear shape changes both in fibroblasts and in the fly embryo but fails to elongate the cortical nuclei in the fly embryo. Kuk- Δ 353-404 and Kuk-cc+ Δ N185 were the only constructs for which localization at the NM was not combined with rescue of the nuclear elongation phenotype in the embryo. This suggests that NM localization is not sufficient for Kuk function during cellularization. Considering the above mentioned observations, it is conceivable that the conserved part 353-404 is essential for maintaining nuclear elongation, but not for inducing nuclear ruffling. It has been shown that MTs are required for maintaining the elongated shape of nuclei in the fly embryo, since upon their destruction the nuclei fail to elongate even though they still ruffle apically (Brandt *et al.*, 2006). One possibility could be that the domain 353-404 takes part in mediating an interaction of the MTs with the NM that could contribute in the maintenance of the elongated nuclear shape.

Ectopic expression of Kuk and LaminDm0 Δ N in yeast was shown to result in the formation of abnormally shaped nuclei. The activity of the two farnesylated NM proteins in yeast, where there is no classical nuclear lamina suggests that the nuclear shape changes could be induced by the incorporation of the proteins at the NM via their lipophilic farnesylated moiety and would therefore be independent of filament formation. The latter is further supported by the fact that there is so far no evidence that Kuk can form filaments as well as by the activity of the truncated, non filament forming LaminDm0 Δ N construct in yeast. The yeast nuclear morphology upon Kuk or LaminDm0 Δ N expression is similar to the morphology observed when Esc1p, a yeast protein of the nuclear periphery is overexpressed (Hattier *et al.*, 2007). Esc1p is a non-membrane and non filament forming protein of the nuclear periphery and despite its coiled coil motifs and its activity on nuclear shape it is not comparable to lamins. Solubilization properties of the protein suggest that it bears a lipid modification via which it associates to membranes (Taddei *et al.*, 2004). Therefore Esc1p could be another example of a lipid modified protein that changes nuclear shape when overexpressed, without depending on filament formation or on the presence of a classical nuclear lamina. Since Esc1p can function as an anchor for chromatin (Taddei *et al.*, 2004), it is possible that chromatin-nuclear periphery interactions can also participate in nuclear shape changes. A potential role of chromatin is also suggested by the nuclear shape changes that were observed upon RNAi mediated depletion of the chromatin interacting protein BAF in S2 cells. Taken together, it is here suggested that the nuclear shape changes induced by the overexpression of Kuk or LaminDm0 Δ N are independent of filament formation and might additionally be related to altered chromatin-NM interactions.

The hypothesis for a lamina independent activity of Kuk is consistent with the results of the RNAi experiments in S2 cells, which indicate that localization of Kuk and lamin Dm0 does not depend on selected lamina and INM proteins. For lamin Dm0 this result was not unexpected since the protein is itself required for structural integrity of the nucleus as well as for the localization of a number of INM proteins. In contrast to the LEM domain proteins otefin, bocksbeutel and dMAN1, and several newly identified nuclear envelope transmembrane proteins that depend on lamins for their INM localization (Wagner *et al.*, 2004; Wagner *et al.*, 2006; Malik *et al.*, 2010), Kuk localizes at the NM even when lamin Dm0 is downregulated, which indicates that Kuk is tethered at the NM without depending on lamin Dm0. The dependence of Kuk NM localization on BAF and p55 was an unexpected finding which suggests that the organization of the NM might depend at a certain extent on its direct or indirect interaction with chromatin. Nevertheless, so far there is no evidence of direct Kuk-chromatin or Kuk-chromatin binding proteins interactions and an interaction of Kuk with BAF and p55 could not be demonstrated by the experiments performed in this study.

BAF, which interacts among others with chromatin and LEM domain proteins (Margalit *et al.*, 2007), is considered to be an adaptor protein between NM and chromatin. The abnormal nuclear morphologies observed upon BAF downregulation, have been attributed to the disruption of interactions between BAF, LEM domain proteins and lamin Dm0 (Furukawa *et al.*, 2003). However, this hypothesis cannot explain the nuclear phenotype of the p55 RNAi treated S2 cells, since p55 is a nucleoplasmic WD-repeat component of histone modifying and chromatin assembly complexes (Tyler *et al.*, 1996; Tyler *et al.*, 2001), which is not expected to interact with NM proteins. Therefore, it seems that changes in chromatin organization induced by downregulation of chromatin associated proteins can affect nuclear shape in a direct or indirect way.

In the *in vitro* liposome binding assay it was observed that farnesylation results in the enrichment of the respective protein in the lipid bound fraction but not in exclusion of the protein from the aqueous phase. This result is consistent with previously published studies using farnesylated peptides (Silvius and l'Heureux, 1994; Rowat *et al.*, 2004), where it was shown that the peptides partition between the aqueous and lipid phases. In the present study, large proteins fragments were used instead of peptides and even the FL protein in the case of Kuk. Therefore the contribution of other protein domains in addition to the CaaX motif, to the determination of the final lipid binding properties cannot be excluded. Nevertheless, the binding affinity of all the protein constructs tested was rather moderate, as expected for farnesylated proteins. Farnesylation is a rather weak lipid modification, and while for other proteins i.e. Ras, a second modification, palmitoylation, follows in order to render the membrane binding more stable (Hancock *et al.*, 1990) nothing similar has been reported to take place in the case of lamins or Kuk.

The goal of this work was to elucidate the mechanism by which nuclear morphology changes are induced when farnesylated NM proteins are overexpressed in the cell. Generally, changes in membrane structure can be primarily achieved by two mechanisms (reviewed in Kozlov, 2010 and schematically shown in Figure 3). The first mechanism involves asymmetric insertion of lipid or protein molecules in one of the two layers of the membrane. The second mechanism involves contraction of boundaries between domains of different lipid phases and in this model, protein molecules can act as scaffolds which stabilize membrane curvature. Considering the results of the liposome deformation assay which showed that farnesylated recombinant proteins interact with liposomes and change their morphology, it is here suggested that farnesylated NM proteins change nuclear shape using the first mechanism, involving asymmetric insertion. Since there is no evidence of altered lipid composition of the bilayer, it is rather proposed that the membrane shape changes are due to asymmetric insertion of

farnesylated protein molecules to the lipid monolayer, which would lead to membrane deformation. Nevertheless, the contribution of lipid asymmetry cannot be excluded. It is possible that the farnesylated moiety of the proteins preferentially associates with specific categories of lipids which would cluster asymmetrically when the protein is inserted to the lipid layer. Contraction of boundaries (second mechanism of membrane deformation) might also in part take place, since it has been shown that prenylated peptides are excluded from lipid raft domains (Zacharias *et al.*, 2002). The exclusion of farnesylated proteins from specific membrane domains could subsequently lead in boundary contraction and altered NM morphology.

In conclusion, the results of this study demonstrate for the first time that farnesylated proteins of the NM affect nuclear shape in absence of a classical nuclear lamina and induce morphological changes to protein free liposomes depending on their farnesylation. The reduction of activity on liposome deformation when the Ig-fold globular part of LaminDm0 Δ N is removed suggests that this domain participates in the membrane deforming activity of lamin Dm0. The absolute requirement of farnesylation for the activity of Kuk and lamin Dm0 constructs on NMs and protein-free liposomes suggests that nuclear morphology changes might be directly arising from the insertion of the proteins to the lipid bilayer of the NM via their lipophilic farnesylated moiety. Nevertheless, the contribution of other mechanisms, including the alteration of NM-chromatin interactions that could consequently affect nuclear structure cannot be excluded.

4.2 Identification of potential Kuk interacting partners

As discussed in 4.1 the experiments in yeast and the *in vitro* liposome deformation assays suggest a direct effect of Kuk on nuclear shape, via interaction with the lipid bilayer of the NM. Nevertheless, the involvement of Kuk-interacting proteins cannot be excluded. The function of Kuk during cellularization in the *Drosophila* embryo can be dissected in two distinct aspects, apical NM ruffling and nuclear elongation. As observed when the Kuk- Δ 353-404 construct was injected in blastoderm embryos, apical nuclear ruffling does not necessarily correlate with nuclear elongation. Even though the Kuk- Δ 353-404 construct has a functional CaaX motif, can be farnesylated and is targeted to the NM it cannot rescue the nuclear elongation phenotype of the *kuk* mutant embryos. These observations imply that only the insertion of farnesylated Kuk into the NM is not sufficient for inducing and maintaining nuclear elongation but other factors might be additionally involved in this process. This hypothesis is further supported by the fact that in HA-LaminDm0 injected *kuk* mutant embryos nuclear elongation cannot be rescued. This indicates that simply increasing the amount of farnesylated NM proteins in the cellularizing embryo is not sufficient for inducing nuclear elongation. The activity of Kuk, either alone or via its interaction with other proteins seems to be specifically required for this process.

Disruption of the MTs in the fly embryo by MT depolymerizing drugs has been shown to result in loss of nuclear elongation during cellularization (Brandt *et al.*, 2006; Pilot *et al.*, 2006). It is therefore possible that MTs or other cytoskeletal elements participate in stabilizing the elongated nuclear shape in the *Drosophila* embryo. The “linkers of nucleoskeleton and cytoskeleton” (LINC) complex, has been shown to link the NM to a variety of cytoskeletal elements (Stewart *et al.*, 2007; Razafsky and Hodzic, 2009) and it involves SUN proteins, nesprins, INM proteins, A-type lamins, MTs and actin filaments. Interaction of Kuk with components of the LINC complex or directly with cytoskeletal elements could explain how Kuk stabilizes nuclear shape during cellularization.

By performing IgG pull down of ZZ-Kuk from *Drosophila* embryonic nuclear lysates, followed by mass spectrometry, a number of potential Kuk interacting partners were identified (Table 7). Among these candidates, cytoskeleton related proteins such as actin isoforms, microtubule binding proteins (i.e. awg) and γ -tubulin were identified. Kuk interaction with γ -tubulin, a component of the centrosome, could explain the disrupted NM-centrosome interaction observed in *kuk* mutants (Pilot *et al.*, 2006). Confirmation of Kuk interaction with the above mentioned candidate proteins is necessary in order to examine their biological significance and to address whether they could participate in the maintenance of nuclear elongation by Kuk during cellularization.

Both downregulation and overexpression of Kuk result in altered heterochromatin structure. Downregulation of Kuk in the fly embryo results in impaired formation of the apically located chromocenter (Brandt *et al.*, 2006), while overexpression of Kuk induces loss of heterochromatin markers, as shown in cultured mammalian cells (Brandt *et al.*, 2008; this study, 3.2.1.2). Identification of Kuk-interacting partners could also provide insight on the effect of Kuk on chromatin structure. Among the potential Kuk interacting partners were regulators of transcription (CtBP, pontin, NotI, moira), transcription factors (DREF), RNA polymerase II and proteins related to chromatin organization (Dp1, su(var)3-9, ISWI, NAP-1, reptin, dMi-2, putzig, tousled-like kinase, nucleoplasmin-like protein) and Nup98, a component of the NPC shown by Kalverda *et al.*, 2010 to be involved in regulation of gene expression in the nucleoplasm. Since A-type lamins have been proposed to regulate gene expression in physiological conditions and in disease by interacting with transcription factors, chromatin binding proteins, chromatin remodeling complex components and even by affecting RNA polymerase II activity (Mattout-Drubezki and Gruenbaum, 2003; Andres and Gonzalez, 2009; Pegoraro *et al.*, 2009), it is interesting to investigate whether Kuk can influence chromatin organization and gene expression using similar mechanisms. The above mentioned identified potential Kuk interacting partners provide a starting point for addressing this possibility.

4.3 The GFP-Kuk HeLa s/a cell line: a quantitative assay for studying ageing related cellular phenotypes

Analysis of Kuk-induced cellular phenotypes such as heterochromatin loss and increased DNA damage in transiently transfected cells renders the quantification of the data difficult and not entirely reliable, due to the variable percentage of transfection efficiency and the non uniform protein expression levels in the transfected cells. In this study, the GFP-Kuk HeLa s/a stable cell line was generated. In this cell line the transgene is integrated in a characterized genomic locus, in which the inducible expression is tightly controlled (mother cell line described in Weidenfeld *et al.*, 2009). Taking advantage of the uniform cell population of this stable cell line, it is possible to perform quantifications by WB, which allows detection of even subtle changes in the levels of the different marker proteins and does not depend on error-prone quantification methods i.e. counting cells showing increased or decreased staining of marker proteins in fixed and stained samples.

The GFP-Kuk HeLa s/a cell line was tested for the characteristic nuclear defects observed in Kuk overexpressing cells, in aged cells or in HGPS cells and these defects, namely abnormal nuclear shape, loss of heterochromatin markers and increased DNA damage could be observed upon induction of GFP-Kuk expression. These results confirm that the cell line recapitulates the cellular phenotypes of ageing or HGPS and is therefore suitable for being used in assays addressing ageing-related cellular phenotypes. Apart from the markers used in this study (HP1, RBBP4, p- γ -H2A.X), other markers can be tested i.e. phosphorylated p53 or Chk2 for detection of DNA damage (Liu *et al.*, 2006), or markers suitable for addressing other aspects of the cellular phenotypes of cells overexpressing La Δ 50, such as hyperproliferative behavior and apoptosis (Bridger and Kill, 2004), impaired DNA repair (Manju *et al.*, 2006; Constantinescu *et al.*, 2010), cell cycle progression defects (Cao *et al.*, 2007; Dechat *et al.*, 2007), accumulation of oxidized proteins (Viteri *et al.*, 2010) and altered Notch signaling (Scaffidi and Misteli, 2008).

In addition, the GFP-Kuk HeLa s/a cell line can be used for testing chemical compounds for their ability to reverse ageing-related cellular phenotypes. Identifying compounds with such activity, could suggest putative therapeutic approaches for HGPS. In this work, it was shown that induction of GFP-Kuk expression in the HeLa s/a cell line in the presence of the FTI ABT-100 can prevent abnormal nuclear shape formation and loss of heterochromatin, which comes in agreement with the results from FTI treatment in cases of La Δ 50 overexpression (Columbaro *et al.*, 2005; Glynn and Glover, 2005; Toth *et al.*, 2005; Yang *et al.*, 2005). Nevertheless, it is not clear whether simply inhibiting the farnesylation of La Δ 50 by FTIs can provide an efficient treatment for HGPS. In a study by Yang *et al.*, 2008, it was shown that in a mouse model, a non

farnesylatable form of La Δ 50 can also induce progeria-like disease phenotypes, albeit less severe than the farnesylatable form. Therefore, additional therapeutic approaches in addition to the FTIs need to be investigated in order to treat the farnesylation independent cellular phenotypes of the HGPS disease. The inducible stable line generated in this study, provides a suitable assay for screening chemical compounds for their efficacy in reversing or preventing ageing- and HGPS-related cellular phenotypes.

FTIs could inhibit the farnesylation of GFP-Kuk in the induced GFP-Kuk HeLa s/a line but not with 100% efficiency, especially at treatments longer than 5 d. Generating a GFP-KukC567S HeLa s/a line and comparing its cellular phenotypes to the ones of the GFP-Kuk expressing line could also be useful. In this way, the cellular phenotypes arising from accumulation of farnesylated GFP-Kuk in the nucleus can be distinguished from the ones that are farnesylation independent.

4.4 Analyzing the interplay of NM alterations and chromatin by DamID

Regulation of gene expression is affected by spatial arrangement of chromatin in the nucleus. Interaction of genes with the components of the nuclear lamina has generally been associated with transcriptional repression (reviewed in Akhtar and Gasser, 2007). Nuclear envelope proteins have been shown to transcriptionally regulate genes at the nuclear periphery by various mechanisms such as direct binding to transcription factors, recruitment of chromatin modifiers or interplay with signal transduction pathways (Shaklai *et al.*, 2007; Andres and Gonzalez 2009). Genomic elements that associate with the nuclear lamina in *Drosophila* cells have already been identified, by using the DamID technique for lamin Dm0 (Pickersgill *et al.*, 2006). The lamin Dm0 associated genomic regions were found to be transcriptionally inactive, late replicating and poor in active histone marks, thus confirming the general view of the nuclear periphery as a platform for mostly inactive chromatin.

In this work, DamID was performed in order to identify Kuk interacting genomic regions in *Drosophila* Kc167 cells. Comparison of the Kuk DamID results to the lamin Dm0 DamID results obtained in parallel, showed that the Kuk and lamin Dm0 interacting genomic regions highly overlap. Since the two proteins show the same topology in the nucleus, this result was rather expected. When the linear maps of Kuk and lamin Dm0 interaction along the chromosomes were compared, Kuk gave stronger peaks, which in general makes the definition of the borders of the Kuk interacting genomic regions easier than the respective borders for lamin Dm0. Considering these observations, Kuk is a suitable NM protein to be used for further analysis of NM-chromatin interactions by DamID.

La Δ 50 expressing HGPS cells, cells overexpressing Kuk or permanently farnesylated lamin variants and aged cells share common cellular phenotypes including altered nuclear shape and loss of heterochromatin markers. All these different situations share a common feature; the altered NM composition due to the overexpression of a farnesylated NM protein. Therefore, analyzing the interplay between components of the NM and chromatin can elucidate how changing the structure of the NM, by overexpressing farnesylated proteins, results in disruption of heterochromatin and potentially altered gene expression.

In order to analyze the interplay of altered NM structure with chromatin, it was examined in this work whether Kuk overexpression in cultured *Drosophila* cells affects the association of lamina interacting genomic regions with the lamina. Comparison of the lamin Dm0 DamID results under control and Kuk overexpression conditions showed that increased Kuk amounts do not affect the interaction of the nuclear lamina with chromatin. Strikingly, a defined number of genomic loci were found to be of increased accessibility upon Kuk overexpression. These loci were not found to interact with Kuk or lamin Dm0. Since the genomic regions interacting with HP1 and Su(var)3-9 (Greil *et al.*, 2003; de Wit *et al.*, 2005, 2007), polycomb group (PcG) proteins (Tolhuis *et al.*, 2006), FL Nup98, Nup50 and Nup62 and NPC tethered Nup98 have already been identified (Kalverda *et al.*, 2010), it would be interesting to investigate whether the genomic loci affected by Kuk overexpression associate with one or more of the above mentioned proteins.

The loss of heterochromatin in aged or HGPS cells has been described by showing that several heterochromatin markers and chromatin remodeling complex components are severely reduced (Scaffidi and Misteli, 2006; Pegoraro *et al.*, 2009). However, identification of specific genes affected by these heterochromatin defects has not been reported. Age-related transcriptional activation of p53 targets has been described by comparative analysis of genes expressed in the skeletal muscle of young and old mice (Edwards *et al.*, 2007) and several downstream components of the Notch signaling pathway were found to be activated in La Δ 50 expressing cells (Scaffidi and Misteli, 2008). Nevertheless, due to the great heterogeneity between ageing-related gene expression patterns in different tissues and different organisms (Somel *et al.*, 2006; Zahn *et al.*, 2007), it is rather difficult to identify ageing-related changes in gene expression simply by comparing the gene expression profiles of young and old (or HGPS) individuals. Using DamID in control and Kuk overexpressing cells as described in this study, it was possible to identify in a defined way genomic regions that respond to NM alterations. The loci showing the highest increase in accessibility upon Kuk overexpression seem to mainly be located in genes and not in intergenic regions. It is therefore important to investigate whether this increased accessibility is followed by altered gene expression. In addition it would be interesting

to examine whether among the genes found to be rendered more accessible there is any enrichment in genes represented in certain gene ontology groups.

Since Kuk overexpression induces life span shortening and ageing-related phenotypes in the adult fly (Brandt *et al.*, 2008), the Kuk overexpressing fly can be used for studying different aspects of ageing. A DamID based assay similar to the one described in this study can also be performed *in vivo*, in Kuk overexpressing flies, in order to examine whether comparable genomic regions to the ones identified in cultured cells are found to be affected by the overexpression of Kuk in the adult organism. The *in vivo* DamID based assay could also be used for comparing the genes affected by Kuk overexpression in different tissues or in different cell types in a defined tissue. Identification of specific genes the expression of which is altered in accelerated ageing or in physiological ageing situations can elucidate whether and how the heterochromatin loss observed in these situations is linked to the organismal defects.

4.5 Involvement of NM components in positioning of the X chromosome in male *Drosophila* cells

In contrast to the nuclear periphery that is generally refractory for gene expression, the NPC is thought to be linked to active transcription. An example of increased gene expression related to the NPC is the dosage compensated X chromosome in *Drosophila*. The association of the X chromosome with the NPC components Nup153 and Mtor in *Drosophila* S2 cells (male cells) was found to be required for its hyperactivation by the MSL complex (Mendjan *et al.*, 2006). Depletion of the above mentioned NPC components by RNAi was found to result in decondensation of the X chromosome, detachment from the nuclear periphery where it is normally found to localize and most importantly loss of dosage compensation. Driven by the observations of Mendjan *et al.*, it was analyzed in this study whether the peripheral localization of the X chromosome in male cells depends on proteins of the NM or other nuclear proteins. Strikingly, RNAi mediated downregulation of Kuk, BAF, p55 and Sbr gave an equally strong effect on mislocalization of the X chromosome as the downregulation of Mtor and Nup153.

An explanation why the NPC is related to active genes is provided by the “gene-gating” hypothesis, according to which association of actively transcribed genes with the NPC enhances the efficiency of the export of newly synthesized mRNA (Blobel, 1985). Kuk, which was found to influence association of the X chromosome with the nuclear periphery, is a NM protein and not a NPC component. This result suggests that there might be functional interactions of non pore components with the NPC in order to achieve efficient mRNA export. Similar functional interaction of a non NPC component with the NPC has been reported for the nuclear periphery protein Esc1p in yeast (Lewis *et al.*, 2007). Coupling of mRNA export with regulation of gene

expression could also explain the effect of Sbr downregulation on X chromosome localization. Sbr is the fly homologue of the human TAP/NXF-1 mRNA export factor and was found to be required for mRNA export throughout development (Wilkie *et al.*, 2001). Another explanation for the role of Kuk in the peripheral localization of the X chromosome, independent from mRNA export, might be that NM components are required for stabilizing the X chromosome at the nuclear periphery. This idea could also explain why BAF was found to influence X chromosome localization. As discussed in 4.1, BAF serves as an adaptor protein between chromatin and NM. Depletion of BAF could disturb the NM-chromatin interaction thus leading in mislocalization of the X chromosome. Nevertheless, careful interpretation is required concerning data obtained by BAF downregulation, since the cells show a variety of nuclear defects such as severe alterations of nuclear shape, nuclear division defects and loss of lamina and INM components (Furukawa *et al.*, 2003; Margalit *et al.*, 2005; this study 3.1.8 and Figure 22). p55, the fly homolog of RBBP4/RBBP7 is a nucleoplasmic WD-repeat component of the nucleosome remodeling factor (NURF) and chromatin assembly complex 1 (CAF-1) (Martinez-Balbas *et al.*, 1998). The observed decondensation and mislocalization of the X chromosome upon p55 downregulation might be due to defective chromatin assembly. Since like in the case of BAF, p55 depletion leads in nuclear defects, in particular enlargement of the nuclei as described in 3.1.8 and shown in Figure 22, the possibility that the X chromosome decondensation is due to indirect consequences of the p55 depletion cannot be excluded.

Apart from analyzing the mechanism via which the above mentioned nuclear proteins affect the localization of the X chromosome in male cells, it is important to investigate whether the observed mislocalization and/or decondensation correlates with defective hyperactivation of X-linked genes. Even though in the study of Mendjan *et al.*, Nup153 and Mtor were found to be essential for dosage compensation, when similar experiments were performed by Grimaud and Becker, 2009, in S2 cells and in *Drosophila* larvae, assembly of the dosage compensation complex, targeting of the X chromosome and conformation of the X chromosome were not found to depend on Nup153 and Mtor. According to Grimaud and Becker, the observations of Mendjan *et al.*, are due to indirect consequences of cell death induced by the loss of the two NPC proteins. In addition, enrichment of Nups could not be observed on the male X chromosome in polytene chromosome stainings or by DamID experiments using male cell lines (Kalverda *et al.*, 2010). In the same study, by performing DamID experiments for different Nups, it was found that the NPC seems to interact with not particularly active genes and that NPC components indeed stimulate gene expression, not at the NPC but in the nucleoplasm. Similar data was obtained by Capelson *et al.*, 2010, suggesting a direct function of Nups in regulating gene expression away from the NPC. It is therefore highly possible that the role of NM or chromatin

associated proteins in regulating X chromosome localization and potentially hyperactivation is not linked to the NPC.

Taken together, the results from the DamID experiments upon Kuk overexpression, where specific genomic loci were found to be of increased accessibility and the results from the downregulation of Kuk in male *Drosophila* cells which induced mislocalization of the X chromosome, indicate that modification of the levels of NM components can affect chromatin structure. What remains to be investigated, is whether the observed modifications of chromatin structure are accompanied by changes in gene expression levels.

5. References

- Akhtar, A., and Gasser, S.M. (2007). The nuclear envelope and transcriptional control. *Nature reviews* 8, 507-517.
- Alberts, B. (2002). *Molecular biology of the cell*. (Garland Science: New York).
- Andres, V., and Gonzalez, J.M. (2009). Role of A-type lamins in signaling, transcription, and chromatin organization. *J Cell Biol* 187, 945-957.
- Andrulis, E.D., Neiman, A.M., Zappulla, D.C., and Sternglanz, R. (1998). Perinuclear localization of chromatin facilitates transcriptional silencing. *Nature* 394, 592-595.
- Beaudouin, J., Gerlich, D., Daigle, N., Eils, R., and Ellenberg, J. (2002). Nuclear envelope breakdown proceeds by microtubule-induced tearing of the lamina. *Cell* 108, 83-96.
- Ben-Harush, K., Wiesel, N., Frenkiel-Krispin, D., Moeller, D., Soreq, E., Aebi, U., Herrmann, H., Gruenbaum, Y., and Medalia, O. (2009). The supramolecular organization of the *C. elegans* nuclear lamin filament. *Journal of molecular biology* 386, 1392-1402.
- Blobel, G. (1985). Gene gating: a hypothesis. *Proc Natl Acad Sci U S A* 82, 8527-8529.
- Bengtsson, L., and Wilson, K.L. (2006). Barrier-to-autointegration factor phosphorylation on Ser-4 regulates emerin binding to lamin A in vitro and emerin localization in vivo. *Mol Biol Cell* 17, 1154-1163.
- Brandt, A., Krohne, G., and Grosshans, J. (2008). The farnesylated nuclear proteins KUGELKERN and LAMIN B promote aging-like phenotypes in *Drosophila* flies. *Aging Cell* 7, 541-551.
- Brandt, A., Papagiannouli, F., Wagner, N., Wilsch-Brauninger, M., Braun, M., Furlong, E.E., Loserth, S., Wenzl, C., Pilot, F., Vogt, N., Lecuit, T., Krohne, G., and Grosshans, J. (2006). Developmental control of nuclear size and shape by Kugelkern and Kurzkern. *Curr Biol* 16, 543-552.
- Bridger, J.M., and Kill, I.R. (2004). Aging of Hutchinson-Gilford progeria syndrome fibroblasts is characterised by hyperproliferation and increased apoptosis. *Exp Gerontol* 39, 717-724.
- Broers, J.L., Hutchison, C.J., and Ramaekers, F.C. (2004). Laminopathies. *J Pathol* 204, 478-488.
- Campelo, F., McMahon, H.T., and Kozlov, M.M. (2008). The hydrophobic insertion mechanism of membrane curvature generation by proteins. *Biophys J* 95, 2325-2339.
- Broers, J.L., Machiels, B.M., van Eys, G.J., Kuijpers, H.J., Manders, E.M., van Driel, R., and Ramaekers, F.C. (1999). Dynamics of the nuclear lamina as monitored by GFP-tagged A-type lamins. *J Cell Sci* 112 (Pt 20), 3463-3475.
- Cao, K., Capell, B.C., Erdos, M.R., Djabali, K., and Collins, F.S. (2007). A lamin A protein isoform overexpressed in Hutchinson-Gilford progeria syndrome interferes with mitosis in progeria and normal cells. *Proc Natl Acad Sci U S A* 104, 4949-4954.
- Capanni, C., Cenni, V., Haraguchi, T., Squarzoni, S., Schuchner, S., Ogris, E., Novelli, G., Maraldi, N.M., and Lattanzi, G. (2010). Lamin A precursor induces barrier-to-autointegration factor nuclear localization. *Cell Cycle* 9.
- Capanni, C., Del Coco, R., Mattioli, E., Camozzi, D., Columbaro, M., Schena, E., Merlini, L., Squarzoni, S., Maraldi, N.M., and Lattanzi, G. (2009). Emerin-prelamin A interplay in human fibroblasts. *Biol Cell* 101, 541-554.

- Capell, B.C., and Collins, F.S. (2006). Human laminopathies: nuclei gone genetically awry. *Nature reviews* 7, 940-952.
- Capell, B.C., Erdos, M.R., Madigan, J.P., Fiordalisi, J.J., Varga, R., Conneely, K.N., Gordon, L.B., Der, C.J., Cox, A.D., and Collins, F.S. (2005). Inhibiting farnesylation of progerin prevents the characteristic nuclear blebbing of Hutchinson-Gilford progeria syndrome. *Proc Natl Acad Sci U S A* 102, 12879-12884.
- Capelson, M., Liang, Y., Schulte, R., Mair, W., Wagner, U., and Hetzer, M.W. (2010). Chromatin-bound nuclear pore components regulate gene expression in higher eukaryotes. *Cell* 140, 372-383.
- Chi, Y.H., Chen, Z.J., and Jeang, K.T. (2009). The nuclear envelopathies and human diseases. *J Biomed Sci* 16, 96.
- Cohen, M., Lee, K.K., Wilson, K.L., and Gruenbaum, Y. (2001). Transcriptional repression, apoptosis, human disease and the functional evolution of the nuclear lamina. *Trends Biochem Sci* 26, 41-47.
- Cohen, T.V., Hernandez, L., and Stewart, C.L. (2008). Functions of the nuclear envelope and lamina in development and disease. *Biochem Soc Trans* 36, 1329-1334.
- Columbaro, M., Capanni, C., Mattioli, E., Novelli, G., Parnaik, V.K., Squarzone, S., Maraldi, N.M., and Lattanzi, G. (2005). Rescue of heterochromatin organization in Hutchinson-Gilford progeria by drug treatment. *Cell Mol Life Sci* 62, 2669-2678.
- Constantinescu, D., Csoka, A.B., Navara, C.S., and Schatten, G.P. (2010). Defective DSB repair correlates with abnormal nuclear morphology and is improved with FTI treatment in Hutchinson-Gilford progeria syndrome fibroblasts. *Exp Cell Res*.
- De Sandre-Giovannoli, A., Bernard, R., Cau, P., Navarro, C., Amiel, J., Boccaccio, I., Lyonnet, S., Stewart, C.L., Munnich, A., Le Merrer, M., and Levy, N. (2003). Lamin A truncation in Hutchinson-Gilford progeria. *Science* 300, 2055.
- de Wit, E., Greil, F., and van Steensel, B. (2005). Genome-wide HP1 binding in *Drosophila*: developmental plasticity and genomic targeting signals. *Genome Res* 15, 1265-1273.
- de Wit, E., Greil, F., and van Steensel, B. (2007). High-resolution mapping reveals links of HP1 with active and inactive chromatin components. *PLoS Genet* 3, e38.
- DeBusk, F.L. (1972). The Hutchinson-Gilford progeria syndrome. Report of 4 cases and review of the literature. *J Pediatr* 80, 697-724.
- Dechat, T., Gajewski, A., Korbei, B., Gerlich, D., Daigle, N., Haraguchi, T., Furukawa, K., Ellenberg, J., and Foisner, R. (2004). LAP2alpha and BAF transiently localize to telomeres and specific regions on chromatin during nuclear assembly. *J Cell Sci* 117, 6117-6128.
- Dechat, T., Korbei, B., Vaughan, O.A., Vlcek, S., Hutchison, C.J., and Foisner, R. (2000). Lamina-associated polypeptide 2alpha binds intranuclear A-type lamins. *J Cell Sci* 113 Pt 19, 3473-3484.
- Dechat, T., Shimi, T., Adam, S.A., Rusinol, A.E., Andres, D.A., Spielmann, H.P., Sinensky, M.S., and Goldman, R.D. (2007). Alterations in mitosis and cell cycle progression caused by a mutant lamin A known to accelerate human aging. *Proc Natl Acad Sci U S A* 104, 4955-4960.
- Delbarre, E., Tramier, M., Coppey-Moisan, M., Gaillard, C., Courvalin, J.C., and Buendia, B. (2006). The truncated prelamin A in Hutchinson-Gilford progeria syndrome alters segregation of A-type and B-type lamin homopolymers. *Hum Mol Genet* 15, 1113-1122.

- Edwards, M.G., Anderson, R.M., Yuan, M., Kendziorski, C.M., Weindruch, R., and Prolla, T.A. (2007). Gene expression profiling of aging reveals activation of a p53-mediated transcriptional program. *BMC Genomics* 8, 80.
- Erber, A., Riemer, D., Bovenschulte, M., and Weber, K. (1998). Molecular phylogeny of metazoan intermediate filament proteins. *J Mol Evol* 47, 751-762.
- Eriksson, M., Brown, W.T., Gordon, L.B., Glynn, M.W., Singer, J., Scott, L., Erdos, M.R., Robbins, C.M., Moses, T.Y., Berglund, P., Dutra, A., Pak, E., Durkin, S., Csoka, A.B., Boehnke, M., Glover, T.W., and Collins, F.S. (2003). Recurrent de novo point mutations in lamin A cause Hutchinson-Gilford progeria syndrome. *Nature* 423, 293-298.
- Finlan, L.E., Sproul, D., Thomson, I., Boyle, S., Kerr, E., Perry, P., Ylstra, B., Chubb, J.R., and Bickmore, W.A. (2008). Recruitment to the nuclear periphery can alter expression of genes in human cells. *PLoS Genet* 4, e1000039.
- Foisner, R. (2001). Inner nuclear membrane proteins and the nuclear lamina. *J Cell Sci* 114, 3791-3792.
- Foisner, R., and Gerace, L. (1993). Integral membrane proteins of the nuclear envelope interact with lamins and chromosomes, and binding is modulated by mitotic phosphorylation. *Cell* 73, 1267-1279.
- Fong, L.G., Ng, J.K., Meta, M., Cote, N., Yang, S.H., Stewart, C.L., Sullivan, T., Burghardt, A., Majumdar, S., Reue, K., Bergo, M.O., and Young, S.G. (2004). Heterozygosity for *Lmna* deficiency eliminates the progeria-like phenotypes in *Zmpste24*-deficient mice. *Proc Natl Acad Sci U S A* 101, 18111-18116.
- Furukawa, K., Sugiyama, S., Osouda, S., Goto, H., Inagaki, M., Horigome, T., Omata, S., McConnell, M., Fisher, P.A., and Nishida, Y. (2003). Barrier-to-autointegration factor plays crucial roles in cell cycle progression and nuclear organization in *Drosophila*. *J Cell Sci* 116, 3811-3823.
- Gant, T.M., Harris, C.A., and Wilson, K.L. (1999). Roles of LAP2 proteins in nuclear assembly and DNA replication: truncated LAP2beta proteins alter lamina assembly, envelope formation, nuclear size, and DNA replication efficiency in *Xenopus laevis* extracts. *J Cell Biol* 144, 1083-1096.
- Gilford H (1904) Ateleiosis and progeria: continuous youth and premature old age. *British Medical Journal* 2: 914-918.
- Giot, L., Bader, J.S., Brouwer, C., Chaudhuri, A., Kuang, B., Li, Y., Hao, Y.L., Ooi, C.E., Godwin, B., Vitols, E., Vijayadamar, G., Pochart, P., Machineni, H., Welsh, M., Kong, Y., Zerhusen, B., Malcolm, R., Varrone, Z., Collis, A., Minto, M., Burgess, S., McDaniel, L., Stimpson, E., Spriggs, F., Williams, J., Neurath, K., Ioime, N., Agee, M., Voss, E., Furtak, K., Renzulli, R., Aanensen, N., Carroll, S., Bickelhaupt, E., Lazovatsky, Y., DaSilva, A., Zhong, J., Stanyon, C.A., Finley, R.L., Jr., White, K.P., Braverman, M., Jarvie, T., Gold, S., Leach, M., Knight, J., Shimkets, R.A., McKenna, M.P., Chant, J., and Rothberg, J.M. (2003). A protein interaction map of *Drosophila melanogaster*. *Science* 302, 1727-1736.
- Glynn, M.W., and Glover, T.W. (2005). Incomplete processing of mutant lamin A in Hutchinson-Gilford progeria leads to nuclear abnormalities, which are reversed by farnesyltransferase inhibition. *Hum Mol Genet* 14, 2959-2969.
- Goldberg, M., Lu, H., Stuurman, N., Ashery-Padan, R., Weiss, A.M., Yu, J., Bhattacharyya, D., Fisher, P.A., Gruenbaum, Y., and Wolfner, M.F. (1998). Interactions among *Drosophila* nuclear envelope proteins lamin, otefin, and YA. *Mol Cell Biol* 18, 4315-4323.
- Goldman, R.D., Gruenbaum, Y., Moir, R.D., Shumaker, D.K., and Spann, T.P. (2002). Nuclear lamins: building blocks of nuclear architecture. *Genes Dev* 16, 533-547.

- Goldman, R.D., Shumaker, D.K., Erdos, M.R., Eriksson, M., Goldman, A.E., Gordon, L.B., Gruenbaum, Y., Khuon, S., Mendez, M., Varga, R., and Collins, F.S. (2004). Accumulation of mutant lamin A causes progressive changes in nuclear architecture in Hutchinson–Gilford progeria syndrome. *Proc Natl Acad Sci U S A* *101*, 8963-8968.
- Greil, F., van der Kraan, I., Delrow, J., Smothers, J.F., de Wit, E., Bussemaker, H.J., van Driel, R., Henikoff, S., and van Steensel, B. (2003). Distinct HP1 and Su(var)3-9 complexes bind to sets of developmentally coexpressed genes depending on chromosomal location. *Genes Dev* *17*, 2825-2838.
- Grimaud, C., and Becker, P.B. (2009). The dosage compensation complex shapes the conformation of the X chromosome in *Drosophila*. *Genes Dev* *23*, 2490-2495.
- Guelen, L., Pagie, L., Brasset, E., Meuleman, W., Faza, M.B., Talhout, W., Eussen, B.H., de Klein, A., Wessels, L., de Laat, W., and van Steensel, B. (2008). Domain organization of human chromosomes revealed by mapping of nuclear lamina interactions. *Nature* *453*, 948-951.
- Haithecock, E., Dayani, Y., Neufeld, E., Zahand, A.J., Feinstein, N., Mattout, A., Gruenbaum, Y., and Liu, J. (2005). Age-related changes of nuclear architecture in *Caenorhabditis elegans*. *Proc Natl Acad Sci U S A* *102*, 16690-16695.
- Hancock, J.F., Paterson, H., and Marshall, C.J. (1990). A polybasic domain or palmitoylation is required in addition to the CAAX motif to localize p21ras to the plasma membrane. *Cell* *63*, 133-139.
- Haque, F., Lloyd, D.J., Smallwood, D.T., Dent, C.L., Shanahan, C.M., Fry, A.M., Trembath, R.C., and Shackleton, S. (2006). SUN1 interacts with nuclear lamin A and cytoplasmic nesprins to provide a physical connection between the nuclear lamina and the cytoskeleton. *Mol Cell Biol* *26*, 3738-3751.
- Harbury, P.B., Zhang, T., Kim, P.S., and Alber, T. (1993). A switch between two-, three-, and four-stranded coiled coils in GCN4 leucine zipper mutants. *Science* *262*, 1401-1407.
- Hattier, T., Andrulis, E.D., and Tartakoff, A.M. (2007). Immobility, inheritance and plasticity of shape of the yeast nucleus. *BMC Cell Biol* *8*, 47.
- Herrmann, H., Strelkov, S.V., Burkhard, P., and Aebi, U. (2009). Intermediate filaments: primary determinants of cell architecture and plasticity. *J Clin Invest* *119*, 1772-1783.
- Hoffmann, K., Sperling, K., Olins, A.L., and Olins, D.E. (2007). The granulocyte nucleus and lamin B receptor: avoiding the ovoid. *Chromosoma* *116*, 227-235.
- Holaska, J.M., Lee, K.K., Kowalski, A.K., and Wilson, K.L. (2003). Transcriptional repressor germ cell-less (GCL) and barrier to autointegration factor (BAF) compete for binding to emerin in vitro. *J Biol Chem* *278*, 6969-6975.
- Houben, F., Ramaekers, F.C., Snoeckx, L.H., and Broers, J.L. (2007). Role of nuclear lamina-cytoskeleton interactions in the maintenance of cellular strength. *Biochim Biophys Acta* *1773*, 675-686.
- Hutchinson J (1886) Case of congenital absence of hair, with atrophic condition of the skin and its appendages, in a boy whose mother had been almost wholly bald from alopecia areata from the age of six. *Lancet* *1*: 923.
- Hutchison, C.J., Bridger, J.M., Cox, L.S., and Kill, I.R. (1994). Weaving a pattern from disparate threads: lamin function in nuclear assembly and DNA replication. *J Cell Sci* *107 (Pt 12)*, 3259-3269.
- Ichijima, Y., Sakasai, R., Okita, N., Asahina, K., Mizutani, S., and Teraoka, H. (2005). Phosphorylation of histone H2AX at M phase in human cells without DNA damage response. *Biochem Biophys Res Commun* *336*, 807-812.

- Ivorra, C., Kubicek, M., Gonzalez, J.M., Sanz-Gonzalez, S.M., Alvarez-Barrientos, A., O'Connor, J.E., Burke, B., and Andres, V. (2006). A mechanism of AP-1 suppression through interaction of c-Fos with lamin A/C. *Genes Dev* 20, 307-320.
- Janke, C., Magiera, M.M., Rathfelder, N., Taxis, C., Reber, S., Maekawa, H., Moreno-Borchart, A., Doenges, G., Schwob, E., Schiebel, E., and Knop, M. (2004). A versatile toolbox for PCR-based tagging of yeast genes: new fluorescent proteins, more markers and promoter substitution cassettes. *Yeast* 21, 947-962.
- Ji, J.Y., Lee, R.T., Vergnes, L., Fong, L.G., Stewart, C.L., Reue, K., Young, S.G., Zhang, Q., Shanahan, C.M., and Lammerding, J. (2007). Cell nuclei spin in the absence of lamin b1. *J Biol Chem* 282, 20015-20026.
- Kalverda, B., Pickersgill, H., Shloma, V.V., and Fornerod, M. (2010). Nucleoporins directly stimulate expression of developmental and cell-cycle genes inside the nucleoplasm. *Cell* 140, 360-371.
- Kapinos, L.E., Schumacher, J., Mucke, N., Machaidze, G., Burkhard, P., Aebi, U., Strelkov, S.V., and Herrmann, H. (2009). Characterization of the Head-to-Tail Overlap Complexes Formed by Human Lamin A, B1 and B2 "Half-minilamin" Dimers. *Journal of molecular biology*.
- Kelley, L.A., and Sternberg, M.J. (2009). Protein structure prediction on the Web: a case study using the Phyre server. *Nat Protoc* 4, 363-371.
- Kitten, G.T., and Nigg, E.A. (1991). The CaaX motif is required for isoprenylation, carboxyl methylation, and nuclear membrane association of lamin B2. *J Cell Biol* 113, 13-23.
- Kozlov, M.M. (2010). Biophysics: Joint effort bends membrane. *Nature* 463, 439-440.
- Krohne, G. (1998). Lamin assembly in vivo. *Subcell Biochem* 31, 563-586.
- Kumaran, R.I., and Spector, D.L. (2008). A genetic locus targeted to the nuclear periphery in living cells maintains its transcriptional competence. *J Cell Biol* 180, 51-65.
- Lammerding, J., Fong, L.G., Ji, J.Y., Reue, K., Stewart, C.L., Young, S.G., and Lee, R.T. (2006). Lamins A and C but not lamin B1 regulate nuclear mechanics. *J Biol Chem* 281, 25768-25780.
- Lammerding, J., Hsiao, J., Schulze, P.C., Kozlov, S., Stewart, C.L., and Lee, R.T. (2005). Abnormal nuclear shape and impaired mechanotransduction in emerin-deficient cells. *J Cell Biol* 170, 781-791.
- Lammerding, J., Schulze, P.C., Takahashi, T., Kozlov, S., Sullivan, T., Kamm, R.D., Stewart, C.L., and Lee, R.T. (2004). Lamin A/C deficiency causes defective nuclear mechanics and mechanotransduction. *J Clin Invest* 113, 370-378.
- Larkin, M.A., Blackshields, G., Brown, N.P., Chenna, R., McGettigan, P.A., McWilliam, H., Valentin, F., Wallace, I.M., Wilm, A., Lopez, R., Thompson, J.D., Gibson, T.J., and Higgins, D.G. (2007). Clustal W and Clustal X version 2.0. *Bioinformatics* 23, 2947-2948.
- Lee, K.K., Haraguchi, T., Lee, R.S., Koujin, T., Hiraoka, Y., and Wilson, K.L. (2001). Distinct functional domains in emerin bind lamin A and DNA-bridging protein BAF. *J Cell Sci* 114, 4567-4573.
- Lewin, B. (2004). *Genes VIII*. Pearson Prentice Hall: Upper Saddle River, NJ.
- Lewis, A., Felberbaum, R., and Hochstrasser, M. (2007). A nuclear envelope protein linking nuclear pore basket assembly, SUMO protease regulation, and mRNA surveillance. *J Cell Biol* 178, 813-827.
- Lin, F., Blake, D.L., Callebaut, I., Skerjanc, I.S., Holmer, L., McBurney, M.W., Paulin-Levasseur, M., and Worman, H.J. (2000). MAN1, an inner nuclear membrane protein that shares the LEM domain with lamina-associated polypeptide 2 and emerin. *J Biol Chem* 275, 4840-4847.

- Liu, Y., Rusinol, A., Sinensky, M., Wang, Y., and Zou, Y. (2006). DNA damage responses in progeroid syndromes arise from defective maturation of prelamin A. *J Cell Sci* *119*, 4644-4649.
- Lloyd, D.J., Trembath, R.C., and Shackleton, S. (2002). A novel interaction between lamin A and SREBP1: implications for partial lipodystrophy and other laminopathies. *Hum Mol Genet* *11*, 769-777.
- Malik, P., Korfali, N., Srsen, V., Lazou, V., Batrakou, D.G., Zuleger, N., Kavanagh, D.M., Wilkie, G.S., Goldberg, M.W., and Schirmer, E.C. (2010). Cell-specific and lamin-dependent targeting of novel transmembrane proteins in the nuclear envelope. *Cell Mol Life Sci*.
- Manju, K., Muralikrishna, B., and Parnaik, V.K. (2006). Expression of disease-causing lamin A mutants impairs the formation of DNA repair foci. *J Cell Sci* *119*, 2704-2714.
- Mansharamani, M., and Wilson, K.L. (2005). Direct binding of nuclear membrane protein MAN1 to emerin in vitro and two modes of binding to barrier-to-autointegration factor. *J Biol Chem* *280*, 13863-13870.
- Margalit, A., Brachner, A., Gotzmann, J., Foisner, R., and Gruenbaum, Y. (2007). Barrier-to-autointegration factor--a BAFfling little protein. *Trends Cell Biol* *17*, 202-208.
- Margalit, A., Segura-Totten, M., Gruenbaum, Y., and Wilson, K.L. (2005). Barrier-to-autointegration factor is required to segregate and enclose chromosomes within the nuclear envelope and assemble the nuclear lamina. *Proc Natl Acad Sci U S A* *102*, 3290-3295.
- Markiewicz, E., Dechat, T., Foisner, R., Quinlan, R.A., and Hutchison, C.J. (2002). Lamin A/C binding protein LAP2alpha is required for nuclear anchorage of retinoblastoma protein. *Mol Biol Cell* *13*, 4401-4413.
- Martinez-Balbas, M.A., Tsukiyama, T., Gdula, D., and Wu, C. (1998). Drosophila NURF-55, a WD repeat protein involved in histone metabolism. *Proc Natl Acad Sci U S A* *95*, 132-137.
- Mattout-Drubezki, A., and Gruenbaum, Y. (2003). Dynamic interactions of nuclear lamina proteins with chromatin and transcriptional machinery. *Cell Mol Life Sci* *60*, 2053-2063.
- Mazumdar, A., and Mazumdar, M. (2002). How one becomes many: blastoderm cellularization in *Drosophila melanogaster*. *Bioessays* *24*, 1012-1022.
- Mendjan, S., Taipale, M., Kind, J., Holz, H., Gebhardt, P., Schelder, M., Vermeulen, M., Buscaino, A., Duncan, K., Mueller, J., Wilm, M., Stunnenberg, H.G., Saumweber, H., and Akhtar, A. (2006). Nuclear pore components are involved in the transcriptional regulation of dosage compensation in *Drosophila*. *Mol Cell* *21*, 811-823.
- Meshorer, E., and Gruenbaum, Y. (2008). Gone with the Wnt/Notch: stem cells in laminopathies, progeria, and aging. *J Cell Biol* *181*, 9-13.
- Mislow, J.M., Holaska, J.M., Kim, M.S., Lee, K.K., Segura-Totten, M., Wilson, K.L., and McNally, E.M. (2002). Nesprin-1alpha self-associates and binds directly to emerin and lamin A in vitro. *FEBS Lett* *525*, 135-140.
- Morgan, D.O. (2007). *The cell cycle: principles of control*. Published by New Science Press in association with Oxford University Press.
- Moulson, C.L., Go, G., Gardner, J.M., van der Wal, A.C., Smitt, J.H., van Hagen, J.M., and Miner, J.H. (2005). Homozygous and compound heterozygous mutations in ZMPSTE24 cause the laminopathy restrictive dermopathy. *J Invest Dermatol* *125*, 913-919.

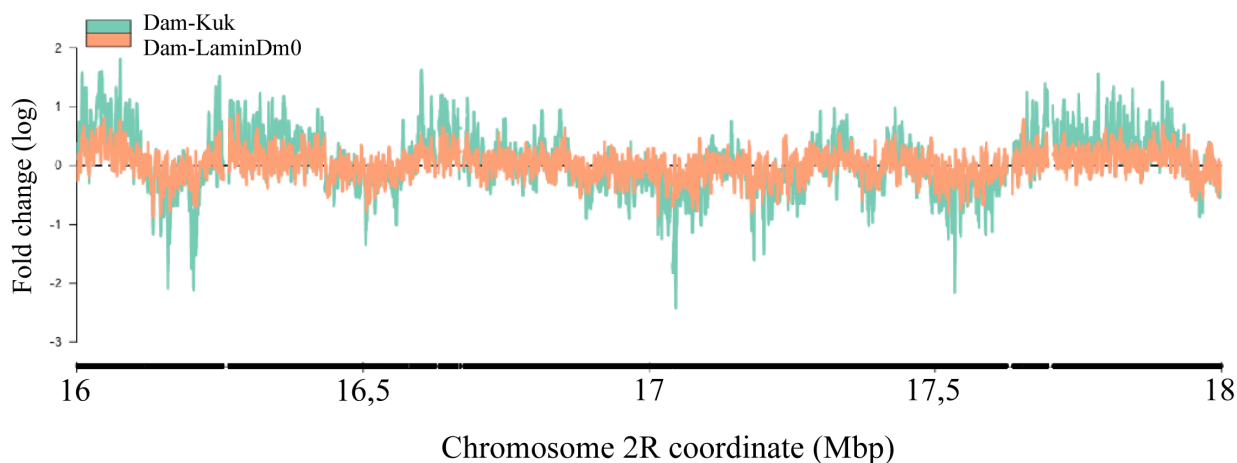
- Navarro, C.L., Cadinanos, J., De Sandre-Giovannoli, A., Bernard, R., Courrier, S., Boccaccio, I., Boyer, A., Kleijer, W.J., Wagner, A., Giuliano, F., Beemer, F.A., Freije, J.M., Cau, P., Hennekam, R.C., Lopez-Otin, C., Badens, C., and Levy, N. (2005). Loss of ZMPSTE24 (FACE-1) causes autosomal recessive restrictive dermopathy and accumulation of Lamin A precursors. *Hum Mol Genet* *14*, 1503-1513.
- Olins, A.L., and Olins, D.E. (2005). The mechanism of granulocyte nuclear shape determination: possible involvement of the centrosome. *Eur J Cell Biol* *84*, 181-188.
- Ozaki, T., Saijo, M., Murakami, K., Enomoto, H., Taya, Y., and Sakiyama, S. (1994). Complex formation between lamin A and the retinoblastoma gene product: identification of the domain on lamin A required for its interaction. *Oncogene* *9*, 2649-2653.
- Pegoraro, G., Kubben, N., Wickert, U., Gohler, H., Hoffmann, K., and Misteli, T. (2009). Ageing-related chromatin defects through loss of the NURD complex. *Nat Cell Biol* *11*, 1261-1267.
- Pickersgill, H., Kalverda, B., de Wit, E., Talhout, W., Fornerod, M., and van Steensel, B. (2006). Characterization of the *Drosophila melanogaster* genome at the nuclear lamina. *Nat Genet* *38*, 1005-1014.
- Pilot, F., Philippe, J.M., Lemmers, C., Chauvin, J.P., and Lecuit, T. (2006). Developmental control of nuclear morphogenesis and anchoring by charleston, identified in a functional genomic screen of *Drosophila* cellularisation. *Development* *133*, 711-723.
- Prufert, K., Vogel, A., and Krohne, G. (2004). The lamin CxxM motif promotes nuclear membrane growth. *J Cell Sci* *117*, 6105-6116.
- Ralle, T., Grund, C., Franke, W.W., and Stick, R. (2004). Intranuclear membrane structure formations by CaaX-containing nuclear proteins. *J Cell Sci* *117*, 6095-6104.
- Razafsky, D., and Hodzic, D. (2009). Bringing KASH under the SUN: the many faces of nucleocytoskeletal connections. *J Cell Biol* *186*, 461-472.
- Reddy, K.L., Zullo, J.M., Bertolino, E., and Singh, H. (2008). Transcriptional repression mediated by repositioning of genes to the nuclear lamina. *Nature* *452*, 243-247.
- Rothbauer, U., Zolghadr, K., Muyldermans, S., Schepers, A., Cardoso, M.C., and Leonhardt, H. (2008). A versatile nanotrap for biochemical and functional studies with fluorescent fusion proteins. *Mol Cell Proteomics* *7*, 282-289.
- Rowat, A.C., Brask, J., Sparrman, T., Jensen, K.J., Lindblom, G., and Ipsen, J.H. (2004). Farnesylated peptides in model membranes: a biophysical investigation. *Eur Biophys J* *33*, 300-309.
- Rowat, A.C., Lammerding, J., and Ipsen, J.H. (2006). Mechanical properties of the cell nucleus and the effect of emerin deficiency. *Biophys J* *91*, 4649-4664.
- Rozema, M.J., Kruger, A.W., Rohde, B.D., Shelat, B., Bhagavatula, L., Tien, J.T., Zhang, W., and Henry, R.F. (2005). Synthesis of a novel farnesyl transferase inhibitor, ABT-100; selective preparation of a stereogenic tertiary carbinol. *Tetrahedron*, Volume 61, Issue 18, (2005) 4419-4425
- Ruault, M., Dubarry, M., and Taddei, A. (2008). Re-positioning genes to the nuclear envelope in mammalian cells: impact on transcription. *Trends Genet* *24*, 574-581.
- Sakaki, M., Koike, H., Takahashi, N., Sasagawa, N., Tomioka, S., Arahata, K., and Ishiura, S. (2001). Interaction between emerin and nuclear lamins. *J Biochem* *129*, 321-327.
- Sambrook and Russel, 2001: *Molecular Cloning, A Laboratory Manual*.

- Sasseville, A.M., and Langelier, Y. (1998). In vitro interaction of the carboxy-terminal domain of lamin A with actin. *FEBS Lett* 425, 485-489.
- Scaffidi, P., and Misteli, T. (2006). Lamin A-dependent nuclear defects in human aging. *Science* 312, 1059-1063.
- Scaffidi, P., and Misteli, T. (2008). Lamin A-dependent misregulation of adult stem cells associated with accelerated ageing. *Nat Cell Biol* 10, 452-459.
- Schejter, E.D., and Wieschaus, E. (1993). Bottleneck acts as a regulator of the microfilament network governing cellularization of the *Drosophila* embryo. *Cell* 75(2), 373-85.
- Shaklai, S., Amariglio, N., Rechavi, G., and Simon, A.J. (2007). Gene silencing at the nuclear periphery. *FEBS J* 274, 1383-1392.
- Shumaker, D.K., Lee, K.K., Tanhehco, Y.C., Craigie, R., and Wilson, K.L. (2001). LAP2 binds to BAF.DNA complexes: requirement for the LEM domain and modulation by variable regions. *EMBO J* 20, 1754-1764.
- Silvius, J.R., and l'Heureux, F. (1994). Fluorimetric evaluation of the affinities of isoprenylated peptides for lipid bilayers. *Biochemistry* 33, 3014-3022.
- Smith, S., and Blobel, G. (1994). Colocalization of vertebrate lamin B and lamin B receptor (LBR) in nuclear envelopes and in LBR-induced membrane stacks of the yeast *Saccharomyces cerevisiae*. *Proc Natl Acad Sci U S A* 91, 10124-10128.
- Somel, M., Khaitovich, P., Bahn, S., Paabo, S., and Lachmann, M. (2006). Gene expression becomes heterogeneous with age. *Curr Biol* 16, R359-360.
- Stewart, C.L., Roux, K.J., and Burke, B. (2007). Blurring the boundary: the nuclear envelope extends its reach. *Science* 318, 1408-1412.
- Stierle, V., Couprie, J., Ostlund, C., Krimm, I., Zinn-Justin, S., Hossenlopp, P., Worman, H.J., Courvalin, J.C., and Duband-Goulet, I. (2003). The carboxyl-terminal region common to lamins A and C contains a DNA binding domain. *Biochemistry* 42, 4819-4828.
- Straub, T., and Becker, P.B. (2007). Dosage compensation: the beginning and end of generalization. *Nature reviews* 8, 47-57.
- Stuurman, N., Heins, S., and Aebi, U. (1998). Nuclear lamins: their structure, assembly, and interactions. *J Struct Biol* 122, 42-66.
- Taddei, A., Hediger, F., Neumann, F.R., Bauer, C., and Gasser, S.M. (2004). Separation of silencing from perinuclear anchoring functions in yeast Ku80, Sir4 and Esc1 proteins. *EMBO J* 23, 1301-1312.
- Taniura, H., Glass, C., and Gerace, L. (1995). A chromatin binding site in the tail domain of nuclear lamins that interacts with core histones. *J Cell Biol* 131, 33-44.
- Thanbichler, M., Wang, S.C., and Shapiro, L. (2005). The bacterial nucleoid: a highly organized and dynamic structure. *J Cell Biochem* 96, 506-521.
- Tolhuis, B., de Wit, E., Muijters, I., Teunissen, H., Talhout, W., van Steensel, B., and van Lohuizen, M. (2006). Genome-wide profiling of PRC1 and PRC2 Polycomb chromatin binding in *Drosophila melanogaster*. *Nat Genet* 38, 694-699.

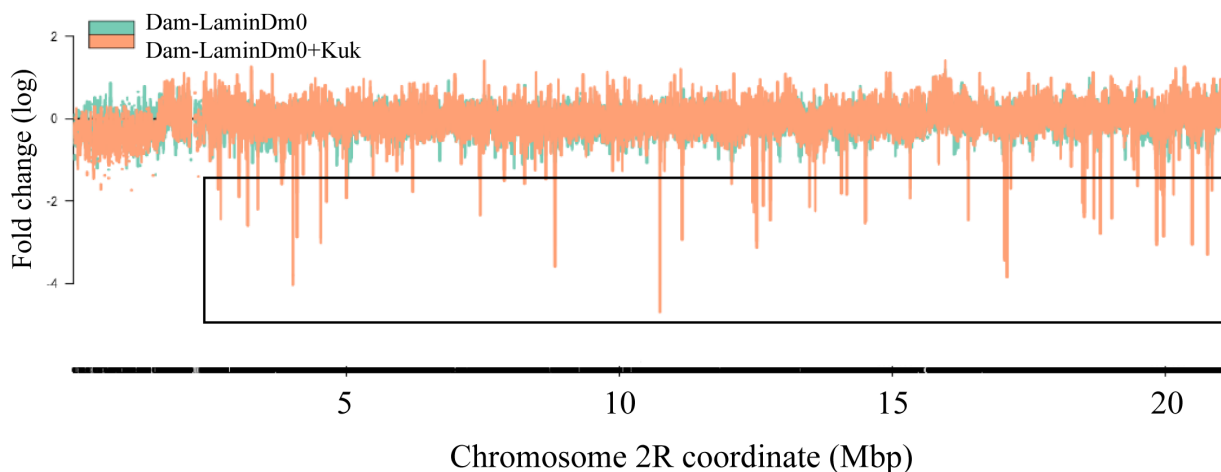
- Toth, J.I., Yang, S.H., Qiao, X., Beigneux, A.P., Gelb, M.H., Moulson, C.L., Miner, J.H., Young, S.G., and Fong, L.G. (2005). Blocking protein farnesyltransferase improves nuclear shape in fibroblasts from humans with progeroid syndromes. *Proc Natl Acad Sci U S A* *102*, 12873-12878.
- Tyler, J.K., Bulger, M., Kamakaka, R.T., Kobayashi, R., and Kadonaga, J.T. (1996). The p55 subunit of *Drosophila* chromatin assembly factor 1 is homologous to a histone deacetylase-associated protein. *Mol Cell Biol* *16*, 6149-6159.
- Tyler, J.K., Collins, K.A., Prasad-Sinha, J., Amriott, E., Bulger, M., Harte, P.J., Kobayashi, R., and Kadonaga, J.T. (2001). Interaction between the *Drosophila* CAF-1 and ASF1 chromatin assembly factors. *Mol Cell Biol* *21*, 6574-6584.
- van Steensel, B., and Henikoff, S. (2000). Identification of in vivo DNA targets of chromatin proteins using tethered dam methyltransferase. *Nat Biotechnol* *18*, 424-428.
- Viteri, G., Chung, Y.W., and Stadtman, E.R. (2010). Effect of progerin on the accumulation of oxidized proteins in fibroblasts from Hutchinson Gilford progeria patients. *Mech Ageing Dev* *131*, 2-8.
- Vogel, M.J., Peric-Hupkes, D., and van Steensel, B. (2007). Detection of in vivo protein-DNA interactions using DamID in mammalian cells. *Nat Protoc* *2*, 1467-1478.
- Wagner, N., Kagermeier, B., Loserth, S., and Krohne, G. (2006). The *Drosophila melanogaster* LEM-domain protein MAN1. *Eur J Cell Biol* *85*, 91-105.
- Wagner, N., Schmitt, J., and Krohne, G. (2004). Two novel LEM-domain proteins are splice products of the annotated *Drosophila melanogaster* gene CG9424 (Bocksbeutel). *Eur J Cell Biol* *82*, 605-616.
- Webster, M., Witkin, K.L., and Cohen-Fix, O. (2009). Sizing up the nucleus: nuclear shape, size and nuclear-envelope assembly. *J Cell Sci* *122*, 1477-1486.
- Weidenfeld, I., Gossen, M., Low, R., Kentner, D., Berger, S., Gorlich, D., Bartsch, D., Bujard, H., and Schonig, K. (2009). Inducible expression of coding and inhibitory RNAs from retargetable genomic loci. *Nucleic Acids Res* *37*, e50.
- Wiesel, N., Mattout, A., Melcer, S., Melamed-Book, N., Herrmann, H., Medalia, O., Aebi, U., and Gruenbaum, Y. (2008). Laminopathic mutations interfere with the assembly, localization, and dynamics of nuclear lamins. *Proc Natl Acad Sci U S A* *105*, 180-185.
- Wilkie, G.S., Zimyanin, V., Kirby, R., Korey, C., Francis-Lang, H., Van Vactor, D., and Davis, I. (2001). Small bristles, the *Drosophila* ortholog of NXF-1, is essential for mRNA export throughout development. *RNA* *7*, 1781-1792.
- Worby, C.A., Simonson-Leff, N., and Dixon, J.E. (2001). RNA interference of gene expression (RNAi) in cultured *Drosophila* cells. *Sci STKE* *2001*, p11.
- Wright, L.P., and Philips, M.R. (2006). Thematic review series: lipid posttranslational modifications. CAAX modification and membrane targeting of Ras. *J Lipid Res* *47*, 883-891.
- Yang, L., Guan, T., and Gerace, L. (1997). Lamin-binding fragment of LAP2 inhibits increase in nuclear volume during the cell cycle and progression into S phase. *J Cell Biol* *139*, 1077-1087.
- Yang, S.H., Andres, D.A., Spielmann, H.P., Young, S.G., and Fong, L.G. (2008). Progerin elicits disease phenotypes of progeria in mice whether or not it is farnesylated. *J Clin Invest* *118*, 3291-3300.
- Yang, S.H., Bergo, M.O., Toth, J.I., Qiao, X., Hu, Y., Sandoval, S., Meta, M., Bendale, P., Gelb, M.H., Young, S.G., and Fong, L.G. (2005). Blocking protein farnesyltransferase improves nuclear blebbing in

- mouse fibroblasts with a targeted Hutchinson-Gilford progeria syndrome mutation. *Proc Natl Acad Sci U S A* *102*, 10291-10296.
- Ye, Q., Callebaut, I., Pezhman, A., Courvalin, J.C., and Worman, H.J. (1997). Domain-specific interactions of human HP1-type chromodomain proteins and inner nuclear membrane protein LBR. *J Biol Chem* *272*(23), 14983-9.
- Ye, Q., and Worman, H.J. (1994). Primary structure analysis and lamin B and DNA binding of human LBR, an integral protein of the nuclear envelope inner membrane. *J Biol Chem* *269*, 11306-11311.
- Young, S.G., Meta, M., Yang, S.H., and Fong, L.G. (2006). Prelamin A farnesylation and progeroid syndromes. *J Biol Chem* *281*, 39741-39745.
- Yu, Y., Vroman, J.A., Bae, S.C., and Granick, S. (2010). Vesicle budding induced by a pore-forming peptide. *J Am Chem Soc* *132*, 195-201.
- Yuan, H., Michelsen, K., and Schwappach, B. (2003). 14-3-3 dimers probe the assembly status of multimeric membrane proteins. *Curr Biol* *13*, 638-646.
- Zacharias, D.A., Violin, J.D., Newton, A.C., and Tsien, R.Y. (2002). Partitioning of lipid-modified monomeric GFPs into membrane microdomains of live cells. *Science* *296*, 913-916.
- Zahn, J.M., Poosala, S., Owen, A.B., Ingram, D.K., Lustig, A., Carter, A., Weeraratna, A.T., Taub, D.D., Gorospe, M., Mazan-Mamczarz, K., Lakatta, E.G., Boheler, K.R., Xu, X., Mattson, M.P., Falco, G., Ko, M.S., Schlessinger, D., Firman, J., Kummerfeld, S.K., Wood, W.H., 3rd, Zonderman, A.B., Kim, S.K., and Becker, K.G. (2007). AGEMAP: a gene expression database for aging in mice. *PLoS Genet* *3*, e201.
- Zastrow, M.S., Vlcek, S., and Wilson, K.L. (2004). Proteins that bind A-type lamins: integrating isolated clues. *J Cell Sci* *117*, 979-987.
- Zink, D., Fischer, A.H., and Nickerson, J.A. (2004). Nuclear structure in cancer cells. *Nat Rev Cancer* *4*, 677-687.

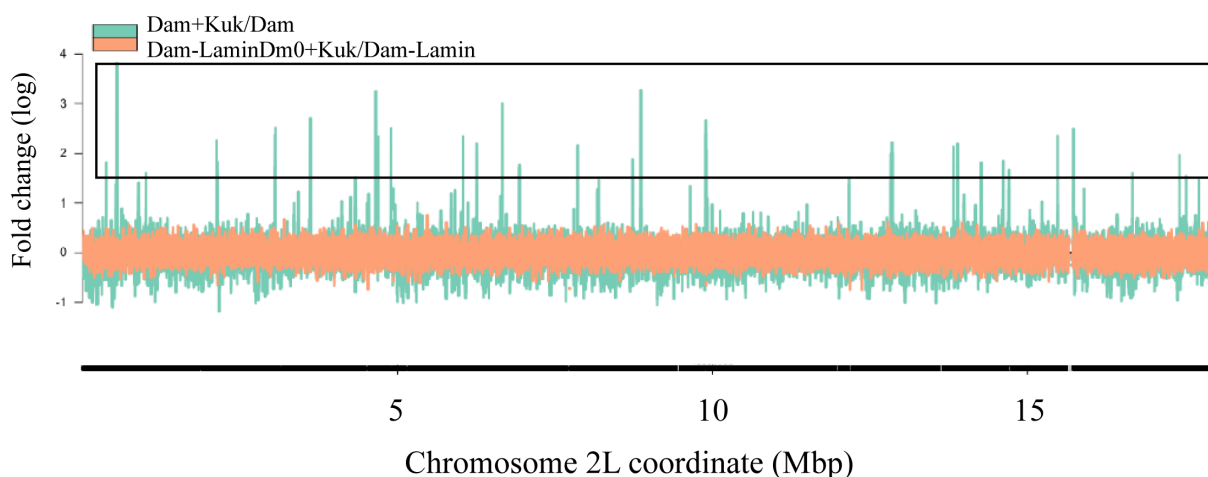
6. Appendix



Appendix 6.1: Interaction of Kuk (teal) and LaminDm0 (orange) with a part of the right arm of chromosome 2 (2R). Similar results were obtained for 2L and for chromosomes 3 and X. This part of chromosome 2R is shown here as a representative example. The data were obtained using *Drosophila* genome tiling arrays. (Analysis performed by M. Fornerod.)



Appendix 6.2: Interaction of LaminDm0 (teal) and LaminDm0+Kuk (orange) with a part of the right arm of chromosome 2 (2R). Similar results were obtained for 2L and for chromosomes 3 and X. This part of chromosome 2R is shown here as a representative example. The data were obtained using *Drosophila* genome tiling arrays. In the black box, the dips observed under Kuk overexpression conditions are selected. (Analysis performed by M. Fornerod.)



Appendix 6.3: Chromatin accessibility under Kuk overexpression conditions (teal) and LaminDm0 chromatin interaction under Kuk overexpression conditions (orange) with a part of the left arm of chromosome 2 (2L). Similar results were obtained for 2R and for chromosomes 3 and X. This part of chromosome 2L is shown here as a representative example. The data were obtained using *Drosophila* genome tiling arrays. In the black box, the peaks in chromatin accessibility observed under Kuk overexpression conditions are selected. (Analysis performed by M. Fornerod.)

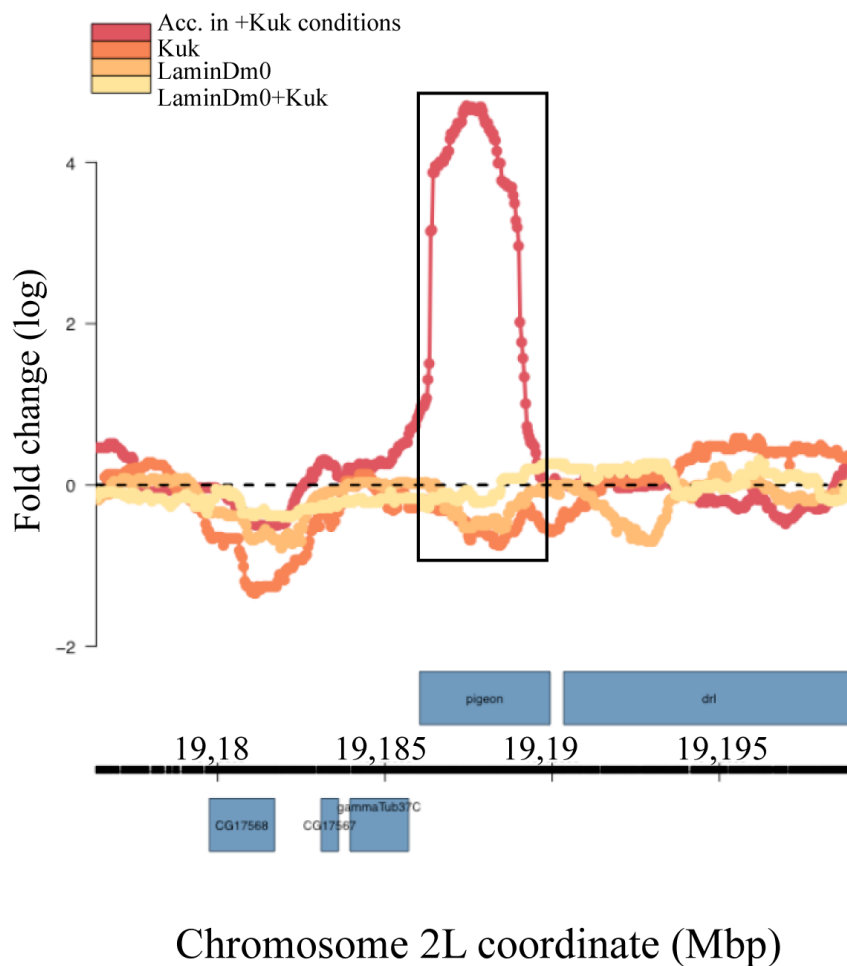
Appendix 6.4: Table of genomic regions showing increased chromatin accessibility upon Kuk overexpression. (Analysis performed by M. Fornerod.)

Chromosome	Start	End	FBID	Max Level	Score	Name
BDGPv5;chr2L	19186215	19189209	FBgn0010309	4,7032882	222,5224	pigeon
BDGPv5;chr3R	19235623	19238286	FBgn0039078	4,5574482	150,144	-
BDGPv5;chr2R	10743908	10747821	FBgn0053506	3,9626573	219,1759	-
BDGPv5;chrX	14641754	14644272	FBgn0015774	3,897958	93,76545	Netrin-B
BDGPv5;chr3L	16058974	16061356	FBgn0005536	3,8752362	114,619	Myosin binding subunit
BDGPv5;chr3L	17503846	17507171	FBgn0036733	3,8432108	159,116	U4-U6 small nuclear riboprotein factor 60K
BDGPv5;chrX	21184148	21187304	FBgn0031171	3,8296258	107,8072	-
BDGPv5;chr2L	553518	555910	FBgn0031262	3,8138403	115,4016	
BDGPv5;chrX	8331642	8334281	FBgn0030038	3,7261281	107,1349	-
BDGPv5;chrX	20122919	20125268	FBgn0015789	3,5280927	77,19378	Rab-protein 10
BDGPv5;chr2R	17063881	17065856	FBgn0003162	3,4171242	85,75983	Punch
BDGPv5;chr3L	18990787	18993209	FBgn0036838	3,4018248	105,4699	-
BDGPv5;chr3L	15598479	15600132	FBgn0036518	3,4003208	69,99734	RhoGAP71E
BDGPv5;chr3L	11565518	11567651	FBgn0053490	3,386456	102,4651	-
BDGPv5;chr3L	17349288	17352429	FBgn0036714	3,3183744	105,7157	-
BDGPv5;chr2L	8864092	8867083	FBgn0052988	3,27401	111,6045	-
BDGPv5;chr3R	18206221	18208799	FBgn0051169	3,2256162	79,89178	-
BDGPv5;chr3L	7587544	7590417	FBgn0035802	3,2176016	80,12819	-
BDGPv5;chr3L	15962538	15965186	FBgn0000212	3,2168373	83,09733	brahma

BDGPv5;chr2R	4020285	4022241	FBgn0005648	3,2036789	65,948	Pabp2
BDGPv5;chr3R	20478123	20480103	FBgn0051125	3,1731013	74,54185	-
BDGPv5;chr2R	20772028	20774865	FBgn0085442	3,1436905	73,36673	Na,K-ATPase Interacting
BDGPv5;chr3L	16708848	16712619	FBgn0000414	3,1257237	108,8664	Disabled
BDGPv5;chrX	10216262	10218063	FBgn0010338	3,0242488	63,23314	
BDGPv5;chr2L	6666921	6669646	FBgn0000392	3,0070327	90,47221	cup
BDGPv5;chr2R	8818825	8822296	FBgn0033783	2,9909082	110,363	-
BDGPv5;chr3R	1200819	1203456	FBgn0037317	2,9384672	80,7555	-
BDGPv5;chr3R	5896864	5899145	FBgn0041105	2,9106516	72,3774	nervous fingers 2
BDGPv5;chr2R	19025198	19027342	FBgn0050192	2,9014382	59,99296	-
BDGPv5;chrX	15986944	15989285	FBgn0030726	2,8876922	58,0871	
BDGPv5;chrX	2236115	2238584	FBgn0003079	2,8730728	61,77363	pole hole
BDGPv5;chrX	21250682	21252751	FBgn0003423	2,8505332	63,59329	sluggish A
BDGPv5;chrX	2499102	2500825	FBgn0004643	2,8434973	49,17772	mitotic 15
BDGPv5;chr3L	9660699	9663835	FBgn0016081	2,7959068	77,85659	furry
BDGPv5;chr3R	6118031	6120948	FBgn0037804	2,7844329	76,5639	-
BDGPv5;chr3L	4858702	4861213	FBgn0047330	2,7608614	61,01208	-
BDGPv5;chrX	1560495	1562410	FBgn0000482	2,7341063	65,32821	deep orange
BDGPv5;chr3R	25676429	25678756	FBgn0039709	2,7270305	65,46555	Cad99C
BDGPv5;chr2L	3624635	3626951	FBgn0000721	2,6971058	69,09852	foraging
BDGPv5;chr2R	18808499	18811586	FBgn0010660	2,680825	83,72832	Nup214
BDGPv5;chrX	6503857	6506502	FBgn0029881	2,669188	62,86449	pickled eggs
BDGPv5;chr2L	9895800	9898447	FBgn0004867	2,6595735	70,6845	string of pearls
BDGPv5;chr3R	5393660	5396169	FBgn0037712	2,6520642	63,60276	-
BDGPv5;chr2R	12514453	12517523	FBgn0040505	2,6484479	64,7643	Alk
BDGPv5;chr2R	20494839	20496986	FBgn0035037	2,6268393	56,65791	
BDGPv5;chr2R	19971815	19974674	FBgn0034974	2,6209446	70,32912	-
BDGPv5;chr2R	12477479	12479113	FBgn0034142	2,6064395	45,48018	-
BDGPv5;chr2R	14500981	14502672	FBgn0034361	2,6064071	48,52292	mitochondrial ribosomal protein S28
BDGPv5;chr2R	2699545	2701058	FBgn0028954	2,6026031	47,70253	-
BDGPv5;chr3L	13842505	13845358	FBgn0029167	2,5990193	82,61942	Hemolectin
BDGPv5;chr3R	25649530	25651779	FBgn0039704	2,5934222	51,30061	-
BDGPv5;chr3R	18118290	18120407	FBgn0051163	2,5805786	44,37764	Shal K[+] channel interacting protein
BDGPv5;chr2R	11153946	11155817	FBgn0083959	2,5386205	49,79736	-
BDGPv5;chr3R	5829886	5831831	FBgn0053208	2,5346299	49,42856	Molecule interacting with CasL
BDGPv5;chr2L	3066103	3069304	FBgn0027571	2,5158219	60,47654	-
BDGPv5;chr2L	4900506	4902893	FBgn0031645	2,5064647	50,38283	-
BDGPv5;chrX	16727379	16728858	FBgn0030797	2,5063141	34,71575	-
BDGPv5;chr2L	15728041	15730548	FBgn0010382	2,4942534	58,85106	Cyclin E
BDGPv5;chr2R	12762876	12765004	FBgn0025833	2,4810569	43,40159	-
BDGPv5;chrX	20070046	20070889	FBgn0067861	2,4797621	11,32389	Sperm-specific dynein intermediate chain 1
BDGPv5;chr3R	6618974	6622019	FBgn0037836	2,4731502	67,03554	-
BDGPv5;chr3R	9035511	9038292	FBgn0038126	2,4725839	58,21157	-
BDGPv5;chr3L	21532229	21534175	FBgn0028663	2,445617	44,21708	VhaM9.7-2
BDGPv5;chrX	3748262	3750057	FBgn0000542	2,4443503	39,0054	echinus
BDGPv5;chr3L	5229784	5232320	FBgn0052423	2,433957	34,20014	alan shepard

BDGPv5;chr3R	21480845	21483686	FBgn0027508	2,4283607	56,30914	tankyrase
BDGPv5;chr3L	4248856	4250971	FBgn0041171	2,4219919	39,93814	archipelago
BDGPv5;chr3R	6067647	6069413	FBgn0037800	2,4163949	42,88245	-
BDGPv5;chr3L	18800142	18802267	FBgn0036814	2,3936603	53,54601	-
BDGPv5;chrX	13041737	13043950	FBgn0052645	2,3876228	45,75169	-
BDGPv5;chr2R	14522842	14525141	FBgn0050122	2,373402	47,5415	-
BDGPv5;chr2L	3060490	3062189	FBgn0027571	2,3728582	37,65121	-
BDGPv5;chr2L	6042927	6045390	FBgn0000052	2,347335	54,62261	adenosine 2
BDGPv5;chr3L	449434	450963	FBgn0001316	2,3472499	37,74167	klarsicht
BDGPv5;chr2L	4701072	4704091	FBgn0085380	2,3424189	62,3897	-
BDGPv5;chrX	9885091	9886918	FBgn0052694	2,3361582	38,24039	-
BDGPv5;chr3R	18002246	18004065	FBgn0051163	2,336007	36,04902	Shal K[+] channel interacting protein
BDGPv5;chrX	8763749	8765623	FBgn0030065	2,33539	29,24183	-
BDGPv5;chr3R	27620979	27623297	FBgn0027620	2,3096137	42,50888	ATP-dependent chromatin assembly factor large subunit
BDGPv5;chrX	7997538	7999766	FBgn0040319	2,3038536	41,26481	Glutamate-cysteine ligase catalytic subunit
BDGPv5;chr3L	16323612	16325426	FBgn0053060	2,2985804	36,30785	-
BDGPv5;chr3L	8485536	8487395	FBgn0035899	2,2936883	30,88856	-
BDGPv5;chr2L	18133898	18136014	FBgn0001301	2,2780724	41,79223	kelch
BDGPv5;chrX	13132579	13134085	FBgn0004456	2,2636306	31,12379	multiple edematous wings
BDGPv5;chr2L	2135771	2137516	FBgn0004507	2,2608594	29,51258	Glycogen phosphorylase
BDGPv5;chr3L	8109637	8111504	FBgn0026252	2,2518066	40,67861	moleskin
BDGPv5;chr3R	18550080	18551776	FBgn0039013	2,196607	32,54068	-
BDGPv5;chrX	18268388	18270546	FBgn0014467	2,1960747	32,96851	Cyclic-AMP response element binding protein B at 17A
BDGPv5;chrX	7793707	7796441	FBgn0004922	2,1954207	39,72193	-
BDGPv5;chr3R	24699991	24702390	FBgn0053203	2,1869526	38,97602	-
BDGPv5;chr3R	16686140	16687424	FBgn0038837	2,1842834	24,16301	-
BDGPv5;chr2L	13888513	13890488	FBgn0028509	2,1820481	38,00163	centaurin gamma 1A
BDGPv5;chr3L	16641695	16643062	FBgn0036650	2,1698652	25,48049	-
BDGPv5;chr2R	6211321	6212787	FBgn0085392	2,166153	32,77287	-
BDGPv5;chrX	13232876	13234702	FBgn0030474	2,1645712	37,79988	-
BDGPv5;chr3L	3457497	3459058	FBgn0026259	2,1400519	34,94582	eIF5B
BDGPv5;chr2L	13824467	13826814	FBgn0004406	2,1328479	43,2121	tamas
BDGPv5;chr2R	18692285	18694160	FBgn0000405	2,1277756	32,44847	Cyclin B
BDGPv5;chrX	1956479	1960862	FBgn0025626	2,1245468	48,35298	-
BDGPv5;chrX	14118360	14120195	FBgn0030551	2,1219311	38,11828	-
BDGPv5;chr2R	17175542	17176976	FBgn0034612	2,1040271	22,4863	-
BDGPv5;chrX	1331154	1332690	FBgn0085416	2,0932711	24,2025	-
BDGPv5;chr3R	26663935	26665941	FBgn0039804	2,0921166	30,71741	-
BDGPv5;chr3L	21171514	21173084	FBgn0021760	2,0863088	33,12748	chromosome bows
BDGPv5;chr3R	22725101	22726486	FBgn0004359	2,0759411	22,84185	Transcript 48
BDGPv5;chrX	16629678	16632017	FBgn0027528	2,0523797	36,29674	-
BDGPv5;chrX	1248809	1251692	FBgn0024364	2,0291626	45,43062	-
BDGPv5;chr3L	15976546	15978037	FBgn0000115	2,0141464	29,1132	Arflike at 72A
BDGPv5;chr3L	15231653	15232632	FBgn0029114	1,9992015	16,92214	Tollo
BDGPv5;chr3R	2931362	2933000	FBgn0037471	1,9943077	19,93735	-

BDGPv5;chr2R	4632397	4634211	FBgn0027585	1,9883184	33,43331	-
BDGPv5;chr3R	11196892	11198219	FBgn0038332	1,9827219	22,09358	-
BDGPv5;chr2R	3379322	3380762	FBgn0033182	1,9800084	16,53282	-
BDGPv5;chr3R	9528334	9530321	FBgn0038172	1,9799602	27,66873	Adenosine deaminase-related growth factor D
BDGPv5;chr2R	15327794	15330382	FBgn0040273	1,9726885	25,31028	Spt5
BDGPv5;chr2L	17411045	17412164	FBgn0032635	1,9701326	19,483	-
BDGPv5;chr3R	59432	60629	FBgn0015331	1,9634286	15,53564	abstrakt
BDGPv5;chr2R	18518304	18520036	FBgn0053143	1,9632421	28,62733	-
BDGPv5;chr3L	11219982	11221725	FBgn0036149	1,9546563	22,51671	
BDGPv5;chr3R	23490763	23492176	FBgn0039536	1,953909	24,90006	-
BDGPv5;chrX	15778945	15781075	FBgn0030702	1,9403658	20,30831	
BDGPv5;chr3R	24639124	24641026	FBgn0039600	1,9309841	26,05644	-
BDGPv5;chr3R	4666097	4668291	FBgn0003177	1,9308184	32,11912	polychaetoid
BDGPv5;chr3L	3049057	3051218	FBgn0052484	1,9254305	36,44855	Sphingosine kinase 2
BDGPv5;chr3R	19816785	19818632	FBgn0039137	1,9217827	28,16926	-
BDGPv5;chr2L	8734894	8736351	FBgn0003209	1,8737024	20,41166	raw
BDGPv5;chr3R	5876405	5878341	FBgn0037781	1,8700803	23,77078	Fancl
BDGPv5;chrX	16377837	16379565	FBgn0003036	1,865619	20,07135	
BDGPv5;chr3L	8725449	8726543	FBgn0003149	1,8609111	12,78924	Paramyosin
BDGPv5;chr3L	11087169	11088975	FBgn0036125	1,8487637	26,39562	-
BDGPv5;chr3R	11148032	11150722	FBgn0026441	1,84769	23,06616	ENL/AF9-related
BDGPv5;chr3R	12653729	12655380	FBgn0000014	1,8435014	22,00367	abdominal A
BDGPv5;chr2R	2650368	2652177	FBgn0085421	1,8393077	27,24655	Epac
BDGPv5;chr2L	2150875	2151913	FBgn0027509	1,8300735	11,15886	-
BDGPv5;chr3L	8466987	8469306	FBgn0035898	1,8243489	25,78312	-
BDGPv5;chr2L	383139	384527	FBgn0000061	1,8192027	19,79657	aristaless
BDGPv5;chr2L	14267589	14269736	FBgn0004002	1,8163286	25,86651	
BDGPv5;chr3R	4841649	4843479	FBgn0015014	1,8090799	19,63501	tango
BDGPv5;chr3L	12053546	12054563	FBgn0041096	1,8055627	13,91839	rolling pebbles
BDGPv5;chr3L	20590194	20591367	FBgn0001323	1,8028708	17,91053	knirps-like
BDGPv5;chr3L	5900505	5902639	FBgn0035648	1,7930612	20,50412	-
BDGPv5;chr3R	2380734	2382897	FBgn0053202	1,7888645	24,19991	dpr11
BDGPv5;chr2L	6938089	6939434	FBgn0031869	1,7616506	20,60659	-
BDGPv5;chrX	14966565	14968164	FBgn0030608	1,7576862	19,33332	Lipid storage droplet-2
BDGPv5;chr3R	1669518	1671524	FBgn0037387	1,7424312	17,60338	-
BDGPv5;chr3L	20843527	20845414	FBgn0052432	1,7423257	23,08746	-
BDGPv5;chr3L	1237559	1240073	FBgn0035192	1,7318881	28,97629	-



Appendix 6.5: Chromatin accessibility under Kuk overexpression conditions (red) and Kuk (orange) LaminDm0 (light orange) and LaminDm0+Kuk (yellow) chromatin interaction, at the *pigeon* locus (chromosome 2L). (Analysis performed by M. Fornerod.)

Appendix 6.6: List of candidates included in the RNAi screen for genes affecting X chromosome localization in S2 cells. The candidates marked with an asterisk were first tested by A. Brandt (unpublished results) and were retested in this work. The rest of the candidates were tested for the first time in this work. Information concerning the different candidates was obtained from the FlyBase.

	Annotation ID	Name	Information
*	CG17952	LBR	INM protein
*	CG1664	sbr	mRNA export related
*	CG9703	Axs	Unknown function Predicted: chromosome segregation
*	CG8409	HP1a, Su(var)2-5	Chromatin binding
*	CG8593	Quemao	Predicted: geranyltransferase activity, farnesyltransferase activity
*	CG7380	Baf	Chromatin binding, LEM domain interacting
*	CG8274	Mtor	NPC component
*	CG5175	Kuk	INM protein
*	CG5581	Otefin	INM protein
	CG5857	Ndc1	NPC component
	CG4236	Caf-1, p55	Chromatin remodelling complex component
	CG4453	Nup153	NPC component
	CG32067	p66, simjang	Regulator of transcription
	CG6743	Nup107	NPC component
	CG12399	Mad	Regulator of transcription
	CG4257	STAT92E	<i>Drosophila</i> STAT
	CG6476	Su(Var)3-9	Chromatin binding, Histone methyltransferase activity
	CG1594	Hopscotch	<i>Drosophila</i> JAK
	CG12389	fpfs	Geranyltransferase activity

